STATE-DEPENDENT ACTIONS OF SODIUM CHANNEL INHIBITOR INSECTICIDES ON MAMMALIAN VOLTAGE-GATED SODIUM CHANNELS

A Dissertation

Presented to the Faculty of the Graduate School

of Cornell University

In Partial Fulfillment of the Requirements for the Degree of

Doctor of Philosophy

by

Richard Thornton von Stein

August 2011

STATE-DEPENDENT ACTIONS OF SODIUM CHANNEL INHIBITOR INSECTICIDES ON MAMMALIAN VOLTAGE-GATED SODIUM CHANNELS

Richard Thornton von Stein, Ph. D.

Cornell University 2011

Sodium channel inhibitor insecticides are an emerging class of neurotoxic insect control agents that selectively inhibit voltage-gated sodium channels at membrane potentials that promote slow sodium channel inactivation. Metaflumizone, a newly-commercialized insecticide in the animal health market, causes state-dependent inhibition of insect sodium channels. The goal of this dissertation was to investigate the state-dependent effects of metaflumizone; indoxacarb, the only other commercialized compound in this insecticide class; DCJW, the bioactivation metabolite of indoxacarb in insects; and RH-3421 and RH-4841, two experimental insecticides, on mammalian sodium channels using the *Xenopus laevis* oocyte expression system. The two-electrode voltage clamp technique was used to measure sodium currents from unfertilized *Xenopus* frog eggs injected with rat $Na_v1.4$ sodium channel and auxiliary β1-subunit cRNA. Characterization of slow inactivation revealed that it is a heterogeneous biophysical process composed on multiple conformational states that are kinetically, functionally, and structurally distinct.

Metaflumizone shifted the voltage dependence of slow inactivation in the direction of hyperpolarization and selectively inhibited mammalian sodium channels at membrane potentials that facilitated slow inactivation. However, perfusion of metaflumizone at a hyperpolarized potential caused a depolarizing shift in the voltage dependence of activation and selectively

antagonized use-dependent lidocaine inhibition. These results imply that metaflumizone binds to sodium channels in the resting and fast-inactivated state in a manner that is distinct from other compounds in this insecticide class.

I substituted alanine, cysteine, or lysine for residue V787 in DII-S6 of $Na_v1.4$ channels to test the hypothesis that the extent of insecticide inhibition is directly related to the availability of slow-inactivated sodium channels. Substitutions at V787 had residue- and compound-specific effects on the actions of sodium channel inhibitor insecticides that were independent of mutation-induced changes in slow inactivation. These results imply that V787 is part of or in close proximity to the binding site for sodium channel inhibitor insecticides on mammalian voltage-gated sodium channels, which may not be identical for all members of this insecticide class.

BIOGRAPHICAL SKETCH

Richard was born to parents Frederick and Janet on July 13, 1983. Growing up in Mount Kisco, NY, Richard was always very active and enjoyed playing sports (most notably lacrosse) and working as an environmental steward at a local Nature Preserve. After graduating high school, Richard attended the State University of New York at Albany where he met his beloved future wife Melissa, received a B.S. in Environmental Biology, graduated summa cum laude, and received the Outstanding Student award from the Department of Earth and Atmospheric Sciences. During college, Richard was also involved in pioneer neurotoxicology research for two years in the laboratory of Dr. David O. Carpenter at the University at Albany's School of Public Health. Driven by his passion for environmental and biological sciences, Richard immediately enrolled in the Ph.D. program at Cornell University in the field of Environmental Toxicology and was awarded one of the first Presidential Life Science Fellowships. At Cornell, Richard worked under the supervision of Dr. David M. Soderlund at the New York State Agricultural Experiment Station in Geneva, NY. After completing his dissertation, Richard intends to continue his scientific career as a postdoctoral research associate in the department of Entomology at Cornell University.

To my darling Melissa, for always believing in me and being my biggest supporter.

To my family, especially my parents, for teaching me so much except how to give up.

Your attitude, not your aptitude, will determine your altitude.

~Zig Ziglar

ACKNOWLEDGMENTS

This work was supported in part by grant number R01-ES014591 from the National Institute of Environmental Health Sciences, National Institute of Health. I kindly thank Dr. David M. Soderlund for all of your helpful guidance, support, and good humor throughout my dissertation research, for shaping me into the scientist that I am and believing in the scientist that I will become. Additionally, I thank Dr. Robert Oswald and Dr. Gregory Weiland for their participation on my special committee and helpful advice in the completion of my research at Cornell. I thank Dr. Jianguo Tan, Dr. Bingjun He, and Scott Kopatz for your technical assistance and patience. I thank Dr. Rubia Araújo and Dr. Samantha McCavera for your words of encouragement and Friday afternoon ales. I thank Pam Adams for always smiling and reminding me that there is light at the end of the tunnel and DNA at the bottom of the tube. I thank G. Carlson (Rohm and Haas Company) and K. Wing (DuPont Agricultural Products) for providing RH-3421 and RH-4841, and DCJW, and R.G. Kallen (University of Pennsylvania, Philadelphia, PA), and W.A. Catterall (University of Washington, Seattle, WA) for providing the sodium channel clones. And finally, my deepest appreciation goes to my wife and family for your undying love and support. I cannot thank you all enough.

TABLE OF CONTENTS

LIST OF FIGURES

LIST OF TABLES

CHAPTER ONE

REVIEW OF THE LITERATURE AND STATEMENT OF THE PROBLEM

Introduction

The nervous system enables animals to receive and respond to internal and external stimuli with both speed and precision. To process and transmit information, the nervous system uses electrochemical gradients across the plasma membrane of the cell to generate an electrical signal called an action potential. An action potential is a brief, spike-like reversal of the voltage across the membrane that is generated primarily by the cellular influx and efflux of sodium and potassium ions, respectively (Hille and Catterall, 1999). Voltage-gated ion channels embedded in the plasma membrane detect changes in the membrane potential, which mediate changes in the channel conformation. A change in the membrane potential to a more positive value causes voltage-gated sodium and potassium channels to open, enabling the selective diffusion of either sodium or potassium ions through their aqueous pores. Abnormal functioning of these ion channels reduces the ability of the nervous system to transmit, receive, and analyze information and can have painful or life-threatening consequences. The importance of normal ion channel function is evident from the wide variety of channel-specific neurotoxins developed by organisms to capture prey or escape predation (Nicholson, 2007).

Voltage-gated sodium channels are a small multigene family of ion channels that are targets for a wide range of natural and synthetic neurotoxins and therapeutic drugs. Disruption of voltage-gated sodium channel function has been an effective means of controlling pest insects. This dissertation focuses on understanding the mechanism of action of sodium channel inhibitor insecticides on rat voltage-gated sodium channels heterologously expressed in *Xenopus laevis*

oocytes.

Voltage-Gated Sodium Channels

Molecular Structure

Voltage-gated sodium channels are integral membrane proteins principally composed of a large (260 kDa) α subunit (Catterall, 2000). Purification and functional reconstitution of the α subunit into liposomes and artificial membranes demonstrates that it confers all of the major structural, functional, and pharmacological properties of voltage-gated sodium channels including pore formation, ion selectivity, and voltage-dependent gating (Koester and Siegelbaum, 1995). The α subunit is composed of 24 transmembrane α-helical segments connected together by smaller intersegmental linkers and organized into four homologous domains, numbered DI-DIV (Fig. 1.1). Each domain contains six transmembrane α-helices, designated S1-S6.

The size and hydrophobic properties of the sodium channel have prevented the elucidation of x-ray crystal structures of the channel. Therefore, current three-dimensional models of the sodium channel are based on low-resolution (19 Å) cryo-electron microscopy images of the voltage-gated sodium channel purified from the electroplax of the electric eel *Electrophorus electricus* (Sato *et al.*, 2001). Additionally, available crystal structures of various distantly related voltage-gated potassium channels have been used as structural templates for constructing high-resolution homology models of voltage-gated sodium channels (Lipkind and Fozzard, 1996; Lipkind and Fozzard, 2000; Lipkind and Fozzard, 2005; O'Reilly *et al.*, 2006; Scheib *et al.*, 2006; Tikhonov and Zhorov, 2005; Tikhonov and Zhorov, 2007). The sodium channel protein is a bell-shaped molecule containing several narrow transmembrane pores

(Catterall, 2001; Sato *et al.*, 2001). The S4 transmembrane segments of each homology domain, which contain positively charged arginine and lysine residues, serve as the voltage sensors of the protein. The net positive charge of the S4 segments allows them to move outward across the plasma membrane in response to changes in the membrane potential. Movement of the S4 segments transduces changes in the voltage across the membrane into conformational changes in the entire protein that results in channel opening. The extracellular loop, known as the P-loop, located between the S5 and S6 segment in each domain, partially folds back into the membrane and forms the outer pore and the ion selectivity filter, which prevents the conduction of ions other than sodium across the membrane. The S6 transmembrane segment in each domain is thought to line the intracellular side of the ion conduction pore and contains a glycine or serine residue that is proposed to function as a flexible hinge, allowing bending of the S6 segments during channel opening (Lipkind and Fozzard, 2005).

α *Subunit Isoforms*

Mammalian genomes possess nine genes that encode voltage-gated sodium channel α subunit isoforms, designated $Na_v1.1$-$Na_v1.9$ (Fig. 1.2). Comparison of all nine primary amino acid sequences reveals that the isoforms share 70-90% sequence identity (Yu and Catterall, 2003).

Sodium channel isoforms exhibit diverse expression profiles in excitable cells. The genes encoding the $Na_v1.1$, $Na_v1.2$, $Na_v1.3$, and $Na_v1.6$ isoforms are abundantly expressed in the central nervous system (CNS) (Duflocq *et al.*, 2008). Though, expression of $Na_v1.1$ mRNA has also been detected in cardiac muscle (Malhotra *et al.*, 2001). Each of these brain sodium channel isoforms is sensitive to inhibition by tetrodotoxin (TTX), a sodium channel-specific neurotoxin found in puffer fish and the blue-ringed octopus (Hwang *et al.*, 1989; Narahashi, 2001).

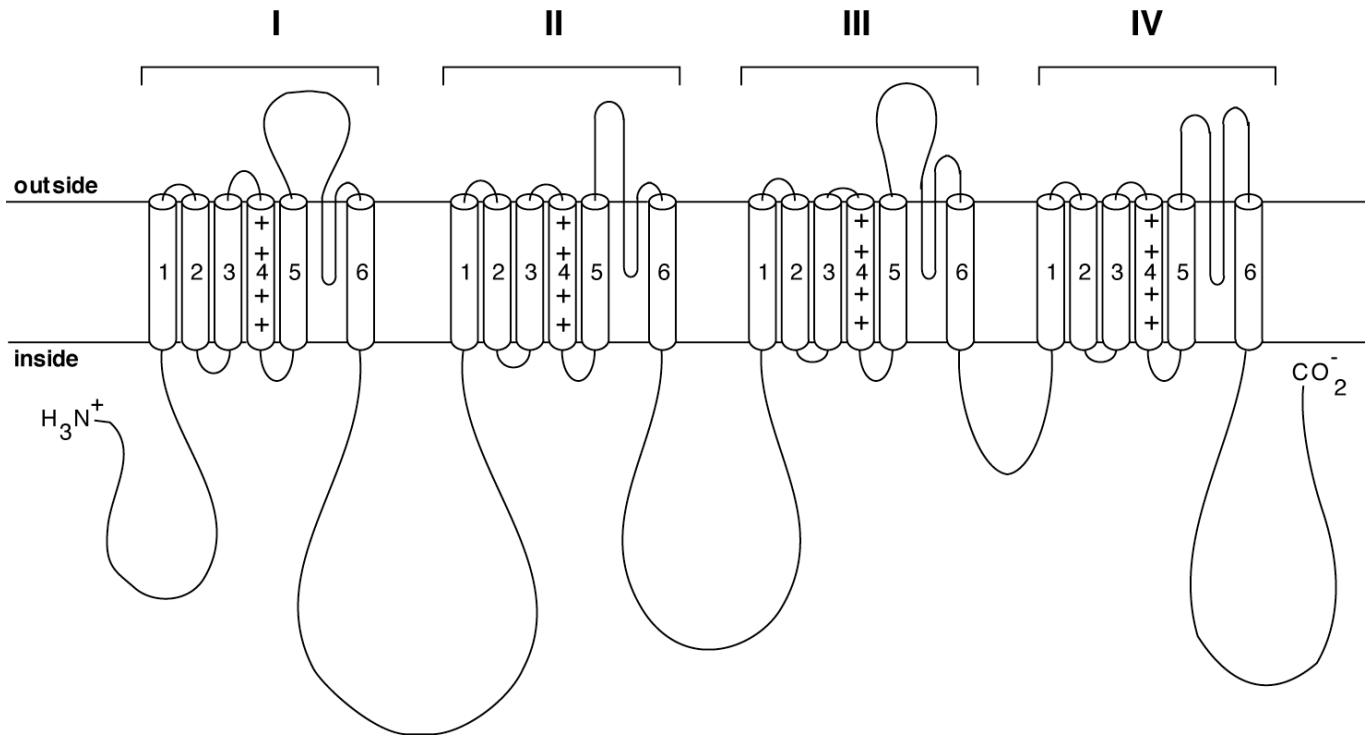

Figure 1.1: The secondary structure of voltage-gated sodium channels

$Na_v1.7$, $Na_v1.8$, and $Na_v1.9$ sodium channel isoforms are abundantly expressed in the PNS. $Na_v1.7$ is a TTX-sensitive (TTX-S) isoform that is widely expressed throughout the PNS, whereas expression of $Na_v1.8$ and $Na_v1.9$, two TTX-resistant (TTX-R) isoforms, is almost exclusively restricted to small-diameter fibers of dorsal root ganglion (DRG) neurons (Goldin, 2001).

$Na_v1.4$ and $Na_v1.5$ sodium channel isoforms are abundantly expressed in muscle fibers. $Na_v1.4$ is TTX-S and is the dominant isoform found in skeletal muscle, whereas $Na_v1.5$ is TTX-R and is the dominant sodium channel expressed in cardiac muscle. $Na_v1.5$ is also expressed in limbic regions of the brain (Hartmann *et al.*, 1999; Wu *et al.*, 2002), as well as in immature small-diameter DRG neurons (Renganathan *et al.*, 2002), neonatal skeletal muscle, and adult skeletal muscle after denervation (Kallen *et al.*, 1990; Goldin, 2001).

Auxiliary β Subunits

Voltage-gated sodium channel α subunits typically form heteromultimeric complexes with one or more smaller (33-36 kDa) auxiliary subunits, called β subunits. To date, four auxiliary subunits, designated β1- β4, have been identified in mammals (Yu *et al.*, 2003). Sodium channel β subunits modulate channel gating properties, regulate channel expression in the plasma membrane, and contribute to cell adhesion and cell-cell communication (Patino and Isom, 2010; Tan and Soderlund, 2011). Each β subunit consists of a small intracellular carboxyl-terminal and a large extracellular amino terminal joined by a single transmembrane segment (Fig. 1.3). The extracellular N-terminal contains several potential N-glycosylation sites and cysteine residues that contribute to the formation of an immunoglobulin-like fold, a motif that is also present throughout the family of neuronal cell adhesion molecules (Johnson and Bennett, 2006). β1 and β3 subunits noncovalently associate with the α subunit, whereas the β2 and β4

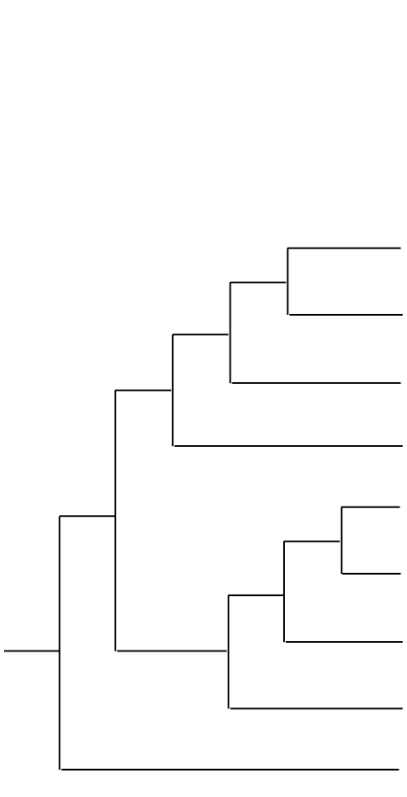

Name	Expression pattern	Auxiliary subunits β1	Auxiliary subunits β2	TTX sensitivity
$Na_v1.9$ (NaN)	PNS	-	-	R
$Na_v1.8$ (SNS/PN3)	PNS	-	-	R
$Na_v1.5$ (H1/SkM2)	cardiac muscle	-	-	R
$Na_v1.4$ (μ1/SkM1)	skeletal muscle	+	-	S
$Na_v1.1$ (brain I)	CNS, PNS	+	+	S
$Na_v1.2$ (brain II/IIa)	CNS	+	+	S
$Na_v1.3$ (brain III)	CNS	+	+	S
$Na_v1.6$ (NaCh6/PN4)	CNS	+	+	S
$Na_v1.7$ (PN1)	CNS, Schwann cells	-	-	S

Figure 1.2: The mammalian voltage-gated sodium channel α subunit gene family (common names are given in parentheses)

subunits covalently bind to the α subunit via disulfide bonds (Yu *et al.*, 2003).

The mechanism by which β subunits alter sodium channel gating is unclear. However, the presence of N-glycosylation sites in the extracellular moiety of β subunits, which are often capped with sialic acids and carry a negative charge at physiological pH, has lead to the hypothesis that β subunits may alter sodium channel gating by increasing the extracellular surface density of negative charges near the S4 voltage sensors (Ferrera and Moran, 2006).

Function

The hallmark of voltage-gated sodium channel function is its ability to undergo rapid, transient conformational changes in response to changes in the voltage difference across the plasma membrane. The conformations adopted by sodium channels can be divided into three distinct categories or states: resting, activated, and inactivated, each of which likely has several substates (Hill, 2001). The resting state is a non-conducting conformation that is predominantly occupied by sodium channels when the membrane potential is very negative, or hyperpolarized. Depolarization of the membrane causes sodium channels to transition from the resting state into the activated channel state briefly before spontaneously undergoing inactivation on a time scale of milliseconds. The activation of sodium channels allows sodium ions to flow across the membrane and into the cell, causing further membrane depolarization.

Sodium channel inactivation can be divided into two distinct biophysical processes, designated fast inactivation and slow inactivation. Fast inactivation, which occurs within milliseconds after membrane depolarization, is responsible for the termination and uni-directional propagation of action potentials and is caused by occlusion of the inner pore of the sodium channel by an inactivating particle. The inactivating particle, formed by the intracellular linker between DIII-DIV (Fig. 1.1), is thought to fold into and block the inner pore by binding to

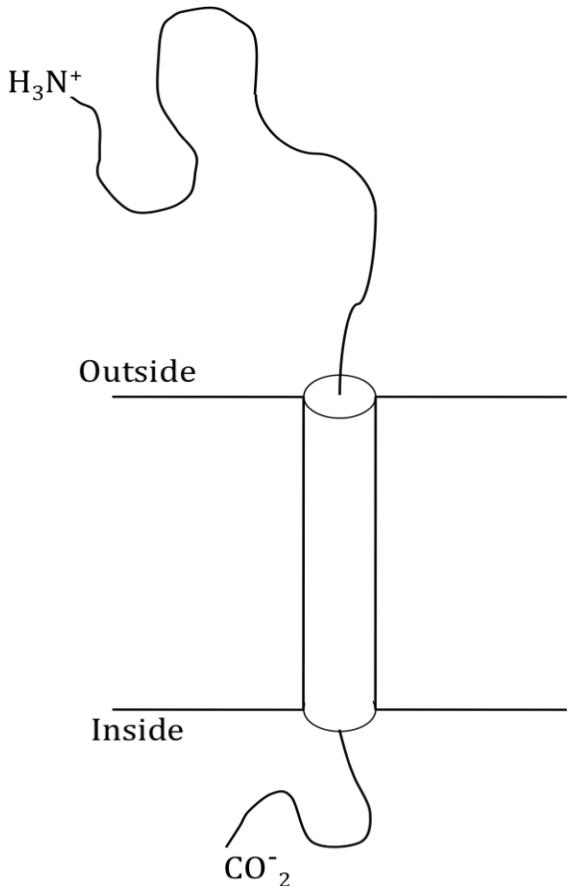

Figure 1.3: The secondary structure of the rat β1 auxiliary subunit.

portions of the intracellular linkers between S4 and S5 in DIII and DIV as well as the intracellular terminus of DIVS6 (Goldin, 2003). The movement of the inactivation gate over the inner mouth of the sodium channel pore prevents further conduction of sodium ions into the cell.

Slow inactivation in sodium channels occurs in response to sustained depolarization or high-frequency bursts of action potentials in spiking cells (Vilin and Ruben, 2001; Goldin, 2003). The slow kinetics of development and recovery from slow inactivation suggests that it is important in regulating membrane excitability, action potential firing properties, and spike-frequency adaptation (Ruff *et al.*, 1988; Sawczuk *et al.*, 1995). Slow inactivation is also thought to be an important mechanism for preventing damage to cells caused by excessive stimulation such as during tissue ischemia and episodic convulsions (Balser *et al.*, 1996). The mechanism of slow inactivation in sodium channels is poorly understood, but it is distinct from fast inactivation because mutations or internal perfusion of proteases that disable the fast-inactivation gate do not disrupt slow inactivation (Goldin, 2003). Slow inactivation may involve a comprehensive conformational change in the protein structure since slow inactivation is altered by mutations in many distant parts of the voltage-gated sodium channel, including all four S6 segments (Ulbricht, 2005), DIVS4 (Mitrovic *et al.*, 2000), the linker between DIIS4 and DIIS5 (Bendahhou *et al.*, 2002), DIIS5 and DIVS5 (Cummins and Sigworth, 1996; Bendahhou *et al.*, 1999), the linker between DII and DIII (Kusmenkin *et al.*, 2003), and the linker DIIS5 and DIIS6 (Goldin, 2003).

The transitioning of sodium channels between conformational states alters sodium ion permeability as well as the sensitivity to some sodium channel specific neurotoxic and therapeutic agents. Consequently, such agents exhibit a preferential state-dependent modification of sodium channel function. Because changes in the transmembrane voltage of the cell drive

changes in the sodium channel conformation, state-dependent interactions are often manifested as voltage-dependent phenomena. According to the "modulated receptor" hypothesis, put forth to account for the apparent voltage-dependent inhibition of sodium channels by local anesthetic, class I anticonvulsant, and class I antiarrhythmic drugs, the transitioning of sodium channels between different states results in conformational changes at the level of the receptor binding site(s) (Hille, 1977). Alternatively, the "guarded-receptor" hypothesis contends that receptor affinity does not change as a result of the sodium channel state; rather it is the accessibility of the neurotoxin or drug to the receptor that changes as a function of the channel state (Starmer *et al.*, 1984). The potential for both receptor affinity and accessibility for some molecules to be modified as a result of sodium channel state transitions cannot be excluded.

Pharmacology

Voltage-gated sodium channels are the molecular targets for a wide range of natural and synthetic neurotoxic and therapeutic agents. Nine distinct neurotoxin or drug binding sites have been identified on voltage-gated sodium channels (Table 1.1) (Wang and Wang, 2003). Although these receptor sites are spatially distinct, they are not independent of one another since the binding of a sodium channel-specific agent at one site can allosterically modulate the binding of agents at other sites.

Site 1 interacts with the water-soluble marine toxins tetrodotoxin (TTX) and saxitoxin (STX), and the large peptidic μ-conotoxins (μ-CTXs). These toxins inhibit sodium ion conductance into the cell by interacting with the ion selectivity filter and occluding the outer pore (Li *et al.*, 2000; Scheib *et al.*, 2006). However, the binding domains for TTX/STX and μ-CTXs do not appear to involve the same amino acid residues since mutations in the DIS5-S6 segment effectively eliminates TTX and STX sensitivity without preventing sodium channel

Table 1.1: The neurotoxin and drug binding sites on voltage-gated sodium channels

Site	Neurotoxin	Physiological Effect	Putative Location
1	Tetrodotoxin Saxitoxin μ-Conotoxin	Inhibit ion transport	DI S5-S6 loop
2	Batrachotoxin Grayanotoxin Veratridine Aconitine *N*-alkylamides	Persistent activation	S6 segments of DI-DIV
3	α-Scorpion toxins Sea anemone toxins δ-atracotoxins	Persistent activation	DIV S3-S4, DI S5-S6, DIV S5-S6 loop
4	β-Scorpion toxins Tarantula huwentoxin-IV	Enhanced activation	DII S1-S2, DII S3-S4
5	Brevetoxin Ciguatoxin	Persistent activation	DI-S6, DIV-S5
6	δ-Conotoxins	Prolonged activation	DIV-S4
7	DDT and pyrethroids	Prolonged activation	DI-S6, DII-S6, DIII-S6
8	Conus striatus toxins *Goniopora* coral toxins	Prolonged activation	?
9	Local anesthetics Class I anticonvulsants Class I antiarrhythmics SCI insecticides	Inhibit ion transport	DI-S6, DIII-S6, DIV-S6

block by μ-CTXs (Stephan *et al.*, 1994).

Site 2 interacts with the lipid-soluble toxins, batrachotoxin, grayanotoxin, veratridine, aconitine, and the *N*-alkylamide insecticides. These compounds bind to the inner-pore forming S6 segments in open sodium channels and shift the voltage dependence of sodium channel activation and fast inactivation in the direction of hyperpolarization and depolarization, respectively (Wang and Wang, 1998; 2003;Wang *et al.*, 2000). The binding of Site 2 toxins results in persistent activation of sodium channels at hyperpolarized resting membrane potentials (Catterall *et al.*, 2007).

Site 3 is the binding site for the α-scorpion toxins, sea anemone toxins, and δ-atracotoxins (Nicholson *et al.*, 2004). These compounds interact with amino acid residues in the extracellular loop between DIVS3-S4 and prolong sodium ion conductance by inhibiting fast inactivation (Wang and Wang, 2003). Additionally, these toxins also appear to interact with residues in the DIS5-S6 and DIVS5-S6 linkers (Nicholson, 2007). The interaction of Site 3 toxins with the voltage sensor in DIV has lead to the hypothesis that these compounds exert their toxic effects by trapping the voltage sensor(s) in the activated state, thereby preventing the conformational changes that mediate closure of the fast-inactivation gate. Indeed, α-scorpion toxins inhibit a component of outward gating charge movement that is correlated with fast inactivation (Catterall *et al.*, 2007; Nicholson, 2007). Site 3 toxins allosterically modulate the binding of Site 2 and Site 5 toxins (Nicholson, 2007).

Site 4 interacts with the scorpion venom β-toxins and tarantula venom huwentoxin-IV. These compounds bind extracellularly to the DIIS1-S2 and DIIS3-S4 linkers and increase the open channel probability of sodium channels in a manner that is thought to be similar to Site 3 neurotoxins (Wang and Wang, 2003). Whereas Site 3 toxins trap the S4 voltage sensor of DIV in the inward position, thereby preventing or slowing transitions into the fast-inactivated state, Site

4 toxins trap the S4 voltage sensor of domain II in the outward position, thereby inhibiting deactivation and also causing strong hyperpolarizing shifts in the voltage dependence of activation (Nicholson, 2007).

Site 5 interacts with the lipid-soluble polyether toxins, brevetoxin and ciguatoxin. These toxins interact with the C-terminus of DIS6 and DIVS5 and cause persistent sodium channel activation in a manner that is thought to be very similar to Site 2 toxins (Trainer *et al.*, 1991; Wang and Wang, 2003). In addition to being allosterically coupled to the Site 3 neurotoxin receptor, Site 5 toxins exert allosteric effects on toxins that interact with Sites 2, 4, 6, and 7 (Trainer *et al.*, 1991).

Sites 6 and 7 are involved in the binding of δ-conotoxins and pyrethroid insecticides, respectively. δ-conotoxins slow the rate of sodium channel inactivation by putatively binding to a hydrophobic peptide motif in the DIVS4 voltage sensor. This interaction is thought to trap the voltage sensor(s) in the activated position (Leipold *et al.*, 2005). The action of pyrethroid insecticides at Site 7 also involves a prolongation of sodium channel opening, though the molecular determinants of pyrethroid binding are unclear. Several amino acid residues that confer pyrethroid insecticide resistance in insects have been identified in DIS6 and DIIS6 (Tan *et al.*, 2005), as well as in DIIIS6 (Wang *et al.*, 2001b). These residues may interact directly with pyrethroid molecules (Wang and Wang, 2003).

Site 8 represents the binding site for the peptidic conus striatus toxin (CsTx) and the *Goniopora* coral toxins (GPTs). CsTx and GPTs prolong sodium channel opening by slowing the rate of inactivation, putatively through an interaction with the cytoplasmic surface of the sodium channel (Gonoi *et al.,* 1986; Gonoi *et al.*, 1987). Furthermore, CsTx shifts the voltage dependence of activation and fast inactivation in the direction of hyperpolarization and depolarization, respectively (Gonoi *et al.*, 1987). The binding of CsTx allosterically enhances the

persistent activation of sodium channels by veratridine (Gonoi *et al.*, 1986) and the binding of batrachotoxinin-A 20-α-benzoate (BTX-B) (Gonoi *et al.*, 1987).

Site 9 represents the binding domain for therapeutic sodium channel inhibitors (local anesthetics, class I antiarrhythmics and anticonvulsants). These compounds interact with residues in DIS6, DIIIS6, and DIVS6 that line the inner ion pore of the sodium channel and shift the voltage dependence of inactivation in the direction of hyperpolarization (Wang and Wang, 1997; Wang *et al.*, 2000; Wang *et al.*, 2001a; Wang *et al.*, 2003). Residues in DIVS6, identified previously as key elements of the therapeutic drug receptor, have also recently been shown to be important determinants of binding and action of sodium channel inhibitor (SCI) insecticides (Silver and Soderlund, 2007). SCI insecticides selectively inhibit sodium conductance at depolarized membrane potentials that produce slow inactivation, cause hyperpolarizing shifts in the voltage dependence of slow inactivation, and retard the rate at which sodium channels recover from slow inactivation at hyperpolarized potentials. Together, these data suggest that SCI insecticides selectively interact with voltage-gated sodium channels in the non-conducting slow-inactivated state (Salgado, 1992; Silver and Soderlund, 2005b). Both SCI drugs and insecticides allosterically inhibit the binding of BTX-B and veratridine to Site 2 (Willow and Catterall, 1982; Postma and Catterall, 1984; Deecher *et al.*, 1991; Leong *et al.*, 2001).

Sodium Channel Inhibitor Insecticides

Development and Insecticidal Properties

Sodium channel inhibitor (SCI) insecticides (Fig. 1.4) are a structurally diverse group of insect control agents that are also referred to as sodium channel blocker insecticides (SCBIs). However, in the strictest sense of the term, “blocker” implies that the molecules impede sodium

ion conductance by physically occluding the channel pore. Therefore, this dissertation prefers the term “SCI insecticide” to recognize additional mechanisms (*e.g*. steric, electrostatic, *etc*.) that may contribute to inhibition of the conduction of ions.

The first SCI insecticides were discovered in the 1970s through a research program at Phillips-Duphar that intended to improve the insecticidal efficacy of the 1-benzoyl-3-phenylureas, such as diflubenzuron (PH 60-40; Fig. 1.5A), which inhibit chitin synthesis and molting in insects (Mulder and Gijswijt, 1973; Mulder *et al.*, 1975). Modification of the benzoylphenylurea structure established a related group of compounds, the 1-phenylcarbamoyl-2-pyrazolines (PH 60-41; Fig 1.5B). These dihydropyrazole derivatives exhibited high levels of insecticidal activity with symptoms of intoxication that were completely different from diflubenzuron and its congeners (Silver and Soderlund, 2005a). Initial assays with PH 60-41 on various larval and adult *Coleopteran* and *Lepidopteran* species reported that contact exposure causes a series of neurological symptoms of intoxication including uncoordinated movements, tremors, convulsions, cessation of feeding, and death (Mulder *et al.*, 1975).

Further research at Philips-Duphar aimed at improving the efficacy of PH 60-41 and related congeners resulted in the discovery of 3-phenyl, 3,4- and 3,5-diphenyl derivatives (Wellinga *et al.*, 1977; van Hes *et al.*, 1978; Grosscurt *et al.*, 1979). The 3,4-diphenyl -1-phenylcarbamoyl-2-pyrazoline derivatives, exemplified by PH 60-42 (Fig. 1.5C), possess exceptionally high levels of insecticidal activity against a wide range of insect pests. However, commercial development of these compounds was prevented due to their unfavorable environmental properties. PH 60-42 is chemically labile due to its high propensity for photoaromatization, ultimately resulting in rapid loss of insecticidal activity. Additionally, the persistence of PH 60-42 in soil samples is long with a calculated soil half-life of ~17 months (Jacobson, 1989).

In the late 1980s, Rohm and Haas disclosed the discovery of a second generation of dihydropyrazole insecticides with both structural and functional similarity to the original series. These compounds, exemplified by RH3421 (Fig. 1.5D), retained a central pyrazoline moiety but possessed additional surrounding structural components. A quantitative analysis of substituent effects on convulsant and insecticidal activity revealed a linear relationship between the hydrophobicity and electronegatively of the surrounding substituents, particularly at the *N*-phenyl moiety, and the overall potency of the RH dihydropyrazoles (Hasan *et al.*, 1994).

The insecticidal activity of RH3421 and other dihydropyrazoles is strongly stereoselective. The *S* enantiomer of RH3421 is reportedly 10- and 100-times more active in American cockroaches and house flies, respectively, than its *R* counterpart (Hasan *et al.*, 1996). Furthermore, inhibition of metabolic enzyme activity with agents such as piperonyl butoxide indicates that stereoselectivity does not reflect a difference in metabolic stability (Hasan *et al.*, 1996).

In addition to the high level of broad-spectrum insecticidal activity, RH dihydropyrazoles also exhibit significantly improved environmental properties. Under field conditions, RH3421 was reported to have a relatively short soil half-life of 30 days and was not susceptible to photodegradation (Jacobson, 1989). Despite the improved environmental properties of the dihydropyrazoles, their development as commercial insecticides was limited by their adverse toxicological properties.

The acute oral toxic dose of dihydropyrazoles is high (LD_{50} > 5000 mg/kg in rats). Lower doses administered in the diet produce the delayed onset of neurotoxic symptoms followed by death. In rats, 50 mg/kg/day causes 100% mortality in 15 days, whereas 33 mg/kg/day results in 80% mortality after 28 days (Meier *et al.*, 1992). The large discrepancy between acute and dietary sub-acute toxicity is perhaps explained by the insolubility of dihydropyrazoles. Therefore, it is possible that a single oral dose is efficiently excreted without toxic effects, while

Figure 1.4: Molecular structures of sodium channel inhibitor insecticides. (A) Diflubenzuron. (B) PH 60-41. (C) PH 60-42. (D) RH 3421. (E) Benzhydrolpiperidine (BZP). (F) Indoxacarb and DCJW. (G) Metaflumizone. Chiral centers are marked with asterisks.

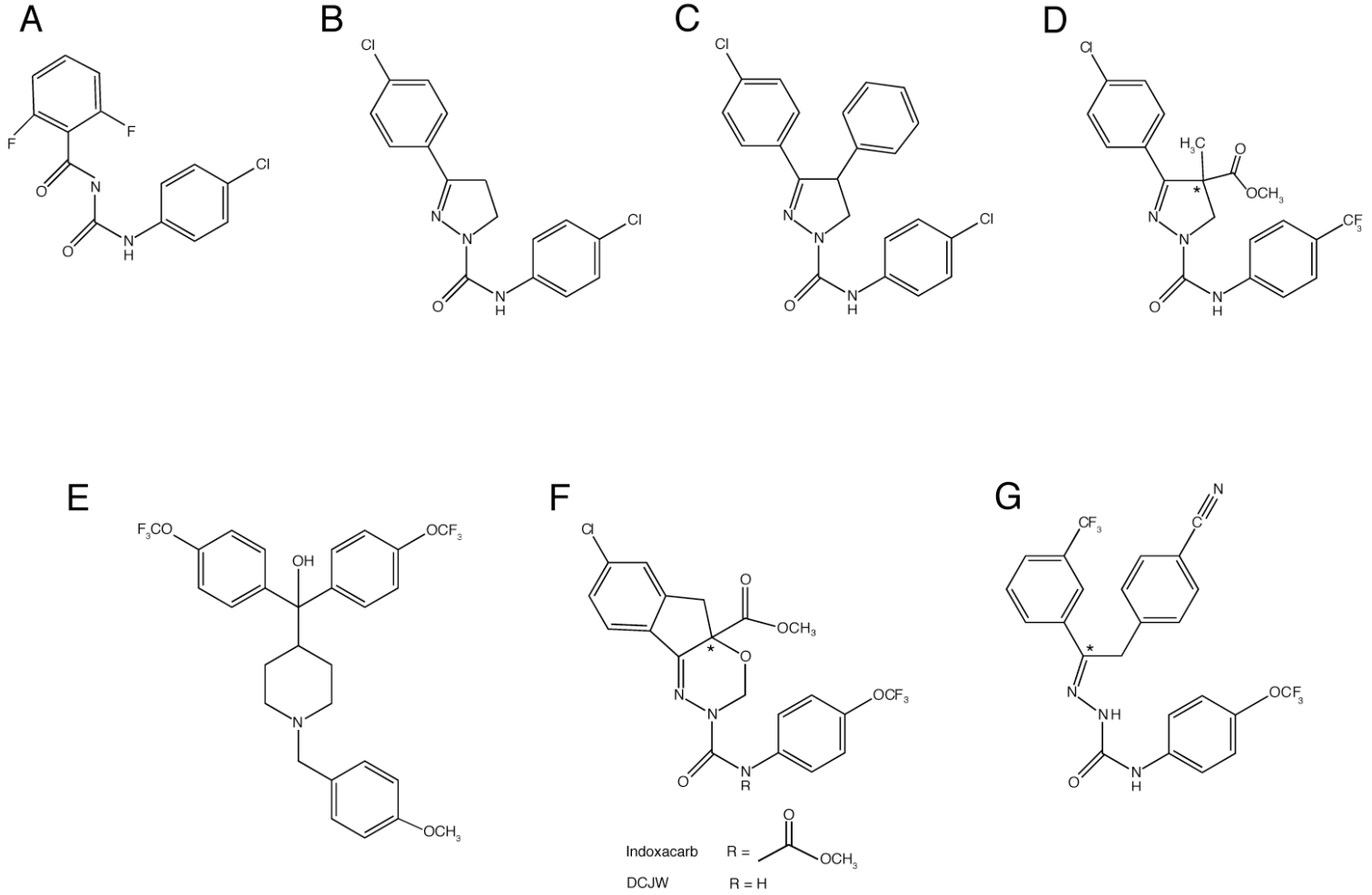
A
B
C
D
E
F
G
Indoxacarb R =
DCJW R = H

sub-acute exposure allows the compound to accumulate at sites necessary to induce the delayed neurotoxic symptoms (Meier *et al.*, 1992). The lipophilicity and metabolic stability of dihydropyrazoles increases their potential for bioaccumulation in adipose tissues (Meier *et al.*, 1992).

Arylalkylbenzhydrolpiperidines (BZPs; Fig. 1.5E), the third subclass of the SCI insecticide family, are based on the structures of the insecticidally active *Aspergillus* metabolites, nominine and aflavinine (Gloer *et al.*, 1988; Leong *et al.*, 2001; Bloomquist *et al.*, 2002). BZPs maintain the rigid, planar structure that is characteristic of pyrazoline SCI insecticides. However, BZPs contain a central piperidine or piperidine *N*-oxide ring moiety (Leong *et al.*, 2001; Bloomquist *et al.*, 2002; Silver and Soderlund, 2005a). BZPs do not have a chiral center, so their insecticidal activity is not stereoselective.

The early BZP series exhibited only weak insecticidal activity. However, subsequent optimization with indole-ring containing substituents markedly improved their efficacy and identified second and third generation compounds containing indolealkyl and indolealkylbenzhydrolpiperazine substituents, respectively. Comparative toxicity studies demonstrated that the tobacco budworm (*Heliothis virescens*) is more sensitive to compounds containing a central piperidine ring, whereas inhibition of nerve activity in mammals is more sensitive to compounds containing a central piperidine *N*-oxide ring (Leong *et al.*, 2001). In rats, BZPs exhibit moderate levels of acute oral toxicity (LD_{50} between 50-500 mg/kg) (Wierenga *et al.*, 2002). Ultimately, the unfavorable toxicological properties of BZPs prevented their development as commercial insecticides.

Oxadiazines are the fourth branch of the SCI insecticide family. The oxadiazine indoxacarb (Fig. 1.5F) is first SCI insecticide to be commercially registered in the United States. Indoxacarb maintains the very rigid, nearly planar structure that is a common feature of other

prototypic SCI insecticides. However, the molecule contains a fused 3-ring structure with a central oxadiazine-ring moiety that replaces the central pyrazoline-ring moiety common amongst the dihydropyrazoles (Silver and Soderlund, 2005a). The insecticidal activity of indoxacarb, like the dihydropyrazoles, is stereospecific. The *S* enantiomer possessing virtually all of indoxacarb's insecticidal properties compared to its *R* counterpart (Payne *et al.*, 1998; Wing *et al.*, 1998; Tsurubuchi *et al.*, 2003).

Indoxacarb is a proinsecticide in insects that requires bioactivation to a significantly more potent insecticidal metabolite, designated DCJW. Bioactivation of indoxacarb occurs in midgut cells where one or more hydrolases cleave the carbomethoxy substituent from the urea linkage (Wing *et al.*, 1998; Wing *et al.*, 2005). Because indoxacarb requires metabolic activation, the rate at which this biochemical process occurs largely determines the relative sensitivity of different insect species. Indoxacarb exhibits exceptionally high lepidoptericidal activity, which is likely due to the high rate at which it is converted into DCJW in these insects. Indoxacarb also shows high efficacy in leafhoppers, fleahoppers, weevils, beetles, as well as some urban pests, such as ants and cockroaches (Wing *et al.*, 2005; Salgado and Hayashi, 2007). In higher animals, such as mammals, the *N*-decarbomethoxylation process is relatively inefficient and indoxacarb is largely metabolized through alternative biochemical pathways, such as cytochrome P450-mediated modification of the indanone- and oxadiazine-rings (Wing *et al.*, 2005). The relatively inefficient rate at which higher animals convert indoxacarb to DCJW partially explains its high selective toxicity between target insects and non-target organisms, such as mammals. Additionally, DCJW is extensively metabolized via alternate pathways and efficiently excreted in the urine (Wing *et al.*, 2005). Acute toxicity tests show that female rats are significantly more sensitive to indoxacarb than males with oral LC_{50} values of 268 mg/kg and 1730 mg/kg, respectively (Wing *et al.*, 2005).

Semicarbazones form the fifth and newest branch of the SCI insecticide family. Metaflumizone (Fig. 1.5G), the second commercialized SCI insecticide, is an example of this group (Salgado and Hayashi, 2007). The overall molecular shape of semicarbazones is very similar to dihydropyrazoles, but some chemical modifications are evident. The most significant difference between semicarbazones and other SCI insecticides is the lack of a central heterocyclic moiety, thus making semicarbazones conformationally flexible molecules. Quantitative structure-activity relationships showed that substitutions at the *meta*-position of the benzene ring have the most profound effects on insect toxicity (Takagi *et al.*, 2007). Whereas substituting a small, lipophilic group (*e.g*. trifluoromethyl) at this position produces the highest levels of insecticidal activity, bulkier substituents cause steric effects that drastically reduce insecticidal activity (Takagi *et al.*, 2007).

Metaflumizone is the first SCI insecticide in the animal health market due to its high efficacy for controlling fleas on domesticated pets. Metaflumizone also shows good insecticidal activity in agriculturally destructive insect pests in the orders *Lepidoptera, Coleoptera, Diptera, Isoptera, Siphonaptera* and *Hypenoptera*. Additionally, metaflumizone is effective against termites, cockroaches, ants, and fire ants, thus potentially extending its usefulness also to wood protection and urban pest insect control (Klein and Oloumi, 2005; Salgado and Hayashi, 2007; Takagi *et al.*, 2007). The insecticidal activity of metaflumizone, like the dihydropyrazoles and oxadiazines, is stereoselective. In lepidopterous larvae, the *E* isomer is 10-times more insecticidally active than the *Z* enantiomer (Takagi *et al.*, 2007).

Symptomology of Intoxication

SCI insecticides are unified by a common mode of action that is manifested through similar symptoms of intoxication. However, different compounds exhibit slightly different

neurotoxic symptoms and at slightly different rates (Salgado, 1988, Silver and Soderlund, 2005a). In American cockroaches (*Periplaneta americana*), RH3421 causes symptoms of intoxication that begin with cessation of feeding and progressive ataxia (Salgado, 1990). As uncoordinated movements worsen, insects transition into a state of prostration and begin to tremor violently while kicking their legs every few seconds when turned upside down and deprived of tarsal contact (Mulder *et al.*, 1975; Salgado, 1990; Salgado, 1992; Meier *et al.*, 1992; Silver and Soderlund, 2005a). Within several hours, insects enter a quiescent state of "pseudo-paralysis" where spontaneous and voluntary movements cease, but a tremor-kick cycle can be induced by tactile stimulation of the insect's trochanter (Salgado, 1990; Silver and Soderlund, 2005a). Ultimately, insects die within 3-4 days, most likely from desiccation (Mulder *et al.*, 1975).

In insects, symptoms of BZP intoxication are very similar to those induced by dihydropyrazoles. In tobacco budworm larvae, BZPs cause cessation of feeding and uncoordinated movements, followed by a quiescent pseudo-paralytic phase during which a characteristic tremor-kick cycle can be induced by tactile disturbance (Bloomquist *et al.*, 2002). BZPs show very high lepidoptericidal activity in foliar feeding assays but lack adequate contact-exposure activity; thus non-foliar feeding insects like fleas and cockroaches are relatively insensitive to BZP poisoning (Bloomquist *et al.*, 2002).

Indoxacarb and DCJW also produce a poisoning profile in insects that is similar to those induced by dihyropyrazoles and BZPs. However, indoxacarb intoxication differs slightly from the other SCI insecticides because it does not invoke a reflex tremor-kick cycle. Rather, indoxacarb causes cessation of feeding, ataxia, followed by a state of flaccid paralysis leading to death (Wing *et al.*, 2005). The rate of onset of indoxacarb intoxication is greatly influenced by the dose and the ambient temperature, with higher doses and temperatures increasing the rate of

onset of symptoms and death (Wing *et al.*, 2005). When larvae are exposed to a sublethal dose of indoxacarb, they are reported to eat less and therefore gain less weight, develop more slowly, and pupate and emerge much later than untreated insects (Wing *et al.*, 2005).

Neurological symptoms of intoxication by SCI insecticides have also been reported in mammals, although there is limited information available in the public literature (Silver and Soderlund, 2005a). In acute oral toxicity tests, a high dose of RH3421 causes ataxia, tremors, salivation, spasms, and a hunched posture in rats (Salgado, 1992; Silver and Soderlund, 2005a). Similar symptoms were reported in rats after being administered a high oral dose of indoxacarb (Zhao *et al.*, 1999). Oral administration of BZPs to rats causes neurological symptoms that include walking in circles on their toes, abnormal body posture, and dilation of the pupils (Silver and Soderlund, 2005a). In sub-acute toxicity assays in mice, high dietary concentrations (>200 ppm) of metaflumizone cause body-weight loss, ataxia, convulsions, and death (Food and Agriculture Organization, 2009).

SCI Insecticide Mode of Action in Invertebrates

The action of SCI insecticides at neuronal target sites was implicated shortly after their discovery in the 1970s (Mulder *et al.*, 1975). However, the first evidence of a neurological mechanism for the characteristic symptoms of intoxication was not offered until the late 1980s when it was demonstrated that dihydropyrazoles cause a profound loss of spontaneous nerve activity in both the peripheral and central nervous system (Salgado, 1988; Salgado, 1990). Low nanomolar concentrations of RH3421 injected into the thorax of American cockroaches (*Periplaneta americana*) blocked afferent activity recorded from the crural nerve, cercal nerve, abdominal stretch receptors and connective arches between the meso-and meta-thoracic ganglia (Salgado, 1990). However, inhibition of spontaneous activity in sensory neurons did not prevent

motor spikes in the crural nerve from being elicited by tactile stimulation of the trochanter, even 24 hrs after the initial onset of paralysis. These intact reflex pathways may mediate the stimulation-induced tremor-kick cycle observed in pseudo-paralyzed insects following dihydropyrazole exposure (Salgado, 1990).

Experiments using crayfish slowly-adapting stretch receptors and giant axons showed that dihydropyrazoles inhibit the initiation of action potentials without affecting their amplitude or modulating the resting membrane potential or input resistance (Salgado, 1990). These data imply a selective dihydropyrazole-induced inhibition of voltage-gated sodium channels, which are responsible for the initiation of action potentials in almost all types of excitable cells. Voltage-clamp experiments revealed that the inhibition of sodium currents by dihydropyrazoles is strongly voltage dependent, with greater inhibition occurring at depolarized membrane potentials (Salgado, 1990). In crayfish giant axons, dihydropyrazoles shifted the voltage-dependent relationship of sodium channel inactivation in the direction of hyperpolarization, implicating a preferential interaction with sodium channels in the inactivated state. This state-dependent action was realized to be similar to that of local anesthetic, class I anticonvulsant, and class I antiarrhythmic drugs, which preferentially target activated or fast-inactivated sodium channels (Salgado, 1992). However, the very slow kinetics of SCI insecticides, on the order of several minutes and much slower than the kinetics of activation or fast inactivation, restricts their inhibition of sodium channels to involve an interaction with channels in the slow-inactivated state (Salgado, 1992). The trapping of sodium channels by insecticides in the nonconducting slow-inactivated state would effectively reduce the availability of resting channels and produce channel inhibition and paralysis at the cellular and whole animal level, respectively.

Since the initial reports of the action of dihydropyrazoles on invertebrate voltage-gated sodium channels, preferential inhibition of slow-inactivated insect voltage-gated sodium

channels by BZPs (Bloomquist *et al.*, 2002), indoxacarb and DCJW (Wing *et al.*, 1998; Lapied *et al.*, 2001; Zhao *et al.*, 2005; Song *et al.*, 2006), and metaflumizone (Salgado and Hayashi, 2007; Silver *et al.*, 2009) has been well documented. However, dihydropyrazole inhibition of sodium channels in crayfish giant axons is not disrupted by progressive disabling of the fast- and slow-inactivation gates by internal perfusion of *N*-bromoacetamide and trypsin, respectively (Salgado, 1992). These data suggest that at least some SCI insecticides can inhibit sodium channels in a non-inactivated state that, nevertheless, may not reflect the native open state (Salgado, 1992).

SCI Insecticide Action on the Mammalian Nervous System

Actions on Voltage-Gated Sodium Channels

The first evidence for the action of SCI insecticides on mammalian voltage-gated sodium channels came from biochemical experiments showing dihydropyrazole-induced inhibition of spontaneous and veratridine (VTD)-, deltamethrin- and crude scorpion (*Leiurus quinquestriatus*) venom-induced release of cytosolic [^{3}H]-γ-aminbutyric acid (^{3}H-GABA) from superfused guinea pig brain synaptosomes (Nicholson and Merletti, 1990). Shortly after, reciprocal competitive interactions between RH3421 and Site 2 neurotoxins (VTD and batrachotoxin) were reported using a radiosodium uptake assay in mouse brain synaptosomes (Deecher and Soderlund, 1991). Further, inhibition of VTD-induced radiosodium uptake is stereospecific, with the *S* enantiomer approximately 6-fold more effective than the *R* counterpart (Payne *et al.*, 1998). Subsequent biochemical experiments demonstrated that RH3421 allosterically inhibits the binding of [^{3}H]-batrachotoxin A 20-α-benzoate (BTX-B) by interacting with a receptor that is allosterically coupled to Site 2 of the sodium channel (Deecher *et al.*, 1991). Similar experiments were also conducted using BZPs as the unlabeled ligand, which also showed allosteric inhibition of BTX-B

binding to Site 2 (Leong *et al.*, 2001), an effect very similar to those of therapeutic SCI drugs (Willow and Catterall, 1982; Postma and Catterall, 1984).

The commercialization of indoxacarb and metaflumizone has led to a renewed interest in the molecular mechanism of action of SCI insecticides. Whole-cell patch-clamp recordings from rat dorsal root ganglion (DRG) neurons have shown that indoxacarb and DCJW inhibit tetrodotoxin-resistant (TTX-R) and sensitive (TTX-S) sodium currents in a voltage-dependent manner (Zhao *et al.*, 2003). Although SCI insecticides appear to selectively inhibit sodium channels under experimental conditions that promote slow inactivation, both indoxacarb and DCJW also cause hyperpolarizing shifts in the voltage dependence of fast inactivation in rat DRG neurons (Zhao *et al.*, 2003). Moreover, exposure of sodium channels in rat DRG neurons to indoxacarb or DCJW at a hyperpolarized membrane potential, at which no inhibition is observed, accelerates the development of slow inactivation following subsequent depolarization. This finding suggests that indoxacarb and DCJW bind to sodium channels in the resting state without inhibiting them (Zhao *et al.*, 2003).

Voltage-gated sodium channel isoforms exhibit differences in their relative sensitivity to inhibition by SCI insecticides. In rat DRG neurons, TTX-sensitive sodium currents were shown to be more sensitive than TTX-R sodium currents to block by the oxadiazine insecticides, indoxacarb and its *N*-decarbomethoxylated metabolite, DCJW (Zhao *et al.*, 2003). Consistent with these data, rat sodium channel isoforms heterologously expressed in *Xenopus laevis* oocytes were shown to also exhibit significant differences their sensitivity to inhibition by RH3421 and DCJW (Silver and Soderlund, 2006). In particular, the TTX-R $Na_v1.5$ and $Na_v1.8$ sodium channel isoforms were significantly less sensitive than the TTX-S $Na_v1.4$ and $Na_v1.2$ isoforms (Silver and Soderlund, 2006). These differences may reflect the relatively low propensity of TTX-R isoforms to undergo slow inactivation compared to TTX-S isoforms (Vilin *et al.*, 1999;

Zhao *et al.*, 2003).

Several lines of evidence suggest a common site of action for SCI insecticides and therapeutic drugs. Biochemical studies of radioligand binding demonstrated reciprocal competitive interactions between RH3421 and the local anesthetic dibucaine as inhibitors of BTX-B binding to sodium channels in mouse brain synaptosomes (Payne *et al.*, 1998). Two-electrode voltage clamp recordings from *Xenopus* oocytes transiently expressing rat sodium channels also showed mutual competitive interactions between the anticonvulsant phenytoin and RH3421 or DCJW (Silver and Soderlund, 2005b). Further, site-directed mutagenesis experiments indicate that DIV-S6 residues (F1579 and Y1586) in rat $Na_v1.4$ sodium channels, identified previously as key determinants of state-dependent inhibition by SCI drugs (Wang *et al.*, 1998; Mike and Lukacs, 2010), also are important determinants of SCI insecticide binding and action (Silver and Soderlund, 2007). The F1579A mutation significantly reduces sodium channel sensitivity to inhibition by RH3421 or DCJW, a finding that is consistent with the impact of this mutation on the action of SCI drugs (Silver and Soderlund, 2007). Paradoxically, the Y1586A mutation significantly increases sodium channel sensitivity to RH3421, indoxacarb, or DCJW compared to wildtype channels. The effect of the Y1586A mutation on SCI insecticide inhibition is opposite to that which has been observed for SCI drug binding. Replacing the bulky aromatic side chain of tyrosine at this position to that of alanine perhaps reduces steric hindrance at this position and promotes a more favorable interaction between the insecticide and its receptor (Silver and Soderlund, 2007). In German cockroach (*Blattella germanica*) sodium channels, alanine substitution of DIV-S6 residues (analogous to F1579 and Y1586 in rat $Na_v1.4$ sodium channels) either does not affect or markedly increases sodium channel sensitivity to SCI insecticides (Silver *et al.*, 2009). These data imply different SCI insecticide receptors on mammalian and insect sodium channels.

Action on Voltage-Gated Calcium Channels

In mammals, voltage-gated sodium channels are not the exclusive neuronal target site of SCI insecticides. An interaction of SCI insecticides with voltage-gated calcium channels was first implicated when the dihydropyrazole RH5529 but not RH3421 was shown to inhibit the release of [^{3}H]GABA from guinea pig cortical synaptosomes, evoked by potassium depolarization (Nicholson and Merletti, 1990). Depolarization of nerve terminals activated voltage-gated calcium channels, which causes influx of calcium ions and triggers the release of neurotransmitters. The inhibition of potassium-evoked release of neurotransmitter by RH5529 but not tetrodotoxin (TTX), a selective blocker of voltage-gated sodium channels, implies that RH5529 interacts with voltage-gated calcium channels at presynaptic sites in the mammalian central nervous system (Nicholson and Merletti, 1990). Additional biochemical experiments using rodent brain synaptosomes preloaded with a calcium sensitive fluorescent indicator (fura-2) show that RH3421, RH5529, and BZPs inhibit veratridine- or potassium-induced increases in intraterminal free calcium (Zhang and Nicholson, 1993; Zhang and Nicholson, 1994; Leong *et al.*, 2001). The ability of RH3421 to prevent potassium-evoked radiolabeled ($^{45}Ca^{2+}$) calcium uptake into nerve terminals is blocked by cobalt ions and unaffected by TTX, thus implying that calcium channels are also a potential target of RH3421 (Zhang and Nicholson, 1994). Additionally, RH3421 and RH5529 inhibit veratridine- and potassium-evoked phosphorylation of synapsin I, blocking the release of L-glutamate from mouse brain synaptosomes (Zhang and Nicholson, 1996a). Binding assays using RH3421 and RH5529 show noncompetitive inhibition of radiolabeled dihydropyridine ([^{3}H]nitrendipine) binding to voltage-gated calcium channels in mouse brain synaptosomes (Zhang and Nicholson, 1996b). The inability of RH3421 or RH5529 to increase the rate of [^{3}H]nitrendipine dissociation at saturating concentrations suggests that is unlikely for these insecticides to interact with dihydropyridine-bound calcium channels (Zhang

and Nicholson, 1996b). RH3421 and RH5529 have also been shown to prevent ATP-dependent calcium uptake into rat brain synaptosomes (Hasan *et al.*, 1996). There is no published evidence for the action of indoxacarb, DCJW, or metaflumizone on mammalian calcium channels; however, whole-cell patch clamp recordings on cockroach DUM neurons indicate that DCJW has no effect on the calcium currents recorded from those cells (Lapied *et al.*, 2001).

The relative potency of SCI insecticides on sodium channels and calcium channels appears to depend strongly on chemical structure (Zhang and Nicholson, 1993). The relative affinity of sodium channels for RH3421 is about 15-fold higher than the affinity of calcium channels for RH3421, whereas sodium and calcium channels have about an equal affinity for RH5529 (Zhang and Nicholson, 1993). This variation in the affinity of sodium and calcium channels for SCI insecticides is likely to influence the relative importance of calcium channels in intoxication.

Actions on Nicotinic Acetylcholine Receptors

To date, only a single study has reported the action of SCI insecticides on mammalian neuronal nicotinic acetylcholine receptors (nAChRs) (Zhao *et al.* 1999). Whole-cell patch-clamp recordings from primary rat cortical neurons demonstrated the ability of indoxacarb to cause irreversible suppression of the acetylcholine (ACh)-induced rapid-decaying currents of α-bungarotoxin (α-BuTX)-sensitive (α7-like) nAChRs. By contrast, indoxacarb was reported to slowly enhance the slow-decaying currents of the α-BuTX-insensitive (α4β2-like) receptors (Zhao *et al.*, 1999). Further, indoxacarb accelerates the desensitization rate of these slowly-decaying currents, thus indicating an indoxacarb-linked increase in the affinity of the AChR for ACh in a manner similar to that of the general anesthetic, halothane. Interestingly, despite DCJW being the more potent insecticide and sodium channel block, it is significantly less effective that

indoxacarb at modulating either the α-BuTX-sensitive or α-BuTX- insensitive receptors (Zhao *et al.*, 1999). The slow rate of potentiation of α-BuTX-insensitive currents by indoxacarb may be indicative of an indirect action on AChRs via an intracellular secondary messenger-mediated pathway (Zhao *et al.*, 1999). By contrast, indoxacarb may act at an intracellular site on nAChRs, thus attributing the slow process of current potentiation to the slow rate of diffusion across the cell membrane (Zhao *et al.*, 1999). The inhibition of neuronal nicotinic acetylcholine receptors could partially explain some of the cholinergic activation-like symptoms (incoordination, hunched posture, spasms, tremors) observed in mammals after being administered a single high oral dose of indoxacarb (Zhao *et al.*, 1999).

Statement of the Problem and Research Objectives

Metaflumizone, a newly-commercialized insecticide in the animal health market, is classified as a sodium channel inhibitor (SCI) insecticide on the basis of its mode of action on insect voltage-gated sodium channels. Previous studies suggest a relationship between slow inactivation and channel inhibition by these compounds at a site that is closely associated with the local anesthetic receptor. However, it is not known whether SCI insecticides bind and act exclusively through the slow-inactivated state. Therefore, the goals of this dissertation project were to characterize the action of metaflumizone on cloned mammalian sodium channels and investigate the state-dependent mechanism of channel inhibition by sodium channel inhibitor insecticides. The experimental objectives in this research were to: (1) characterize slow inactivation in a model rat voltage-gated sodium channel ($Na_v1.4$) in detail to determine the experimental conditions necessary to study the action of SCI insecticides; (2) investigate the state-dependent action of metaflumizone on $Na_v1.4$ sodium channels; and (3) elucidate the state-

dependent mechanism of action of SCI insecticides using $Na_v1.4$ sodium channel specifically mutated to exhibit altered slow inactivation.

Experimental Approach

I employed the two-electrode voltage clamp technique in conjunction with the *Xenopus laevis* oocyte expression system to investigate the state-dependent actions of SCI insecticides on cloned rat $Na_v1.4$ sodium channels. The two-electrode voltage clamp method, which uses one electrode for passing current and another for voltage recording, was first established in the 1950s to study voltage-dependent sodium and potassium currents in the giant axon of squid (*Loligo*) (Hodgkin and Huxley 1952a; Hodgkin and Huxley 1952b; Hodgkin and Huxley 1952c; Hodgkin and Huxley 1952d; Hodgkin *et al.*, 1952). This technique enables precise control of the transmembrane voltage of the cell, allowing detailed analysis of the pharmacological and biophysical properties on ion channels.

The *Xenopus laevis* oocyte expression system is a well-established system for studying the pharmacological and biophysical properties of specific ion channel isoforms (Goldin, 1992). The stability of electrophysiological recordings from oocytes over extended periods of time makes this system an ideal platform for studying the very slow actions of SCI insecticides on individual sodium channel isoforms. The combined use of site-directed mutagenesis offers a powerful means to study ion channel structure-function relationships and define the binding sites of compounds.

The $Na_v1.4$ sodium channel isoform was chosen for these studies for several reasons. First, it has been used previously as a model for investigating both the mechanism and site of action of SCI insecticides (Silver and Soderlund, 2005b; 2007) and therapeutic drugs (Wang *et*

al., 1998; Wang *et al.*, 2000; Wang *et al.*, 2001; Wang *et al.*, 2004) on mammalian sodium channels, as well as for studying the molecular details of slow inactivation (Balser *et al.*, 1996; Vilin *et al.*, 1999; O'Reilly *et al.*, 2001; Bendahhou *et al.*, 2002). Second, the $Na_v1.4$ gene (*SCN4A*) is stably replicated in *E. coli* bacteria and routinely generates robust levels of sodium current expression in oocytes, thereby facilitating electrophysiological analysis under experimental conditions that severely limit sodium channel availability due to partial inactivation and insecticide inhibition. Third, this isoform has been used to construct some of the highest resolution structural models of the local anesthetic receptor in the inner pore region (Lipkind and Fozzard, 2000; Lipkind and Fozzard, 2005), thereby providing a conceptual and structural framework for studying SCI insecticide-drug interactions.

References

Balsar JR, Nuss HB, Chiamvimonvat N, Perez-Garcia MT, Marbán E and Tomaselli GF (1996) External pore residue mediates slow inactivation in μ1 rat skeletal muscle sodium channels. *J. Physiol.* **494**:431-442.

Bendahhou S, Cummins TR, Tawil R, Waxman SG and Ptácek LJ (1999) Activation and inactivation of the voltage-gated sodium channel: role of segment S5 revealed by a novel hyperkalaemic periodic paralysis mutation. *J. Neurosci.* **19**:4762-4771.

Bendahhou S, Cummins TR, Kula RW, Fu Y-H and Ptácek LJ (2002) Impairment of slow inactivation as a common mechanism for periodic paralysis in DIIS4-S5. *Neurology* **58**:1266-1272.

Bloomquist JR, Payne GT, Kinne L, Lyga J, Leong D and Nicholson RA (2002) Toxicity and mode of action of benzhydrolypiperidines and related compounds on insects. *Pestic. Biochem. Phys.* **73**: 18-26.

Catterall WA (2000) From ionic currents to molecular mechanisms: the structure and function of voltage-gated sodium channels. *Neuron* **26**:13-25.

Catterall WC (2001) A 3D view of sodium channels. *Nature* **409**:988-991.

Catterall WA, Cestèle S, Yarov-Yarovoy V, Yu FH, Konoki K and Scheuer T (2007) Voltage-gated ion channels and gating modifier toxins. *Toxicon* **49**:124-141.

Cummins TR and Sigworth FJ (1996) Impaired slow inactivation in mutant sodium channels. *Biophys. J.* **71**:227-236.

Deecher DC and Soderlund DM (1991) RH-3421, an insecticidal dihydropyrazole, inhibits sodium channel-dependent sodium uptake in mouse brain preparations. *Pestic. Biochem. Phys.* **39**:130-137.

Deecher DC, Payne GT and Soderlund DM (1991) Inhibition of [^{3}H]batrachotoxin A 20-a-benzoate binding to mouse brain sodium channels by the dihydropyrazole insecticide RH-3421. *Pestic. Biochem. Physiol.* **41**:265-273.

Duflocq A, Bras BL, Bullier E, Couraud F and Davenne M (2008) Nav1.1 is predominantly expressed in nodes of Ranvier and axon initial segments. *Mol. Cell. Neurosci.* **39**:180-192.

Ferrera L and Moran O (2006) β1-subunit modulates the Nav1.4 sodium channel by changing the surface charge. *Exp. Brain Res.* **172**:139-150.

Food and Agricultural Organization of the United Nations (2009) Evaluation of data for acceptable daily intake and acute dietary intake for humans, maximum residue levels and

supervised trial median residue values, in *Pesticide Residues in Food*, *Joint FAO/WHO Meeting on Pesticide Residues*, Food and Agriculture Organization of the United Nations, Rome.

Gloer JB, TePaske MR, Sima JS, Wicklow DT and Dowd PF (1988) Antiinsectan aflavinine derivatives from the sclerotia of Aspergillus flavus. *J. Org. Chem.* **53**:5457-5460.

Goldin AL (1992) Maintenance of *Xenopus laevis* and oocyte injection. *Methods Enzymol.* **207**:266-297.

Goldin AL (2001) Resurgence of sodium chanel research. *Annu. Rev. Physiol.* **63**:871-894.

Goldin AL (2003) Mechanisms of sodium channel inactivation. *Curr. Opin. Neurobiol.* **13**:284-290.

Gonoi T, Ashida K, Feller D, Schmidt J, Fujiwara M and Catterall WA (1986) Mechanism of action of a polypeptide neurotoxin from the coral *Goniopora* on sodium channels in mouse neuroblastoma cells. *Mol. Pharmacol.* **29**:347-354.

Gonoi T, Ohizumi Y, Kobayashi J, Nakamura H and Catterall WA (1987) Actions of a polypeptide toxin from the marin snail *Conus striatus* on voltage-sensitive sodium channels. *Mol. Pharmacol.* **32**:691-698.

Grosscurt AC, van Hes R and Wellinga K (1979) 1-Phenylcarbamoyl-2-pyrazolines: a new class of insecticides. 1. Synthesis and insecticidal properties of 3,4-Diphenyl-1-phenylcarbamoyl-2-pyrazolines. *J. Agric. Food Chem.* **27**:406-409.

Hartmann HA, Colom LV, Sutherland ML and Noebels JL (1999) Selective localization of cardiac SCN5A sodium channels in limbic regions of rat brain. *Nature Neurosci.* **2**:593-595.

Hasan R, Nishimura K and Ueno T (1994) Quantitative structure-activity relationships of insecticidal pyrazolines. *Pestic. Sci.* **42**:291-298.

Hasan R, Nishimura K, Nakagawa Y, Kurihara N and Ueno T (1996) Structural effects of *N*-arylcarbamoylpyrazolines on calcium uptake in rat brain synaptosomes. *Pestic. Sci.* **46**:221-225.

Hille B (1977) Local anesthetics: hydrophilic and hydrophobic pathways for drug receptor reaction. *J. Gen. Physiol*. **69**:497-515.

Hille B (2001) *Ion Channels of Excitable Membranes*. Sinauer Associates, Inc., Sunderland, MA.

Hille B and Catterall WA (1999) Electrical excitability and ion channels, in *Basic Neurochemistry* (Siegel GJ, Agranoff BW, Albers RW, Fisher SK and Uhler MD eds) pp. 119-137, Lippincott Williams & Wilkins, Pennsylvania.

Hodgkin AL and Huxley AF (1952a) Currents carried by sodium and potassium ion through the

membrane of the giant axon of *Loligo*. *J. Physiol*. **116**:449-472.

Hodgkin AL and Huxley AF (1952b) The components of membrane conductance in the giant axon of *Loligo*. *J. Physiol.* **116**:473-496.

Hodgkin AL and Huxley AF (1952c) The dual effect of membrane potential on sodium conductance in the giant axon of *Loligo*. *J. Physiol.* **116**:497-506.

Hodgkin AL and Huxley AF (1952d) A quantitative description of membrane current and its application to conduction and excitation of nerve. *J. Physiol.* **117**:500-544.

Hodgkin AL, Huxley AF and Katz B (1952) Measurement of the current-voltage relations in the membrane of the giant axon of *Loligo*. *J. Physiol.* **116**:424-448.

Hwang DF, Arakawa O, Saito T, Noguchi T, Simidu U, Tsukamoto K, Shida Y and Hashimoto K (1989) Tetrodotoxin-producing bacteria from the blue-ringed octopus *Octopus maculosus*. *Mar. Biol.* **100**:327-332.

Jacobson RM (1989) A new class of insecticidal dihydropyrazoles, in *Recent Advances in the Chemistry of Insect Control II* (Crombie L ed.) pp. 206-211, Royal Society of Chemistry, London.

Johnson D and Bennett ES (2006) Isoform-specific effects of the β_2 subunit on voltage-gated sodium channel gating. *J. Biol. Chem.* **281**:25875-25881.

Kallen RG, Sheng Z-H, Yang J, Chen L, Rogart RB and Barchi RL (1990) Primary structure and expression of a sodium channel characeristic of denervated and immature rat skeletal muscle. *Neuron* **4**:233-242.

Koester J and Siegelbaum S (1995) Ion Channels, in *Essentials of Neuronal Science and Behavior* (Kandel ER, Schwartz JH and Jessel TM eds.) pp. 115-131, Appleton & Lange, Connecticut.

Klein CD and Oloumi H (2005) Metaflumizone: a new insecticide for urban insect control from BASF, in *Proceedings of the Fifth International Conference on Urban Pests* (Lee CY and Robinson WH eds.) pp. 101-105, P&Y Design Network, Malaysia.

Kuzmenkin A, Jurkat-Rott K, Lehmann-Horn F and Mitrovic N (2003) Impaired slow inactivation due to polymorphism and substitutions of Ser-906 in the II-III loop of the human $Na_v1.4$ channel. *Pflug. Arch. Eur. J. Phys*. **447**:71-77.

Lapied B, Grolleau F and Sattelle DB (2001) Indoxacarb, an oxadiazine insecticide, blocks insect neuronal sodium channels. *Brit. J. Pharmacol.* **132**:587-595.

Leipold E, Hansel A, Olivera BM, Terlau H and Heinemann SH (2005) Molecular interaction of d-conotoxins with voltage-gated sodium channels. *FEBS Lett.* **579**:3881-3884.

Leong D, Bloomquist JR, Bempong J, Dybas JA, Kinne LP, Lyga JW, Marek FL and Nicholson

RA (2001) Insecticidal arylalkylbenzyhydrolpiperidines: novel inhibitors of voltage-sensitive sodium and calcium channels in mammalian brain. *Pest Manag. Sci.* **57**:889-895.

Li RA, Ennis IL, Vélez P, Tomaselli GF and Marbán E (2000) Novel structural determinants of m-conotoxin (GIIIB) block in rat skeletal muscle (μ1) Na^+ channels. *J. Biol. Chem.* **275**:27551-27558.

Lipkind GM and Fozzard HA (1994) A structural model of the tetrodotoxin and saxitoxin binding site of the Na^+ channel. *Biophys. J.* **66**:1-13.

Lipkind GM and Fozzard HA (1996) Structure and function of voltage-dependent sodium channels: comparison of brain II and cardiac isoforms. *Physiol. Rev.* **76**:887-926.

Lipkind GM and Fozzard HA (2000) KcsA crystal structure as framework for a molecular model of the Na^+ channel pore. *Biochemistry-US* **39**:8161-8170.

Lipkind GM and Fozzard HA (2005) Molecular modeling of local anesthetic drug binding by voltage-gated sodium channels. *Mol. Pharmacol.* **68**:1611-1622.

McPhee JC, Ragsdale DS, Scheuer T and Catterall WA (1994) A mutation in segment IVS6 disrupts fast inactivation of sodium channels. *P. Natl. Acad. Sci. USA* **91**:12346-12350.

McPhee JC, Ragsdale DS, Scheuer T and Catterall WA (1995) A critical role for transmembrane segment IVS6 of the sodium channel α subunit in fast inactivation. *J. Biol. Chem.* **270**:12025-12034.

Meier GA, Silverman IR, Ray PS, Cullen TG, Ali SF, Marek FL and Webster CA (1992) Insecticidal dihydropyrazoles with reduced lipophilicity, in *Synthesis and Chemistry of Agrochemicals III* (Baker DR, Fenyes JG and Steffens JJ eds) pp. 313-326, American Chemical Society, Washington D.C.

Mickus T, Jung H-Y and Spruston N (1999) Properties of slow, cumulative sodium channel inactivation in rat hippocampal CA1 pyramidal neurons. *Biophys. J.* **76**:846-860.

Mike A and Lukacs P (2010) The enigmatic drug binding site for sodium channel inhibitors. *Curr. Mol. Pharmacol.* **3**:129-144.

Mitrovic N, George AL and Horn R (2000) Role of domain 4 in sodium channel slow inactivation. *J. Gen. Physiol.* **115**:707-717.

Mulder R and Gijswijt M (1973) The laboratory evaluation of two promising new insecticides which interfere with cuticle deposition. *Pestic. Sci.* **4**:737-745.

Mulder R, Wellinga K and van Daalen JJ (1975) A new class of insecticides. *Naturwissenschaften* **62**:531-532.

Narahashi T (2001) Pharmacology of tetrodotoxin. *J. Toxicol*. **20**:67-84.

Nicholson GM, Little MJ and Birinyi-Strachan LC (2004) Structure and function of d-atracotoxins: lethal neurotoxins targeting the voltage-gated sodium channel. *Toxicon* **43**:587-599.

Nicholson GM (2007) Insect-selective spider toxins targeting voltage-gated sodium channels. *Toxicon* **49**:490-512.

Nicholson RA and Merletti EL (1990) The effect of dihydropyrazoles on release [^{3}H]GABA from nerve terminals isolated from mammalian cerebral cortex. *Pestic. Biochem. Phys.* **37**:30-40.

O'Reilly AO, Khambay BPS, Williamson MS, Field LM, Wallace BA and Davies TGE (2006) Modeling insecticide-binding sites in the voltage-gated sodium channel. *Biochemistry-US* **396**:255-263.

Patino GA and Isom LL (2010) Electrophysiology and beyond: multiple roles of Na^+ channel β subunits in development and disease. *Neurosci. Lett.* **486**:53-59.

Payne GT, Deecher DC and Soderlund DM (1998) Structure-activity relationships for the action of dihydropyrazole insecticides on mouse brain sodium channels. *Pestic. Biochem. Phys.* **60**:177-185.

Postma W and Catterall WA (1984) Inhibition of [^{3}H]batrachotoxinin A 20-a-benzoate binding to sodium channels by local anesthetics. *Mol. Pharmacol.* **25**:219-227.

Ruff RL, Simoncini L and Stuhmer W (1988) Slow sodium channel inactivation in mammalian muscle: a possible role in regulating excitability. *Muscle Nerve* **11**:502-510.

Salgado VL (1988) Mode of action of 1-phenylcarbamoyl-2-pyrazoline insecticides. *Pestic. Sci.* **24**:343-344.

Salgado VL (1990) Mode of action of insecticidal dihydropyrazoles: selective block of impulse generation in sensory nerves. *Pestic. Sci.* **28**:389-411.

Salgado VL (1992) Slow voltage-dependent block of sodium channels in crayfish nerve by dihydropyrazole insecticides. *Mol. Pharmacol.* **41**:120-126.

Salgado VL and Hayashi JH (2007) Metaflumizone is a novel sodium channel blocker insecticide. *Vet. Parasitol.* **150**:182-189.

Sato C, Ueno Y, Asai K, Takahashi K, Sato M, Engel A and Fujiyoshi Y (2001) The voltage-sensitive sodium channel is a bell-shaped molecule with several cavities. *Nature* **409**:1047-1051.

Sawczuk A, Powers RK and Binder MD (1995) Spike frequency adaptation studies in hypoglossal motoneurons of the rat. *J. Neurophysiol*ogy **73**:1799-1810.

Scheib H, McLay I, Guex N, Clare JJ, Blaney FE, Dale TJ, Tate SN and Robertson GM (2006)

Modeling the pore structure of voltage-gated sodium channels in closed, open, and fast-inactivated conformation reveals details of site 1 toxin and local anesthetic binding. *J. Mol. Model.* **12**:813-822.

Silver KS and Soderlund DM (2005a) Action of sodium channel blocker insecticides at neuronal target sites *Pestic. Biochem. Phys.* **81**:136-143.

Silver K and Soderlund DM (2005b) State-dependent block of rat $Na_v1.4$ sodium channels expressed in *Xenopus* oocytes by pyrazoline-type insecticides. *Neurotox.* **26**:397-406.

Silver KS and Soderlund DM (2006) Differential sensitivity of rat voltage-sensitive sodium channel isoforms to pyrazoline-type insecticides. *Toxicol. Appl. Pharm.* **214**:209-217.

Silver KS and Soderlund DM (2007) Point mutations at the local anesthetic receptor site modulate the state-dependent block of rat $Na_v1.4$ sodium channels by pyrazoline-type insecticides. *Neurotox.* **28**: 655-663.

Silver KS, Nomura Y, Salgado VL and Dong K (2009) Role of the sixth transmembrane segment of domain IV of the cockroach sodium channel in the action of sodium channel-blocker insecticides. *Neurotox.* **30**:613-621.

Song W, Liu Z and Dong K (2006) Molecular basis of differential sensitivity of insect sodium channels to DCJW, a bioactive metabolite of the oxadiazine insecticide indoxacarb. *Neurotox.* **27**:237-44.

Starmer CF, Grant O and Strauss HC (1984) Mechanisms of use-dependent block of sodium channels in excitable membranes by local anesthetics. *Biophys. J.* **46**:15-27.

Stephan MM, Potts JF and Agnew WS (1994) The mI skeletal muscle sodium channel: mutation E403Q eliminates sensitivitity to tetrodotoxin but not to m-conotoxins GIIIA and GIIIB. *J. Membr. Biol.* **137**:1-8.

Tan J, Liu Z, Wang R, Huang ZY, Chen AC, Gurevitz M and Dong K (2005) Identification of amino acid residues in the insect sodium channel critical for pyrethroid binding. *Mol. Pharmacol.* **67**:513-522.

Tan J and Soderlund DM (2011) Independent and joint modulation of rat $Na_v1.6$ voltage-gated sodium channels by coexpression with the auxiliary β1 and β2 subunits. *Biochem. Biophys. Res. Comm.* **407**:788-792.

Takagi K, Hamaguchi H, Nishimatsu T and Konno T (2007) Discovery of metaflumizone, a novel semicarbazone insecticide. *Vet. Parasitol.* **150**:177-181.

Tikhonov DB and Zhorov BS (2005) Modeling P-loops domains of sodium channel: homology with potassium channels and interaction with ligands. *Biophys. J.* **88**:184-197.

Tikhonov DB and Zhorov BS (2007) Sodium channels: ionic model of slow inactivation and state-dependent drug binding. *Biophys. J.* **93**:1557-1570.

Tsurubuchi Y, Zhao X, Nagata K, Kono Y, Nishimuru K, Yeh JZ and Narahashi T (2001) Modulation of tetrodotoxin-resistant sodium channels by dihydropyrazole insecticide RH-3421 in rat dorsal root ganglion neurons. *Neurotox.* **22**:743-753.

Tsurubuchi Y and Kono Y (2003) Modulation of sodium channels by the oxadiazine insecticide indoxacarb and its *N*-decarbomethoxylated metabolite in rat dorsal root ganglion neurons. *Pest Manag. Sci.* **59**:999-1006.

Tsurubuchi Y, Kagaya Y and Kono Y (2003) Suppression of tetrodotoxin-resistant voltage-gated sodium channels by enantiomers of the oxadiazine insecticide indoxacarb in rat dorsal root ganglion neurons. *J. Pestic. Sci.* **28**:315-317.

Ulbricht W (2005) Sodium channel inactivation: molecular determinants and modulation. *Physiol. Rev.* **85**:1271-1301

van Hes R, Wellinga K and Grosscurt AC (1978) 1-Phenylcarbamoyl-2-pyrazolines: a new class of insecticides. 1. Synthesis and insecticidal properties of 3,5-Diphenyl-1-phenylcarbamoyl-2-pyrazolines. *J. Agric. Food Chem.* **26**:915-918.

Vedantham V and Cannon SC (1998) Slow inactivation does not affect the movement of the fast inactivation gate in voltage-gated Na^+ channels. *J. Gen. Physiol.* **111**:83-93.

Vilin YY, Makita N, George AL and Ruben PC (1999) Structural determinants of slow inactivation in human cardiac and skeletal muscle sodium channels. *Biophys. J.* **77**:1384-1393.

Vilin YY and Ruben PC (2001) Slow inactivation in voltage-gated sodium channels. *Cell Biochem. Biophys.* **35**:171-190.

Wang S-Y and Wang GK (1997) A mutation in segment I-S6 alters slow inactivation of sodium channels. *Biophys. J.* **72**:1633-1640.

Wang S-Y and Wang GK (1998) Point mutations in segment I-S6 render voltage-gated Na^+ channels resistant to batrachotoxin. *P. Natl. Acad. Si. USA*. **95**:2653-2658.

Wang S-Y, Nau C and Wang GK (2000) Residues in Na^+ channel D3-S6 segment modulate batrachotoxin and local anesthetic affinities. *Biophys J.* **79**:1379-1387.

Wang S-Y, Barile M and Wang GK (2001a) Disparate role of Na^+ channel D2-S6 residues in batrachotoxin and local anesthetic action. *Mol. Pharmacol.* **59**:1100-1107.

Wang S-Y, Barile M and Wang GK (2001b) A phenylalanine residue at segment D3-S6 in $Na_v1.4$ voltage-gated sodium channels is critical for pyrethroid action. *Mol. Pharmacol.* **60**:620-628.

Wang S-Y and Wang GK (2003) Voltage-gated sodium channels as primary targets of diverse lipid-soluble neurotoxins. *Cell. Signal.* **15**:151-159.

Wellinga K, Grosscurt AC and van Hes R (1977) 1-Phenylcarbamoyl-2-pyrazolines: a new class of insecticides. 1. Synthesis and insecticidal properties of 3-phenyl-1-phenylcarbamoyl-2-pyrazolines. *J. Agric. Food Chem.* **25**:987-992.

Wierenga JM, Warkentin DL, Staetz CA, Pitts DL and Dybas JA (2002). Insecticidal activity of *N*-arylalkylbenzhydrolpiperidines. *Pest Manag. Sci.* **58**:1266-1272.

Willow M and Catterall WA (1982) Inhibition of binding of [^{3}H]batrachotoxinin A 20-a-benzoate to sodium channels by the anticonvulsant drugs diphenylhydantoin and carbamazepine. *Mol. Pharmacol.* **22**:627-635.

Wing KD, Schnee ME, Sacher M and Connair M (1998) A novel oxadiazine insecticide is bioactivated in lepidopteran larvae. *Arch. Insect Biochem. Physiol.* **37**:91-103.

Wing KD, Sacher M, Kagaya Y, Tsurubuchi Y, Mulderig L, Connair M and Schnee M (2000) Bioactivation and mode of action of the oxadiazine indoxacarb in insects. *Crop Prot.* **19**:537-545.

Wing KD, Andaloro JT, McCann SF and Salgado VL (2005) Indoxacarb and the sodium channel blocker insecticides: chemistry, physiology, and biology in insects, in *Comprehensive Molecular Insect Science* (Gilbert LI, Iatrou K and Gill SS eds) pp. 30–53, Elsevier, New York.

Wu L, Nishiyama K, Hollyfield JG and Wang Q (2002) Localization of $Na_v1.5$ sodium channel protein in the mouse brain. *Neuroreport* **13**:2547-2551.

Xiao Y, Bingham J-P, Zhu W, Moczydlowski E, Liang S and Cummins TR (2008) Tarantula Huwentoxin-IV inhibits neuronal sodium channels by binding to receptor site 4 and trapping the domain II voltage sensor in the closed configuration. *J. Biol. Chem.* **283**:27300-27313.

Yu FH and Catterall WA (2003) Overview of the voltage-gated sodium channel family. *Genome Biol.* **4**:1-7.

Zhang A and Nicholson RA (1993) The dihydropyrazole RH-5529 blocks voltage-sensitive calcium channels in mammalian synaptosomes. *Pestic. Biochem. Phys.* **45**:242-247.

Zhang A and Nicholson RA (1994) RH-3421, a potent dihydropyrazole insecticide, inhibits depolarization-stimulated rises in free [Ca^{2+}] and $^{45}Ca^{2+}$ uptake in mammalian synaptosomes. *Comp. Biochem. Physiol.* **108**:307-310.

Zhang A and Nicholson RA (1996a) Dihydropyrazole insecticides: interference with depolarization-dependent phosphorylation of synapsin I and evoked release of L-glutamate in nerve-terminal preparation from mammalian brain. *Pestic. Biochem. Phys.* **54**:24-30.

Zhang A and Nicholson RA (1996b) Presynaptic inhibition of [^{3}H]nitrendipine binding and

modification of membrane properties by insecticidal dihydropyrazoles in mammalian brain. *Pestic. Biochem. Phys.* **55**:200-209.

Zhang Z, Xu Y, Dong PH, Sharma D and Chiamvimonvat N (2003) A negatively charged residue in the outer mouth of rat sodium channel determines the gating kinetics of the channel. *Am. J. Physiol*. **284**:C1247–C1254.

Zhao X, Nagata K, Marszalec W, Yeh JZ and Narahashi T (1999) Effects of the oxadiazine insecticide indoxacarb, DPX-MP062, on nicotinic acetylcholine receptors in mammalian neurons. *Neurotox*. **20**:561-570.

Zhao X, Ikeda T, Yeh JZ and Narahashi T (2003) Voltage-dependent block of sodium channels in mammalian neurons by the oxadiazine insecticide indoxacarb and its metabolite DCJW. *Neurotox*. **24**:83-96.

Zhao X, Ikeda T, Salgado VL, Yeh JZ and Narahashi T (2005) Block of two subtypes of sodium channels in cockroach neurons by indoxacarb insecticides. *Neurotox.* **26**:455-465.

CHAPTER TWO

DISCRETE MECHANISMS OF INTERMEDIATE AND SLOW INACTIVATION IN RAT $NA_V1.4$ SODIUM CHANNELS REVEALED BY COEXPRESSION OF THE β1 SUBUNIT AND SITE-DIRECTED MUTAGENESIS[1]

Introduction

Voltage-gated sodium channels are integral membrane proteins that are responsible for the transient increase in sodium ion permeability during the initial upstroke of the electrical action potential in most types of excitable cells (Hille, 2001). Sodium channels are heteromultimeric complexes containing a large (~260 kDa) pore-forming α subunit and at least one smaller (~33-38 kDa) auxiliary β subunit (Isom, 2001). The $Na_v1.4$ sodium channel isoform constitutes >90% of sodium channels expressed in adult skeletal muscle (Hirn *et al.*, 2008). Coexpression of β1 subunits with skeletal muscle or brain sodium channel α subunits increases the amplitude of the peak sodium current, accelerates its decay, and shifts the voltage dependence of fast inactivation in the direction of hyperpolarization (Isom *et al.*, 1992; Isom, 2001). Thus, the β1 subunit regulates channel expression in the plasma membrane and is an important modulator of channel function.

Sodium channel inactivation is composed of two distinct biophysical processes: fast inactivation and slow inactivation. Fast inactivation of sodium channels, which occurs within milliseconds after depolarization, is responsible for the termination and unidirectional

---

[1]This chapter has been prepared for submission to *Biochemical and Biophysical Research Communications*

propagation of action potentials and involves occlusion of the inner pore of the channel by the DIII-IV inactivation gate (Goldin, 2003). By contrast, slow inactivation of sodium channels occurs after sustained depolarization or prolonged high-frequency stimulation and is thought to regulate membrane excitability, action potential firing patterns, and spike frequency adaptation on a time scale of several seconds (Vilin and Ruben, 2001). The molecular mechanism of slow inactivation remains poorly understood, but it is both functionally and structurally distinct from fast inactivation because internal protease perfusion or mutations that disable the fast-inactivation gate do not disrupt slow inactivation (Goldin, 2003).

Multiple kinetically distinct types of slow inactivation have been identified based on the duration of the sustained depolarizations employed to induce them (Vilin and Ruben, 2001). Intermediate inactivation is typically observed following depolarizations on the order of hundreds of milliseconds (Wang *et al.*, 2000; Veldkamp *et al.*, 2000), classic slow inactivation on the order of seconds (Vilin and Ruben, 2001; O'Reilly *et al.*, 2001), and ultra-slow inactivation on the order of minutes (Todt *et al.*, 1999; Szendroedi *et al.*, 2007). Intermediate, slow, and ultra-slow inactivation may constitute a continuum of overlapping slow-inactivated states (Vilin and Ruben, 2001). However, the extent to which these kinetically distinct modalities represent functionally and structurally distinct conformations is unclear.

Here I characterize intermediate and slow inactivation in rat $Na_v1.4$ sodium channels expressed in *Xenopus* oocytes, either alone or in combination with the rat β1 subunit, and compare the effects on intermediate and slow inactivation of a DII-S6 mutation (V787C) that inhibits slow inactivation gating (O'Reilly *et al.*, 2001). My results demonstrate that intermediate inactivation and slow inactivation are distinct conformations that differ in their voltage dependence and molecular determinants.

Materials and Methods

The rat $Na_v1.4$ α subunit cDNA was a provided by R.G. Kallen (University of Pennsylvania, Philadelphia, PA) and the rat brain β1 subunit cDNA was provided by W.A. Catterall (University of Washington, Seattle, WA). The V787C mutation was introduced by site-directed mutagenesis using a commercial kit (QuikChange XL, Stratagene, La Jolla, CA). Plasmid cDNAs were linearized with restriction enzymes to provide templates from *in vitro* cRNA synthesis using a commercial kit (mMessage mMachine, Ambion, Austin, TX.). The integrity of the cRNAs was verified by electrophoresis in 1% (*w/v*) agarose-formaldehyde gels.

Oocytes were removed from female *X. laevis* (Nasco, Ft Atkinson, WI), as previously described (Smith and Soderlund, 1998). This procedure was performed in accordance with National Institutes of Health guidelines and followed a protocol that was approved by the Cornell University Institutional Animal Care and Use Committee. Stage V-VI oocytes were maintained for 24 hr at 16°C in ND-96 solution (containing in mM: 96 NaCl, 2 KCl, 1.8 $CaCl_2$, 1 $MgCl_2$, and 5 HEPES, adjusted to pH 7.6 with 2 M NaOH) supplemented with 6% horse serum (Sigma-Aldrich), 0.5% penicillin/streptomycin, and 2.5 mM sodium pyruvate (Goldin, 1992). Oocytes were injected with 50 nL of a cRNA solution containing either wildtype or mutated α subunit cRNA alone or in a 1:1 (Fig. 2.1A and Fig. 2.1B only) or 1:2 (mass ratio) mixture of α and β1 subunit cRNAs. Oocytes were incubated at 16°C in supplemented ND-96 media for 2-6 days prior to their use.

The two-electrode voltage clamp technique was employed to record sodium currents from oocytes perfused with ND-96 at room temperature (22-24°C) using an Axon Geneclamp 500B amplifier (Molecular Devices, Foster City, CA), as previously described (Smith and Soderlund, 1998). To determine the time course of entry into intermediate inactivation (I_M) and

slow inactivation (I_S), a conditioning pulse from -120 mV to 0 mV of varying duration was followed by a hyperpolarized (50-ms) to -120 mV (to fully recover fast-inactivated channels) and a test pulse (20-ms) to -10 mV. To determine the time course of recovery from I_M or I_S, a 300 msec (I_M), 60 sec (I_S; α alone) or 100 sec (I_S; α+β1) conditioning pulse from -120 mV to 0 mV was followed by a hyperpolarization to -120 mV of varying duration and a test pulse (20-ms) to -10 mV. To determine the voltage dependence of I_M or I_S, a 300-ms (I_M), 60-s (I_S; α alone), or 100-s (I_S; α+β1) conditioning pulse from -120 mV to potentials ranging from -120 mV to 0 mV in 10-mV increments was followed by a hyperpolarization (50-ms) and a test pulse (20-ms) to -10 mV. Capacitive transients and leak currents were subtracted using the P/4 method (Bezanilla and Armstrong, 1977).

Statistical analyses were performed using Prism 5.0 (GraphPad Software, La Jolla, CA). Comparisons of two or more mean values to a single control data set were assessed by one-way analysis of variance (ANOVA) followed by Dunnett's *post-hoc* analysis. Details of statistical analyses and levels of significance are provided in footnotes to the Tables.

Results

Fig. 2.1A shows representative sodium currents recorded from oocytes expressing the $Na_v1.4$ sodium channel α subunit alone (hereafter designated $Na_v1.4$ channels) and in combination with the β1 subunit ($Na_v1.4$+β1 channels). In the absence of the β1 subunit, inward sodium currents through $Na_v1.4$ channels inactivated relatively slowly during a 20-ms test pulse. Oocytes injected with a 1:1 mixture of α:β1 cRNAs gave sodium currents with biphasic kinetics of inactivation, whereas a 1:2 ratio of α:β1 cRNAs consistently gave sodium currents that inactivated rapidly and nearly completely after ~10 ms of depolarization.

Fig. 2.1B shows the development of intermediate and slow inactivation for $Na_v1.4$, $Na_v1.4+\beta1$ (1:1), and $Na_v1.4+\beta1$ (1:2) channels. $Na_v1.4$ channels displayed a substantial intermediate inactivation component after brief (<50-ms) depolarization and a more stable slow inactivation component after prolonged (>1-s) depolarization. The β1 subunit markedly inhibited the development of intermediate inactivation but impeded the development of slow inactivation only slightly. The extent of β1-subunit effects on inactivation were proportional to the ratio of α:β1 cRNAs. Fits of these data using a double-exponential function yielded two time constants (τ_1 and τ_2), reflecting entry into the intermediate and slow-inactivated state, respectively (Table 2.1). Fig. 2.1C illustrates the recovery from intermediate or slow inactivation in the absence and presence of the β1 subunit. The recovery from intermediate inactivation was fitted best using a single-exponential function, whereas curves for recovery from slow inactivation required a double-exponential function. Coexpression of the β1 subunit significantly accelerated the rate of recovery from intermediate inactivation, whereas only the first kinetic component of slow inactivation (τ_1) was significantly altered by the β1 subunit (Table 2.1). The β1 subunit paradoxically reduced the proportion of channels exhibiting faster recovery from slow inactivation (τ_1) and increased the proportion of channels exhibiting slower recovery (τ_2) (Table 2.1). Fig. 2.1D shows the voltage dependence of intermediate and slow inactivation for $Na_v1.4$ and $Na_v1.4+\beta1$ channels. Coexpression of the β1 subunit shifted the midpoint potential of intermediate and slow inactivation by 13.7 mV and 21 mV in the direction of depolarization, respectively (Table 2.2). Moreover, the slope of the voltage response for intermediate and slow inactivation was decreased in the presence of the β1 subunit.

In $Na_v1.4$ channels, mutations at residue V787 in the S6 segment of homology domain II alter slow inactivation gating. In particular, a cysteine substitution (V787C) strongly inhibits

Figure 2.1: Effects of the β1 subunit on $Na_v1.4$ sodium channel inactivation. (A) Representative sodium current traces recorded from oocytes expressing $Na_v1.4$, $Na_v1.4$+β1 (1:1 mass ratio), and $Na_v1.4$+β1 (1:2) sodium channels. Peak transient currents were scaled to emphasize the difference in decay kinetics. (B) Time course of development of intermediate and slow inactivation in sodium channels complexes shown in Panel A. Amplitudes of peak transient currents obtained using the indicated pulse protocol are plotted as a function of prepulse duration. Values are means (± SE) of 4-9 separate experiments with different oocytes. Curves were fitted to the mean values using a double-exponential decay function. (C) Time course of recovery from intermediate (squares) and slow inactivation (circles) in $Na_v1.4$ and $Na_v1.4$+β1 (1:2) channels. Amplitudes of peak transient currents obtained using the indicated pulse protocols for intermediate inactivation (300-ms prepulses) or slow inactivation (60-s or 100-s prepulses for $Na_v1.4$ or $Na_v1.4$+β1, respectively) are plotted as a function of interpulse duration. Values are means (± SE) of 4-10 separate experiments with different oocytes. Curves were fitted using a double-exponential decay function. (D) Voltage dependence of intermediate (squares) and slow inactivation (circles) in $Na_v1.4$ and $Na_v1.4$+β1 (1:2) channels. Amplitudes of peak transient currents obtained using the indicated pulse protocol for intermediate inactivation (300-ms prepulses) or slow inactivation (60-s or 100-s prepulses for $Na_v1.4$ or $Na_v1.4$+β1, respectively) are plotted as a function of prepulse potential (V_p). Values are means (± SE) of 4-11 separate experiments with different oocytes. Curves were fitted using the Boltzmann equation.

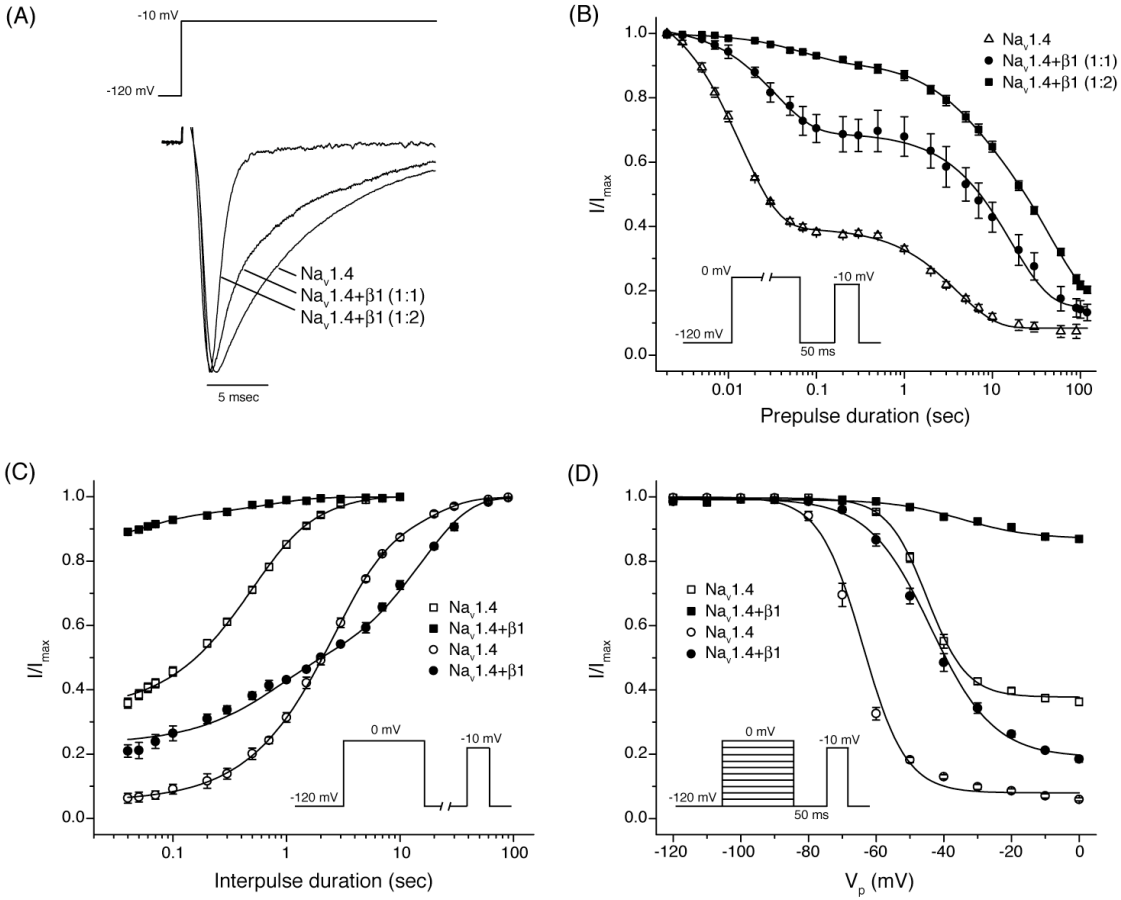
(A)
-10 mV
-120 mV
Na$_v$1.4
Na$_v$1.4+β1 (1:1)
Na$_v$1.4+β1 (1:2)
5 msec
(B)
Na$_v$1.4
Na$_v$1.4+β1 (1:1)
Na$_v$1.4+β1 (1:2)
I/I$_{max}$
0 mV
-10 mV
-120 mV
50 ms
Prepulse duration (sec)
(C)
Na$_v$1.4
Na$_v$1.4+β1
Na$_v$1.4
Na$_v$1.4+β1
I/I$_{max}$
0 mV
-10 mV
-120 mV
Interpulse duration (sec)
(D)
Na$_v$1.4
Na$_v$1.4+β1
Na$_v$1.4
Na$_v$1.4+β1
I/I$_{max}$
0 mV
-10 mV
-120 mV
50 ms
V$_p$ (mV)

slow inactivation compared to wildtype channels (O'Reilly *et al.*, 2001). I therefore examined the effects of the V787C mutation on intermediate and slow inactivation gating in $Na_v1.4$ channels. The V787C mutation did not affect the development of intermediate inactivation but significantly inhibited that of slow inactivation by slowing the rate of entry into the slow-inactivated state by two-fold (Table 2.1) and reducing the fractional extent of slow inactivation (~78% after 60 s at 0 mV) compared to wildtype (~92% after 60 s at 0 mV; Fig. 2.2A). Fig. 2.2B shows the effects of V787C on recovery from intermediate and slow inactivation. The V787C mutation did not affect recovery from intermediate inactivation but significantly reduced τ_1 for recovery from slow inactivation compared to wildtype (Table 2.1). However, the V787C mutation selectively reduced the fraction of channels exhibiting slower recovery (τ_2) from slow inactivation compared to wildtype (Table 2.1). Figure 2.2C shows the effects of the V787C mutation on the voltage dependence of intermediate and slow inactivation. Neither the midpoint potential nor the slope of the intermediate or slow inactivation curve was affected by the V787C mutation (Table 2.2), though slow inactivation was less complete at depolarized potentials (≥-50 mV) in $Na_v1.4$/V787C (~81% slow inactivation at 0 mV) compared to wildtype $Na_v1.4$ channels (~95% slow inactivation at 0 mV).

Fig. 2.3 summarizes the combined effects of the β1 subunit and V787C mutation on intermediate and slow inactivation gating. Figure 2.3A shows the time course of development of intermediate and slow inactivation in $Na_v1.4$+β1 and $Na_v1.4$/V787C+β1 channels. In the presence of β1, the V787C mutation reduced the fractional extent of intermediate inactivation but did not significantly alter the rate of entry into intermediate inactivation compared to $Na_v1.4$+β1 (Table 2.1). However, the V787C mutation reduced both the fractional extent and rate of entry into slow inactivation compared to wildtype. The small residual fraction of $Na_v1.4$/V787C+β1 channels exhibiting intermediate inactivation prevented me from

Figure 2.2: Effects of V787C on intermediate and slow inactivation gating in $Na_v1.4$ channels. (A) Time course of development of intermediate and slow inactivation. Amplitudes of peak transient currents obtained using the slow inactivation protocol described in Fig. 2.1B are plotted as a function of prepulse duration. Values are means (± SE) of 4-6 separate experiments with different oocytes. Curves were fitted to the mean values using a double-exponential decay function. (B) Time course of recovery from intermediate (squares) and slow inactivation (circles). Amplitudes of peak transient currents obtained using the slow inactivation protocol described in Fig. 2.1C are plotted as a function of interpulse duration. Values are means (± SE) of 4-10 separate experiments with different oocytes. Curves were fitted to the mean values using a double-exponential decay function. (C) Voltage dependence of intermediate (squares) and slow inactivation (circles). Amplitudes of peak transient currents obtained using the slow inactivation protocol described in Fig. 2.1D are plotted as a function of prepulse potential (V_p). Values are means (± SE) of 4-11 separate experiments with different oocytes. Curves were fitted to the mean values using the Boltzmann equation.

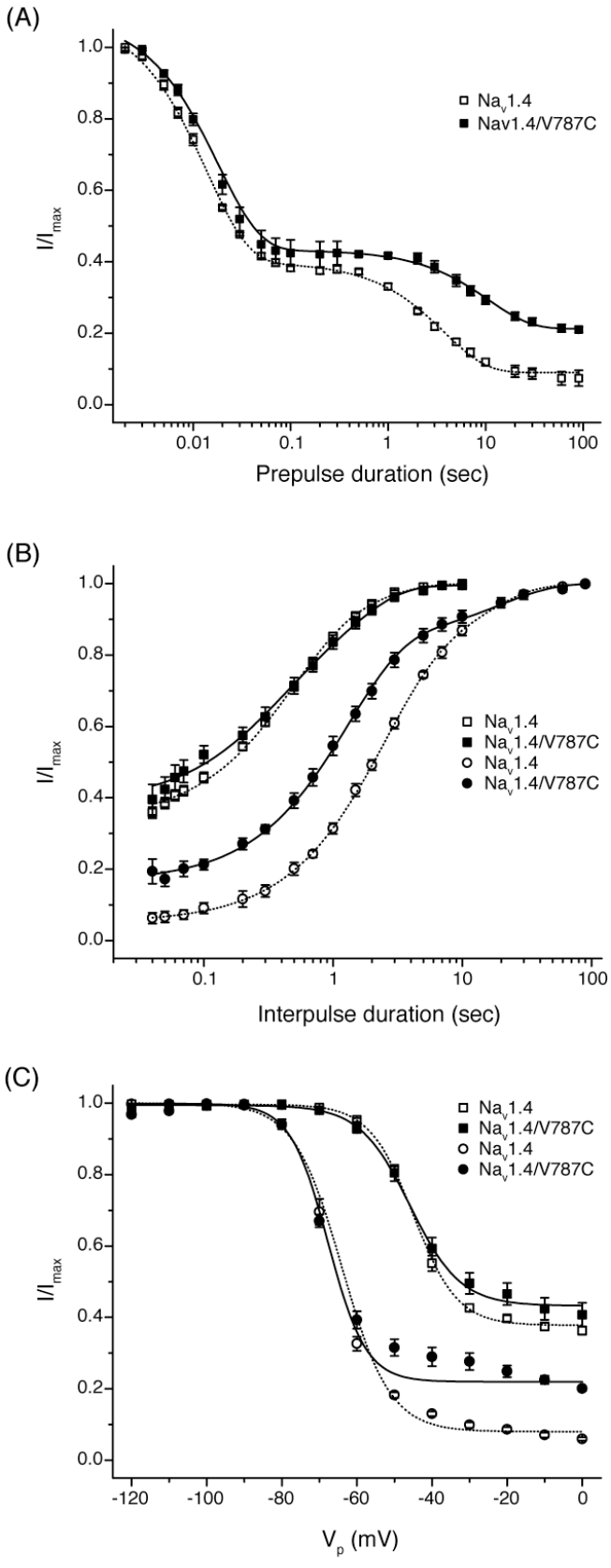
(A)
1.0
0.8
0.6
0.4
0.2
0.0
I/I_max
0.01
0.1
1
10
100
Prepulse duration (sec)
Na_v1.4
Nav1.4/V787C
(B)
1.0
0.8
0.6
0.4
0.2
0.0
I/I_max
0.1
1
10
100
Interpulse duration (sec)
Na_v1.4
Na_v1.4/V787C
Na_v1.4
Na_v1.4/V787C
(C)
1.0
0.8
0.6
0.4
0.2
0.0
I/I_max
-120
-100
-80
-60
-40
-20
0
V_p (mV)
Na_v1.4
Na_v1.4/V787C
Na_v1.4
Na_v1.4/V787C

Figure 2.3: Effects of V787C on intermediate and slow inactivation gating in $Na_v1.4+\beta1$ channels. (A) Time course of development of intermediate and slow inactivation. Amplitudes of peak transient currents obtained using the inactivation protocol described in Fig. 2.1B are plotted as a function of prepulse duration. Values are means (± SE) of 4-9 separate experiments with different oocytes. Curves were fitted to the mean values using a double-exponential decay function. (B) Time course of recovery from slow inactivation. Amplitudes of peak transient currents obtained using the slow inactivation protocol described in Fig. 2.1C are plotted as a function of interpulse duration. Values are means (± SE) of 4-6 separate experiments with different oocytes. Curves were fitted to the mean values using a double-exponential decay function. (C) Voltage dependence of slow inactivation. Amplitudes of peak transient currents obtained using the slow inactivation protocol described in Fig. 2.1D are plotted as a function of prepulse potential (V_p). Values are means (± SE) of 5-6 separate experiments with different oocytes. Curves were fitted to the mean values using the Boltzmann equation.

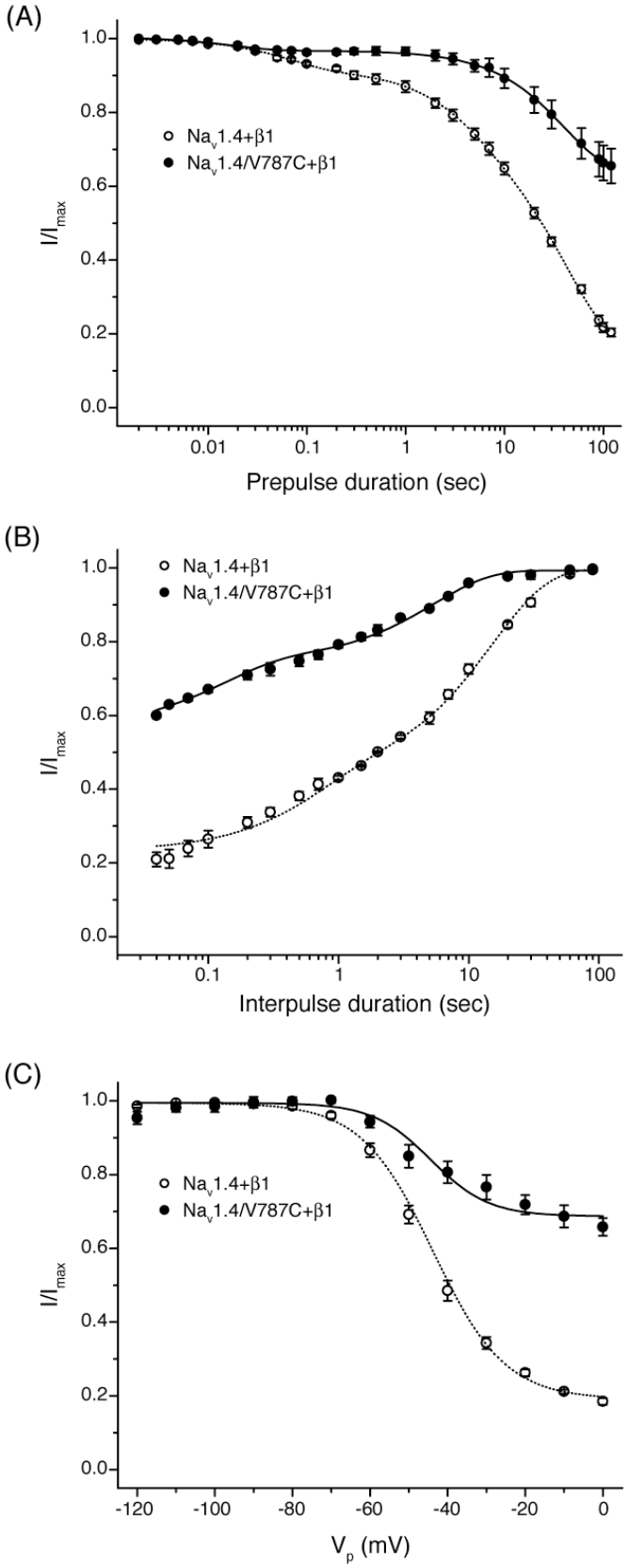
(A)
1.0
0.8
0.6
0.4
0.2
0.0
I/I_max
Na_v1.4+β1
Na_v1.4/V787C+β1
0.01
0.1
1
10
100
Prepulse duration (sec)
(B)
1.0
0.8
0.6
0.4
0.2
0.0
I/I_max
Na_v1.4+β1
Na_v1.4/V787C+β1
0.1
1
10
100
Interpulse duration (sec)
(C)
1.0
0.8
0.6
0.4
0.2
0.0
I/I_max
Na_v1.4+β1
Na_v1.4/V787C+β1
-120
-100
-80
-60
-40
-20
0
V_p (mV)

Table 2.1: Inactivation gating kinetics of wildtype and mutated $Na_v1.4$ sodium channels in the absence and presence of the β1 subunit.

Parameter	$Na_v1.4$			$Na_v1.4$+β1			$Na_v1.4$/V787C			$Na_v1.4$/V787C+β1		
	τ (ms)	(%)	[*n*]	τ (ms)	(%)	[*n*]	τ (ms)	(%)	[*n*]	τ (ms)	(%)	[n]
Entry												
I_M	14.2 ± 0.8	(63 ± 1.6)	[6]	66.0 ± 13.6*	(9 ± 0.6*)	[9]	16.7 ± 1.0	(59 ± 1.5)	[6]	36.5 ± 19.0	(4 ± 0.6*)	[5]
I_S	3957 ± 415	(32 ± 1.2)	[4]	27219 ± 2364*	(70 ± 1.7*)	[6]	8517 ± 700§	(21 ± 0.8†)	[5]	43722 ± 2022†	(34 ± 0.5*)	[4]
Recovery												
I_M	612.5± 32.2	(64 ± 1.1)	[10]	300 ± 45.5*	(11 ± 0.7*)	[5]	677.0 ± 56.1	(57 ± 1.6†)	[6]	---		
I_S	2160 ± 171	(65 ± 5.4)	[4]	328 ± 57.4*	(23 ± 1.5*)	[4]	1153 ± 108§	(62 ± 4.4)	[6]	113 ± 26.2*	(23 ± 3.5)	[6]
	11768 ± 2571	(30 ± 5.2)		13722 ± 944	(57 ± 1.4*)		14350 ± 5977	(19 ± 3.5*)		4705 ± 599*	(25 ± 1.2*)	

Time constants ($\tau_1$and τ_2) for entry and recovery from intermediate and slow inactivation.

Fractional extent (%) of intermediate- and slow-inactivation kinetic components.

Values marked with different symbols were significantly different from wildtype (* = $p < 0.001$, † = $p < 0.01$, § = $p < 0.05$; one-way ANOVA with Dunnett's *post-hoc* analysis).

Table 2.2: Voltage-dependent inactivation gating of wildtype and mutated $Na_v1.4$ sodium channels in the absence or presence of the β1 subunit[a].

State	$Na_v1.4$			$Na_v1.4$+β1			$Na_v1.4$/V787C			$Na_v1.4$/V787C+β1		
	$V_{1/2}$	*k*	[*n*]	$V_{1/2}$	*k*	[*n*]	$V_{1/2}$	*k*	[*n*]	$V_{1/2}$	*k*	[n]
Intermediate	-45.0 ± 0.3	5.7 ± 0.3	[11]	-31.3 ± 4.4*	12.3 ± 3.1*	[6]	-45.1 ± 0.8	7 ± 0.7	[7]	---		
Slow	-65.9 ± 0.5	6 ± 0.5	[4]	-44.9 ± 0.7*	9.3 ± 0.6§	[6]	-67.5 ± 1.2	6.4 ± 1.1	[6]	-41.4 ± 3.4	10.4 ± 3	[5]

[a] Values calculated from fits of the data from indicated number of individual experiments to the Boltzmann equation; $V_{1/2}$, midpoint potential (mV) for voltage-dependent inactivation; *k*, slope factor.

Values marked with different symbols were significantly different from wildtype (* = $p < 0.001$, † = $p < 0.01$, § = $p < 0.05$; one-way ANOVA with Dunnett's *post-hoc* analysis)

characterizing further the combined effects of the V787C mutation and β1 subunit on the time course of recovery from and voltage dependence of this state. Figure 2.3B shows the time course of recovery from slow inactivation for $Na_v1.4$+β1 and $Na_v1.4$/V787C+β1 channels. $Na_v1.4$/V787C+β1 channels recovered from slow inactivation faster than $Na_v1.4$+β1 channels (Table 2.1). In the presence of β1, the V787C mutation reduced only the proportion of channels recovering from slow inactivation with slower kinetics (τ_2), as was also observed in the absence of the β1 subunit. Fig. 2.3C shows the voltage dependence of slow inactivation in $Na_v1.4$+β1 and $Na_v1.4$/V787C+β1 channels. There was a significantly reduced steady-state probability of slow inactivation in $Na_v1.4$/V787C+β1 (~35% slow inactivation at 0 mV) compared to $Na_v1.4$+β1 (~82% slow inactivation at 0 mV). However, the V787C mutation did not significantly affect the midpoint potential or steepness of the voltage response in the presence of the β1 subunit compared to $Na_v1.4$+β1 channels (Table 2.2).

Discussion

Sodium channel α subunits from rat muscle and brain exhibit altered inactivation gating when expressed alone in *Xenopus* oocytes in the absence of the β1 subunit (Balser *et al.*, 1996; Tan and Soderlund, 2011). These channels give macroscopic sodium currents that decay slowly and display a prominent intermediate inactivation component of slow inactivation after very brief (<50-ms) depolarization. Coexpression with the β1 subunit both accelerates sodium current decay and markedly inhibits intermediate inactivation. Whether these concurrent β1-subunit effects involve a single mechanism is unknown.

In the absence of the β1 subunit, the development of slow inactivation in $Na_v1.4$ sodium channels was biphasic. Using diagnostic prepulse durations (*i.e.* 300 ms or 60 s) that favored

either intermediate or slow inactivation revealed that these two states also differed in their voltage dependence. This finding agrees with previous studies of $Na_v1.4$ channels expressed in oocytes (Nuss *et al.*, 1996), which showed that the midpoint potential of steady-state inactivation is shifted in the direction of hyperpolarization by increasing prepulse duration. Coexpression with β1 markedly reduced the fractional extent of the intermediate inactivation component but only modestly inhibited that of the slow inactivation component. Consistent with these results, previous studies have shown that intermediate inactivation in rat $Na_v1.4$ channels is largely eliminated by coexpression of the β1 subunit in oocytes (Balser *et al.*, 1996; Bénitah *et al.*, 1999), whereas slow inactivation is only mildly impeded by β1-subunit coexpression with rat $Na_v1.4$ (Webb *et al.*, 2009) and human $Na_v1.2$ channels (Xu *et al.*, 2007) in mammalian cells. In contrast, the β1 subunit enhances the steady-state probability of slow inactivation in human $Na_v1.4$ channels expressed in oocytes (Vilin *et al.*, 1999). Thus, my data suggest that the β1 subunit exerts opposite effects on slow inactivation gating on orthologous rat and human sodium channels. My data also indicate that the effects of the β1 subunit on the fractional extent of inactivation are independent of its effects on inactivation kinetics. These findings are consistent with other studies in oocytes suggesting that the molecular structures regulating development and recovery kinetics of slow inactivation are different from those controlling the fractional extent of slow inactivation (Vilin *et al.*, 2001).

Mutations at position V787 in the S6 segment of homology domain II either enhance or inhibit slow inactivation (O'Reilly *et al.*, 2001), thus implicating a role for this S6 segment in the molecular mechanism of slow inactivation. The V787C mutation selectively inhibited slow inactivation without affecting intermediate inactivation gating or kinetics. These results imply that intermediate and slow inactivation are functionally distinct biophysical processes with unique structural determinants. The effects of V787C on the fractional extent and kinetics of

slow inactivation agree with previous reports (O'Reilly *et al.*, 2001). However, these studies also reported a mutation-induced depolarizing shift in the voltage dependence of steady-state slow inactivation compared to wildtype, but this effect was not evident in my assays in either the absence or presence of the β1 subunit. This discrepancy may reflect differences in the choice of expression system (HEK293 cells *vs*. oocytes) or in the pulse protocols employed.

I examined the combined effects of β1-subunit coexpression and the V787C mutation on intermediate- and slow-inactivation gating to provide further insight into the independence of these two gating processes. In the presence of the β1 subunit, the V787C mutation impaired slow inactivation despite the virtual lack of intermediate inactivation observed with $Na_v1.4$/V787C+β1 channels. These results provide further evidence that the V787C mutation disrupts slow inactivation by a mechanism that is independent of the β1-subunit induced inhibition of intermediate inactivation.

Previous reports (Vilin and Ruben, 2001) have proposed that intermediate, slow, and ultra-slow inactivation may constitute a continuum of 'slow'-inactivated conformations, but the structural distinction between these states is unresolved. Various amino acid substitutions in the outer-pore forming P-loops modulate intermediate (Kambouris *et al.*, 1998; Chen *et al.*, 2000), slow (Vilin *et al.*, 2001), or ultra-slow inactivation (Todt *et al.*, 1999), thereby implicating conformational changes in the outer pore in 'slow'-inactivated states. Structural rearrangement in the outer pore is also implicated in the molecular pathway for intermediate inactivation by studies showing that intermediate inactivation is potentiated by lowering the extracellular Na^+ concentration (Bénitah *et al.*, 1999; Chen *et al.*, 2000) and is associated with disulfide bond formation between pairs of engineered cysteine residues within the outer pore (Bénitah *et al.*, 1999). The location of V787 suggests that classic slow inactivation also involves structural rearrangement(s) in the channel lumen inside the selectivity filter. Experiments using the

substituted-cysteine accessibility method show that V787C is only accessible to covalent modification by the sulfhydryl-reactive agent methanethiosulfonate ethylammonium under experimental conditions that promote slow inactivation (O'Reilly *et al.*, 2001). These data indicate that slow inactivation involves molecular rearrangement(s) at or near the V787 position.

Studying the mechanistic and structural relationship between these inactivated states is of interest not only in terms of understanding channel function but also because they may represent pharmacologically distinct conformations. The sodium channel local anesthetic (LA) receptor has a relatively higher affinity for lidocaine in the intermediate-inactivated state compared to slow-inactivated channels (Kambouris *et al.*, 1998). Conversely, sodium channel inhibitor (SCI) insecticides, which also bind at the LA receptor (Silver and Soderlund, 2007), preferentially interact with slow-inactivated sodium channels (Silver and Soderlund, 2005).

References

Balser JR, Nuss HB, Romashko DN, Marban E and Tomaselli GF (1996) Functional consequences of lidocaine binding to slow-inactivated sodium channels. *J. Gen. Physiol.* **107**:643-658.

Bénitah J-P, Chen Z, Balser JR, Tomaselli GF and Marbán E (1999) Molecular dynamics of the sodium channel pore vary with gating: interactions between P-segment motions and inactivation. *J Neurosci.* **19**;1577-1585.

Bezanilla F and Armstrong CM (1977) Inactivation of the sodium channel. *J. Gen. Physiol.* **70**:549-566

Chen Z,. Ong B-H, Kambouris NG, Marbán E, Tomaselli GF and Balser JR (2000) Lidocaine induces a slow inactivated state in rat skeletal muscle sodium channels. *J Physiol.* **524**:37-49.

Goldin AL (1992) Maintenance of *Xenopus laevis* and oocyte injection. *Methods Enzymol*. **207**:266-297.

Goldin AL (2003) Mechanisms of sodium channel inactivation. *Curr. Opin*. *Neurobiol.* 13:284-290.

Hille B (2001) Ion Channels of Excitable Membranes, Sinauer, Sunderland, MA.

Hirn C, Shapovalov G, Petermann O, Roulet E and Ruegg UT (2008) $Na_v1.4$ deregulation in dystrophic skeletal muscle leads to Na^+ overload and enhanced cell death. *J. Gen. Physiol*. **132**:199-208.

Isom LL (2001) Sodium channel β subunits: anything but auxiliary. *Neuroscientist* **7**:42-54.

Isom LL, De Jongh KS, Patton DE, Reber BFX, Offord J, Charbonneau H, Walsh K, Goldin AL and Catterall WA (1992) Primary structure and functional expression of the β1 subunit of the rat brain sodium channel. *Science* **256**:839-842.

Kambouris NG, Hastings LA, Stepanovic S, Marbán E, Tomaselli GF and Balser JR (1998) Mechanistic link between lidocaine block and inactivation probed by outer pore mutations in the rat μ1 skeletal muscle sodium channel. *J. Physiol*. **512**:693-705.

Nuss HB, Balser JR, Orias DW, Lawrence JH, Tomaselli GF and Marban E (1996) Coupling between fast and slow inactivation revealed by analysis of a point mutation (F1304Q) in μ1 rat skeletal muscle sodium channels. *J. Physiol.* **494**:411-429.

O'Reilly JP, Wang S-Y and Wang GK (2001) Residue-specific effects on slow inactivation at V787 in D2-S6 of $Na_v1.4$ sodium channels. *Biophys. J.* **81**:2100-2111.

Silver KS and Soderlund DM (2005) State-dependent block of rat $Na_v1.4$ sodium channels expressed in *Xenopus* oocytes by pyrazoline-type insecticides. *Neurotox*. **26**:397-406.

Silver KS and Soderlund DM (2007) Point mutations at the local anesthetic receptor site modulate the state-dependent block of rat $Na_v1.4$ sodium channels by pyrazoline-type insecticides. *Neurotox.* **28**:655-663.

Smith TJ and Soderlund DM (1998)Action of the pyrethroid insecticide cypermethrin on rat brain IIa sodium channels expressed in *Xenopus* oocytes. *Neurotox.* **19**:823-832.

Szendroedi J, Sandtner W, Zarrabi T, Zebedin E, Hilber K, Dudley SC, Fozzard HA and Todt H (2007) Speeding the recovery from ultraslow inactivation of voltage-gated Na^+ channels by metal ion binding to the selectivity filter: a foot-*on*-the door? *Biophys. J.* **93**:4209-4224.

Tan J and Soderlund DM (2011) Independent and joint modulation of rat $Na_v1.6$ voltage-gated sodium channels by coexpression with the auxiliary β1 and β2 subunits. *Biochem. Biophys. Res. Commun.* **407**:788-792

Todt H, Dudley SC, Kyle JW, French RJ and Fozzard HA (1999) Ultra-slow inactivation in μ1 Na^+ channels is produced by a structural rearrangement of the outer vestibule. *Biophys. J.* **76**:1335-1345.

Veldkamp MW, Viswanathan PC, Bezzina C, Baartscheer A, Wilde AAM and Balser JR (2000) Two distinct congenital arrhythmias evoked by a multidysfunctional Na^+ channel. *Circ. Res.* **86**:e91-e97.

Vilin YY, Fujimoto E and Ruben PC (2001) A single residue differentiates between cardiac and skeletal muscle Na^+ channel slow inactivation. *Biophys. J.* **80**:2221-2230.

Vilin YY, Makita N, George AL Jr and Ruben PC (1999) Structural determinants of slow inactivation in human cardiac and skeletal muscle sodium channels. *Biophys. J.* **77**:1384-1393.

Vilin YY and Ruben PC (2001) Slow inactivation in voltage-gated sodium channels. *Cell Biochem. Biophys.* **35**:171-190.

Wang DW, Makita N, Kitabatake A, Balser JR and George AL Jr (2000) Enhanced Na^+ channel intermediate inactivation in Brugada Syndrome. *Circ. Res.* **87**:e37-e43.

Webb J, Wu F and Cannon SC (2009) Slow inactivation of the NaV1.4 sodium channel in mammalian cells is impeded by co-expression of the β1 subunit. *Eur. J. Physiol.* **457**:1253-1263.

Xu R, Thomas EA, Gazina EV, Richards KL, Quick M, Wallace RH, Harkin LA, Heron SE, Berkovic SF, Scheffer IE, Mulley JC and Petrou S (2007) Generalized epilepsy with febrile seizures plus-associated sodium channel β1 subunit mutations severly reduce beta subunit-mediated modulation of sodium channel function. *J. Neurosci*. **148**:164-174.

CHAPTER THREE

ROLE OF THE LOCAL ANESTHETIC RECEPTOR IN THE STATE-DEPENDENT INHIBITION OF VOLTAGE-GATED SODUM CHANNELS BY METAFLUMIZONE[1,2]

Introduction

Sodium channel inhibitor (SCI) drugs represent a structurally diverse group of important therapeutic agents that include local anesthetics, class I anticonvulsants, and class I antiarrhythmics that have been in clinical use for well over a century. Elucidating the molecular details of their action on sodium channels remains an important cornerstone of modern drug discovery efforts. Voltage-gated sodium channels are also the molecular targets for SCI insecticides, a structurally diverse group of insect control agents of increasing importance (Wing *et al.*, 2005; Silver and Soderlund, 2005a). Metaflumizone (Fig. 3.1A), a new drug to control fleas on domesticated animals, is the first SCI insecticide in the animal health market (Salgado and Hayashi, 2007). Indoxacarb (Fig. 3.1C), the first and only other commercialized SCI insecticide, is a proinsecticide that is converted in insects to its active metabolite, DCJW (Fig. 3.1B) (Wing *et al.*, 2005). Other SCI insecticides include dihydropyrazoles (e.g. RH-3421 and RH-4841; Fig. 3.1B) and arylalkylbenzhydrolpiperidines (BZPs) that were not commercialized because of the unacceptable toxic risks they pose to mammals (Payne *et al.*, 1998; Silver and

---

[1]Presented at the 50th Annual Meeting of the Society of Toxicology, Washington D.C., March 6-10, 2011.

[2]This chapter has been prepared for submission to *Molecular Pharmacology*

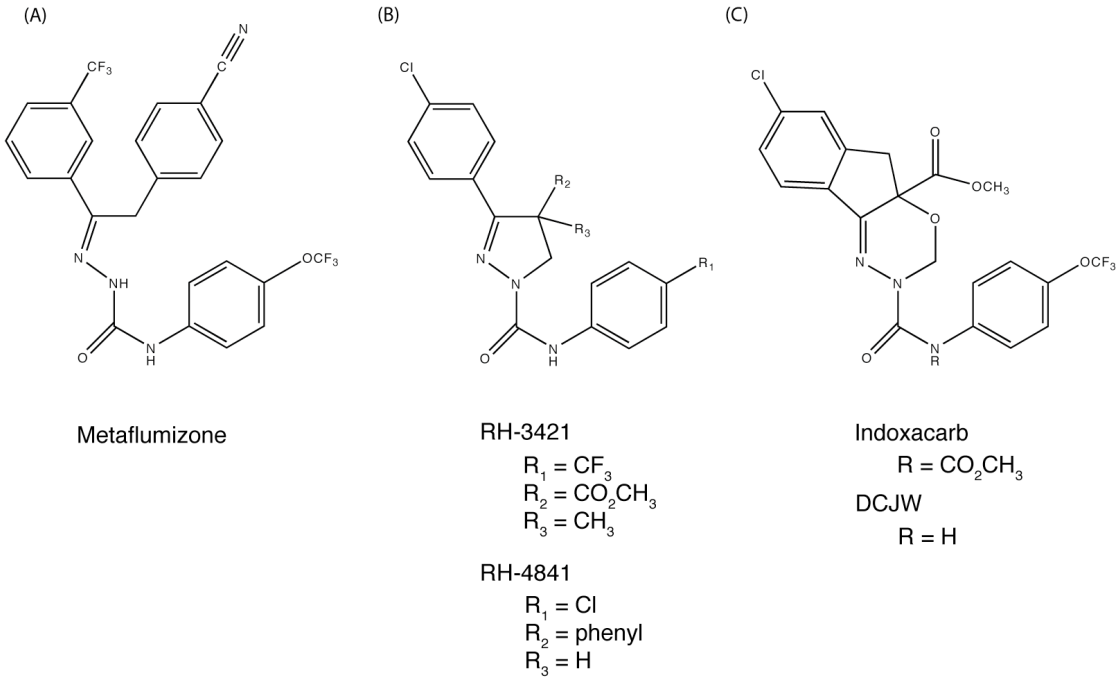

Figure 3.1: Structures of SCI insecticides. (A) Metaflumizone. (B) RH-4841 and RH-3421. (C) Indoxacarb and DCJW.

Soderlund, 2005a). Despite the structural diversity of SCI insecticides, they are functionally unified by a common and novel mode of insecticidal action.

SCI insecticides typically exhibit little or no effect on sodium channels under experimental conditions that promote resting, activated, or fast-inactivated channel conformations, but they cause a slowly-developing inhibition of sodium currents under experimental conditions that promote slow inactivation of channels. Moreover, SCI insecticides cause negative shifts in the voltage dependence of slow inactivation and retard the rate at which channels become available for activation after prolonged depolarization (Salgado, 1992, Zhao *et al.*, 2003, Silver and Soderlund, 2005b, 2007). These properties have been interpreted as evidence that SCI insecticides selectively bind to and stabilize slow-inactivated channel conformation(s). The state-dependent action of SCI insecticides is similar to that of SCI drugs that typically exhibit a preferential interaction with activated or inactivated channels (Ragsdale *et al.*, 1996). Unlike therapeutic drugs, the interactions between insecticides and channels that confer inhibition are very slow, on the order of several minutes. Such slow kinetics preclude the direct inhibition of channels in transient conformations, such as the activated or fast-inactivated states. Therefore, SCI insecticides do not exhibit any frequency- or use-dependent inhibition in response to repetitive stimulation (Silver and Soderlund, 2005b; Salgado and Hayashi, 2007), a hallmark of many SCI drugs.

SCI insecticides share common molecular determinants of binding and action with therapeutic SCI drugs, which bind at the "local anesthetic (LA) receptor" in the inner pore, involving residues in the S6 segments of homology domains I, III and IV (for review, see Mike and Lukacs, 2010). Site-directed mutagenesis experiments (Silver and Soderlund, 2007) indicate that two residues (F1579 and Y1586) in DIV-S6 of rat $Na_v1.4$ sodium channels, identified

previously as critical determinants of state-dependent drug block, also are important determinants of SCI insecticide action. Substitution of alanine for either F1579 or Y1586 significantly reduces use-dependent inhibition by SCI drugs (Ragsdale *et al.*, 1996; Wang *et al.*, 1998; Wagner *et al.*, 2001). By contrast, the extent of inhibition by SCI insecticides is reduced by the F1579A mutation but paradoxically increased by the Y1586A mutation (Silver and Soderlund, 2007). This result implies that Y1586 limits high-affinity interactions of SCI insecticides and that other molecular determinants for the binding of these compounds must exist.

SCI insecticides such as indoxacarb and RH-3421 are conformationally-restricted, nearly planar molecules (Wellinga *et al.*, 1977; Grosscurt *et al.*, 1979; Hasan *et al.*, 1996). Metaflumizone, which lacks the central heterocyclic moiety of other SCI insecticides, is a conformationally flexible molecule that may participate in binding interactions at the LA receptor that are not available to other SCI insecticides. The present study was designed to characterize the action of metaflumizone on cloned rat $Na_v1.4$ sodium channels expressed in *Xenopus laevis* oocytes and test the hypothesis that metaflumizone shares the DIV-S6 binding determinants identified for other SCI insecticides. I report here that metaflumizone is an effective state-dependent inhibitor of $Na_v1.4$ channels and show that replacing alanine at F1579 or Y1586 modulates metaflumizone sensitivity in a manner that is consistent with other SCI insecticides (Silver and Soderlund, 2007). However, my data suggest that metaflumizone may bind to sodium channels without inhibiting them in a manner that is distinct from other compounds in this insecticide class.

Materials and Methods

The cloned rat $Na_v1.4$ cDNA (Kallen *et al.*, 1990) was obtained from R.G. Kallen (University of Pennsylvania, Philadelphia, PA) and the rat β1 subunit cDNA was obtained from W.A. Catterall (University of Washington, Seattle, WA). The F1579A and Y1586A mutations were introduced by site-directed mutagenesis as described previously (Silver and Soderlund, 2007) using a commercial kit (QuikChange XL, Stratagene, La Jolla, CA). Plasmid cDNAs were digested with restriction enzymes to provide linear templates for wildtype and mutated cRNA synthesis *in vitro* using a commercial kit (mMessage mMachine, Ambion, Austin, TX). The integrity of the cRNAs was determined by electrophoresis in 1% agarose-formaldehyde gels.

Oocytes from female *Xenopus laevis* frogs (Nasco, Ft. Atkinson, WI) were washed with Ca^{2+}-free OR-2^+ (containing in mM: 82.5 NaCl, 2 KCl, 1 $MgCl_2$, 5 HEPES, adjusted pH to 7.6 with NaOH) before being digested in 1 mg/mL collagenase (type 1A, Sigma-Aldrich, St. Louis, MO) for approximately 60 min to loosen the surrounding follicle cells. Healthy stage V and VI oocytes were isolated and manually defolliculated with a pair of fine-tipped surgical forceps before being incubated overnight at 16° C in ND-96 (containing in mM: 96 NaCl, 2 KCl, 1.8 CaCl2, 1 MgCl2, and 5 HEPES, adjusted to pH 7.6 with NaOH) solution supplemented with 6% horse serum (Sigma-Aldrich), 0.5% penicillin/streptomycin and 2.5 mM sodium pyruvate (Goldin, 1992). Oocytes were pressure-injected with 50 nL of a 2:1 (mass ratio) mixture of β1 and wildtype or mutated rat $Na_v1.4$ channel α subunit cRNA. The α-subunit concentration ranged from 10 to 50 ng/mL, which yielded sodium current amplitudes between -10 and -30 μA. The injected oocytes were maintained at 16° C in supplemented ND-96 media for 2-5 days before use.

Electrophysiological experiments were conducted in disposable chambers fabricated from

0.25 in. Plexiglass and a glass coverslip sealed together with ethyl cyanoacrylate as described elsewhere (Smith and Soderlund, 1998). Recording microelectrodes were pulled from borosilicate glass capillaries (1.0 mm *o.d.*, 0.78 mm *i.d.*; World Precision Instruments Inc.) on a P-87 Flaming Brown puller (Sutter Instruments, Novato, CA) and filled with 3 M KCl. Filled electrodes had resistances that ranged between 0.5 and 0.7 MΩ when submerged in ND-96 saline. The two-microelectrode voltage-clamp technique was used to record macroscopic sodium currents at room temperature (22-24° C) using a Geneclamp 500B (Molecular Devices, Foster City, CA) amplifier and pClamp 10.2 software (Molecular Devices, Burlingame, CA). Currents were filtered at 5 kHz with a low-pass 4-pole Bessel filter and digitized at 50 kHz with a Digidata 1320A (Molecular Devices). Capacitive transient currents were subtracted using the P/N (N = 4) method (Bezanilla and Armstrong, 1977). Electrophysiological recordings were initiated at least 5 min after clamping oocytes at a hyperpolarized membrane potential of -120 mV. Oocytes were perfused with ND-96 saline at about 0.45 ml/min using a custom-fabricated disposable passive capillary perfusion system similar to that described previously (Tatebayashi and Narahashi, 1994). The entire bath volume could be replaced in ~1 min. All perfusion capillaries, recording chambers and microelectrodes were used only once to prevent potential cross-contamination between experiments.

The voltage dependence of activation was determined by clamping oocytes at a membrane potential of -120 mV and recording sodium currents during 20-ms depolarizing test pulses ranging from -80 mV to 40 mV in 10-mV increments. To determine the voltage dependence of steady-state fast inactivation, oocytes were clamped at a holding potential of -120 mV and stimulated with a 200-ms conditioning prepulse to potentials ranging from -100 mV to 0 mV in 10-mV increments followed by a 20-ms test pulse to -10 mV. The voltage dependence of slow inactivation was determined by clamping oocytes at -120 mV and giving a 100-s

conditioning prepulse to potentials ranging from -90 mV to 0 mV in 10-mV increments followed by a 50-ms hyperpolarization to -120 mV to completely recover fast-inactivated channels and then a 20-ms test pulse to -10 mV ($Na_v1.4$ and $Na_v1.4$/F1579A) or 0 mV ($Na_v1.4$/Y1586A). To avoid potential time-dependent cumulative effects, oocytes were held at -120 mV for >2 min between conditioning pulses. The effects of metaflumizone on activation and inactivation gating was assessed after 15 min of metaflumizone perfusion at a holding potential of -120 mV while sodium currents were measured every minute with a 20-ms test depolarization to -10 mV. The time course of inhibition by the insecticides was studied by clamping oocytes at a holding potential of -30 mV ($Na_v1.4$), -35 mV ($Na_v1.4$/F1579A) or -50 mV ($Na_v1.4$/Y1586A) and giving a 20-ms test depolarization to -10 mV that was preceded by a 2-s hyperpolarization to -120 mV that recovered a fraction (~45%) of sodium channels, thus enabling a sodium current of adequate amplitude to be recorded (Salgado, 1992; Silver and Soderlund, 2005b, 2007). For determinations of use dependence, oocytes were clamped at a holding potential of -120 mV and stimulated at 20 Hz with trains of 0-20 brief (25-ms) conditioning depolarizing pulses to -50 mV, separated by 25-ms interpulse intervals, followed by a 20-ms test pulse to -10 mV. Pulse trains were separated by a 20-s interval at -120 mV to avoid possible time-dependent cumulative effects (Ragsdale *et al.*, 1996). Experiments in the presence of lidocaine were initiated after 10 min of lidocaine perfusion at a holding potential of -120 mV. For experiments characterizing the effects of SCI insecticides on use-dependent lidocaine inhibition, oocytes were clamped at -120 mV and perfused with a given insecticide for 15 min prior to changing the bath perfusate to one containing both the insecticide and lidocaine together for 10 min before pulse protocols were initiated. Additional details of voltage protocols used are provided in the figure legends.

Metaflumizone and lidocaine were purchased from Sigma-Aldrich and indoxacarb was purchased from ChemService (West Chester, PA). RH-4841 and RH-3421 were provided by G.

Carlson (Rohm and Haas Company, Spring House, PA) and DCJW was provided by K. Wing (DuPont Agricultural Product, Newark, DE). Stock solutions of insecticides (10 mM) and lidocaine (200 mM) were prepared in dimethyl sulfoxide (DMSO) and diluted in ND-96 just prior to use to a final concentration of 10 μM (insecticides) and 200 μM (lidocaine). The final DMSO concentration never exceeded 0.2% *v/v*, a concentration that has no effect on sodium currents.

Data analysis was performed using Origin 8.1 (OriginLab Corp., Northampton, MA). Conductance-voltage and sodium channel inactivation data was fitted using the Boltzmann equation [$y = (A_1\text{-}A_2)/\{1 + \exp[(V\text{-}V_{1/2})/k]\} + A_2$] where $V_{1/2}$ is the midpoint of the curve, k is the slope factor, and A_1 and A_2 are the maximum and minimum values in the fit, respectively. Time constants for sodium-current inhibition were obtained by fitting the mean data with a single-exponential decay function [$y = A_1 * \exp(-x/\tau_1) + y_0$], where x is time, τ_1 is the time constant, and y_0 is the non-inactivating component. All fitted data are expressed as means and standard errors. Concentration-effect curves were fitted to the Hill equation [$y = V_{max}(x^n/(k^n + x^n))$].

Statistical analyses were performed using Prism 5.0 (GraphPad Software, La Jolla, CA). Statistical significance between two means was assessed using either paired or unpaired Student's *t*-test, depending on the design of the experiment. Statistical significance of two or more mean values from a single control data set was assessed using one-way analysis of variance (ANOVA) followed by Dunnett's *post-hoc* analysis. Differences were considered statistically significant when $p < 0.05$.

Results

I first characterized the effects of 10 μM metaflumizone, the highest concentration

achievable in ND-96 saline, on the voltage-dependent gating of wildtype $Na_v1.4$ sodium channels (Fig. 3.2). The statistical analyses of these data are summarized in Table 3.1. Perfusion of metaflumizone for 15 min at a holding potential of -120 mV caused a 4.7 mV depolarizing shift in the midpoint potential ($V_{1/2}$) of activation, but did not affect the slope of the voltage response (Fig. 3.2A; Table 3.1). Consequently, the amplitude of sodium currents measured at sub-maximal activation potentials were reduced in the presence of metaflumizone compared to the controls. At test potentials of -30 mV and -20 mV, the reduction in the amplitude of the sodium current by metaflumizone was statistically significant. Metaflumizone had no effect on the voltage dependence of steady-state fast inactivation (Fig. 3.2B). However, slow inactivation was more complete in the presence of metaflumizone (~95% inactivation at 0 mV; Fig. 3.2C) compared to the control (~82% inactivation at 0 mV). Moreover, metaflumizone significantly shifted the midpoint potential for slow inactivation by 3.5 mV in the direction of hyperpolarization and also significantly increased the slope of the voltage response compared to the control.

SCI insecticides selectively inhibit voltage-gated sodium channels at depolarized membrane potentials that promote slow inactivation (Salgado, 1990, 1992; Silver and Soderlund, 2005b). Fig. 3.3 illustrates the inhibition of sodium currents through wildtype $Na_v1.4$ sodium channels by 10 μM metaflumizone (Fig. 3.3A), RH-4841 (Fig. 3.3B) and DCJW (Fig. 3.3C) after 15 min at a holding potential of -30 mV. The time course of sodium current inhibition by SCI insecticides is illustrated is Fig. 3.3D. Inhibition by metaflumizone and RH-4841 increased progressively over the 15 min of exposure, whereas inhibition by DCJW reached an apparent steady state after ~6 min of perfusion. The fractional inhibition of sodium currents through wildtype channels after 15 min of insecticide perfusion is summarized in Table 3.2. Fitting the time course of SCI insecticide inhibition with a first-order exponential decay function yielded

Figure 3.2: Effects of metaflumizone (10 μM) on the voltage dependence of activation, steady-state fast inactivation and slow inactivation. (A) Conductance-voltage plots of activation measured upon depolarization from -120 mV to test potentials ranging from -80 mV to 40 mV. Peak sodium currents were transformed to conductances (G) using the equation $G = I_{Na}/(V_{test} - V_{rev})$, where I_{Na} is the peak sodium current during test depolarization (V), and V_{rev} is the sodium current reversal potential. Data were normalized to maximum peak conductance (G_{Max}) and fitted using the Boltzmann equation; values are means ± SE from 5 oocytes. The asterisks indicate test potentials of sub-maximal activation at which the measured sodium current amplitude in the presence of metaflumizone was significantly (*, $p < 0.05$; **, $p < 0.001$; paired t-test) different from the control. (B) Voltage dependence of steady-state fast inactivation; conditioning pulses (200 ms) from -120 mV to potentials ranging from -100 mV to 0 mV were followed immediately by 20-ms test pulses to -10 mV. Peak sodium currents were normalized to the maximum current obtained during the inactivation protocol for that oocyte and plotted versus the conditioning potential; curves were fitted using the Boltzmann equation; values are means ± SE from 5 oocytes. (C) Voltage dependence of slow inactivation; amplitudes of peak transient currents measured during a 20-ms depolarization to -10 mV following a 100-s conditioning prepulse from a holding potential (V_{hold}) of -120 mV to potentials ranging from -90 to 0 mV and a 50-ms hyperpolarization to -120 mV were normalized to the maximum current obtained during the inactivation protocol for that oocyte and plotted as a function of the conditioning potential. Values are means ± SE from 6 (control) or 5 (metaflumizone) separate experiments in different oocytes; curves are fitted to the Boltzmann equation.

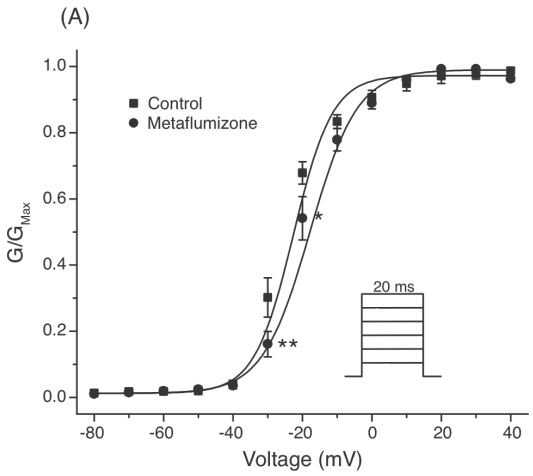
(A)
Control
Metaflumizone
G/G_Max
Voltage (mV)
20 ms
*
**

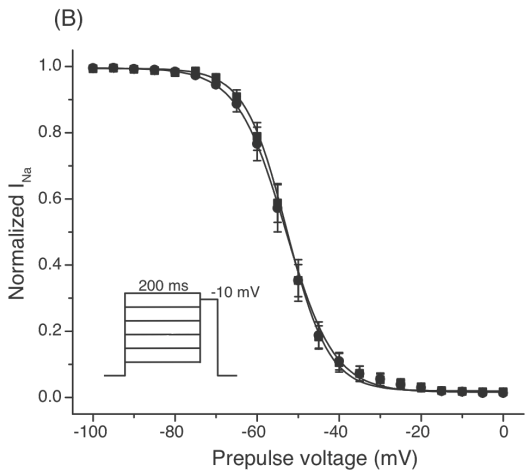
(B)
Normalized I_Na
Prepulse voltage (mV)
200 ms
-10 mV

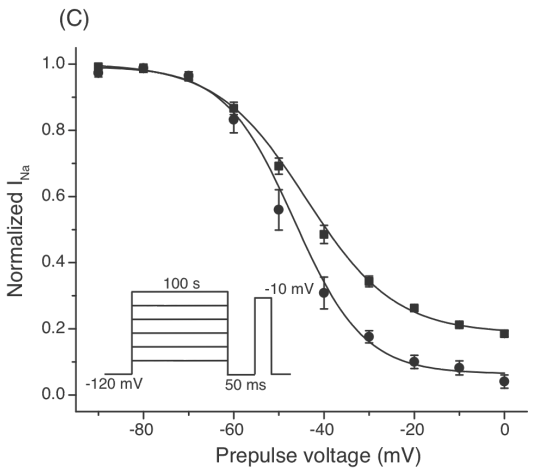
(C)
Normalized I_Na
Prepulse voltage (mV)
100 s
-10 mV
-120 mV
50 ms

Table 3.1: Activation and inactivation gating parameters of $Na_v1.4$ channels in the absence or presence of metaflumizone[a].

Condition	Activation			Fast Inactivation			Slow Inactivation		
	$V_{1/2}$	*k*	*n*	$V_{1/2}$	*k*	*n*	$V_{1/2}$	*k*	*n*
Control	-24.9 ± 0.7	5.9 ± 0.6	5	-53.3 ± 0.2	5.0 ± 0.2	5	-44.9 ± 0.7	9.3 ± 0.6	6
Metaflumizone	-20.2 ± 0.7[*]	6.4 ± 0.6	5	-53.5 ± 0.2	5.2 ± 0.2	5	-48.4 ± 0.9[†]	7.5 ± 0.8[†]	5

[a] Values calculated from fits of data obtained in the absence or presence of 10 μM metaflumizone (Fig. 3.2) to the Boltzmann equation; $V_{1/2}$, midpoint potential (mV) for voltage-dependent activation or inactivation; *k*, slope factor.

[*] Values are significantly different from control (paired *t*-test, $p < 0.05$).

[†] Values are significantly different from control (unpaired *t*-test, $p < 0.05$).

Figure 3.3: Inhibition of $Na_v1.4$ sodium currents by SCI insecticides. (A-C) Representative traces of sodium currents through $Na_v1.4$ channels recorded before and after 15 min of perfusion with 10 μM metaflumizone (A), RH-4841 (B), or DCJW (C). (D) Time course of sodium current inhibition caused by metaflumizone, RH-4841, and DCJW. Oocytes were held at a holding potential of -30 mV and stimulated once every minute with a test pulse (20 ms) to -10 mV that was preceded by a 2-s hyperpolarization to -120 mV. After 4 min of stable control recordings at -30 mV, insecticides were perfused into the bath for 15 min; peak sodium currents were normalized to the mean sodium current amplitude obtained during the 4 min of stable control currents prior insecticide perfusion. Data were fitted using a first-order exponential decay function that yielded a single time constant (τ_1); values are means ± SE of 4 or more individual experiments in separate oocytes.

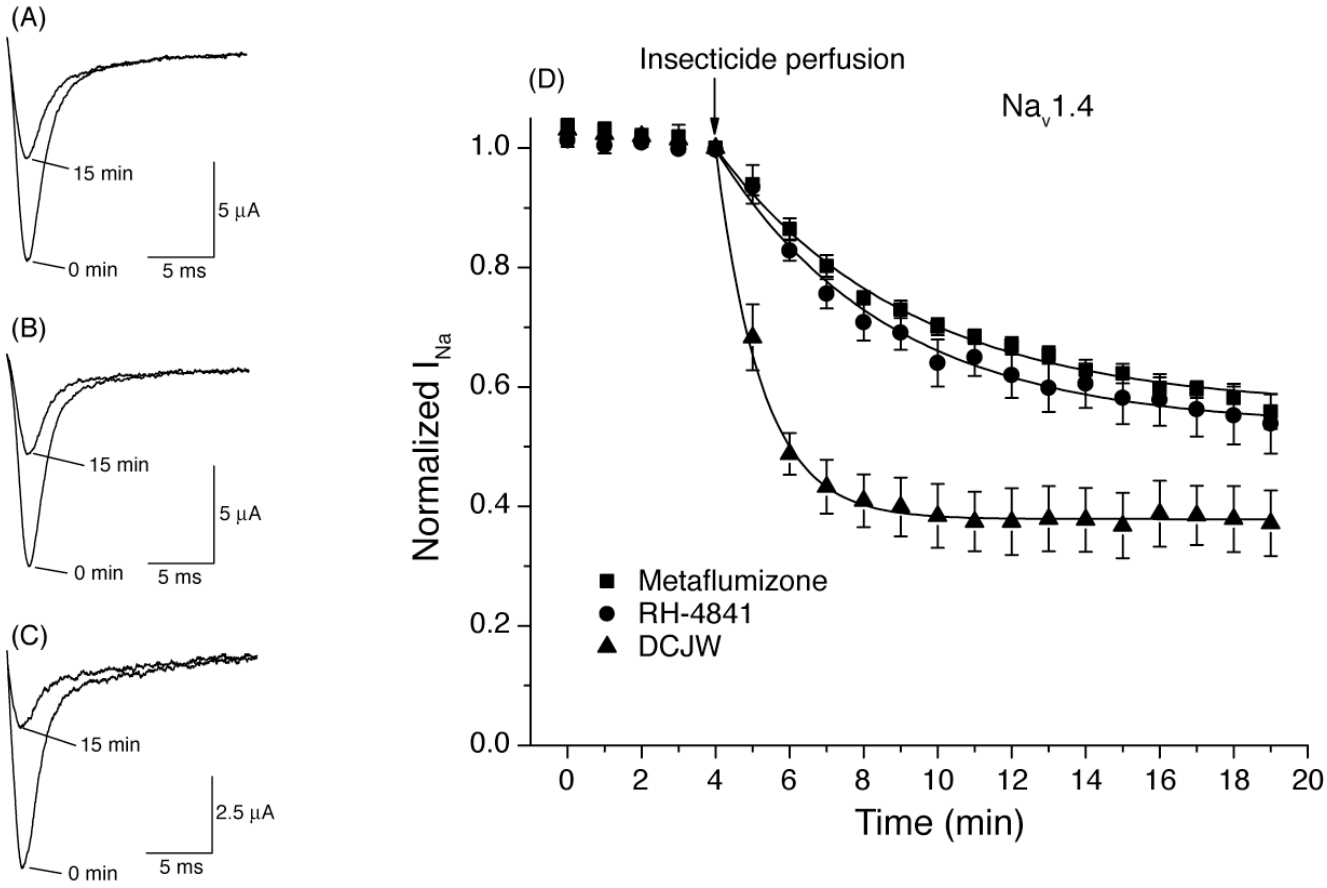
(A)
15 min
0 min
5 μA
5 ms
(B)
15 min
0 min
5 μA
5 ms
(C)
15 min
0 min
2.5 μA
5 ms
(D)
Insecticide perfusion
Na$_v$1.4
Normalized I_{Na}
1.0
0.8
0.6
0.4
0.2
0.0
0
2
4
6
8
10
12
14
16
18
20
Time (min)
Metaflumizone
RH-4841
DCJW

Table 3.2: Percentage SCI insecticide inhibition of rat $Na_v1.4$, $Na_v1.4$/F1579A, and $Na_v1.4$/Y1586A sodium channels[a].

	Metaflumizone		RH-4841		DCJW	
Channel	% Inhibition	*n*	% Inhibition	*n*	% Inhibition	*n*
$Na_v1.4$	43.9 ± 1.7	6	46.2 ± 5.0	4	62.8 ± 5.5	5
F1579A	19.2 ± 1.1*	5	20.6 ± 2.9*	4	44.3 ± 3.7*	4
Y1586A	54.0 ± 2.8*	6	68.9 ± 3.1*	3	88.8 ± 3.0*	4

[a] Values derived from data from Fig. 3.3, Fig.3. 6, and Fig. 3.7 after 15 min of insecticide perfusion

* Values are significantly different from wildtype (one-way ANOVA with Dunnett's *post-hoc* analysis, $p < 0.05$).

time constants (τ) that are given in Table 3.3.

Changes in the transmembrane voltage of the cell determine the conformational state of voltage-gated ion channels, so state-dependent inhibition is often manifested as a voltage-dependent phenomenon (McDonough and Bean, 2006). Fig. 3.4 illustrates the voltage- (*i.e.* state) dependent inhibition of sodium currents through wildtype channels after 15 min of insecticide exposure. Insecticides had little or no effect on peak current amplitude when oocytes were clamped at a holding potential of -120 mV, where channels were almost exclusively in the resting state. However, after 15 min of exposure at a holding potential of -60 mV, peak sodium currents were reduced by 9.6 ± 0.2 (n = 4), 4.2 ± 0.3 (n = 4), 37.9 ± 3.4 (n = 4), 9.7 ± 1.7 (n = 4) and 58.2 ± 3.8% (n = 4) by metaflumizone, RH-4841, RH-3421, indoxacarb and DCJW, respectively. Holding oocytes at -30 mV increased the extent of inhibition by metaflumizone, RH-4841, and RH-3421 (61.2 ± 3.4%; n = 3), whereas the degree of inhibition at -30 mV by the oxadiazine indoxacarb (8.3 ± 1.4%; n = 4) and its bioactive metabolite DCJW was not significantly different from that at -60 mV.

Previous studies (O'Reilly *et al.*, 2000; Bai *et al.*, 2003) have demonstrated that mutations at local anesthetic binding sites in DIV-S6 modulate slow inactivation gating in a residue-specific manner. Therefore, I characterized the effects of the F1579A and Y1586A mutations on the voltage dependence of slow inactivation in the absence of insecticides (Fig. 3.5A). At depolarized potentials (< -50 mV), slow inactivation was more complete in $Na_v1.4$/Y1586A channels (~95% inactivation at 0 mV) than in $Na_v1.4$/F1579A (~80% inactivation at 0 mV) or wildtype channels (~82% inactivation at 0 mV). Neither mutation significantly affected the midpoint potential for the voltage dependence of slow inactivation curve, although the slope was significantly steeper for both $Na_v1.4$/F1579A ($V_{1/2}$ = -44.1 ± 0.5 mV, k = 5.0 ± 0.4) and $Na_v1.4$/Y1586A ($V_{1/2}$ = -45.7 ± 0.4 mV, k = 5.6 ± 0.3) channels compared

Table 3.3: Rate of onset of SCI insecticide inhibition of rat $Na_v1.4$, $Na_v1.4$/F1579A, and $Na_v1.4$/Y1586A sodium channels[a].

	Metaflumizone		RH-4841		DCJW	
Channel	Onset of inhibition τ (min)	*n*	Onset of inhibition τ (min)	*n*	Onset of inhibition τ (min)	*n*
$Na_v1.4$	5.9 ± 0.6	6	4.1 ± 0.4	4	1.3 ± 0.1	5
F1579A	3.2 ± 0.6[*]	5	2.2 ± 0.5[*]	4	1.3 ± 0.1	4
Y1586A	5.9 ± 0.5	6	1.5 ± 0.1[†]	3	1.5 ± 0.1	4

[a] Values calculated by fitting data from Fig. 3.3, Fig. 3.6, and Fig. 3.7 with a single-exponential decay function.

[*] Values are significantly different from wildtype (one-way ANOVA and Dunnett's *post-hoc* analysis, $p < 0.05$).

[†] Values are significantly different from wildtype (one-way ANOVA and Dunnett's *post-hoc* analysis, $p < 0.01$).

Figure 3.4: Voltage-dependent inhibition of $Na_v1.4$ sodium currents by SCI insecticides. Oocytes were clamped at a membrane potential of -120 mV, -60 mV, or -30 mV and stimulated every minute with a test pulse (20 ms) to -10 mV during 15 min of insecticide perfusion; a 2-s hyperpolarization to -120 mV preceded each test pulse in experiments at holding potentials -60 mV and -30 mV. Fractional inhibition was derived from the amplitude of the peak transient sodium current at the end of the perfusion period normalized to the mean sodium current amplitude in that oocyte obtained after 4 min of stable control recordings prior to insecticide application.

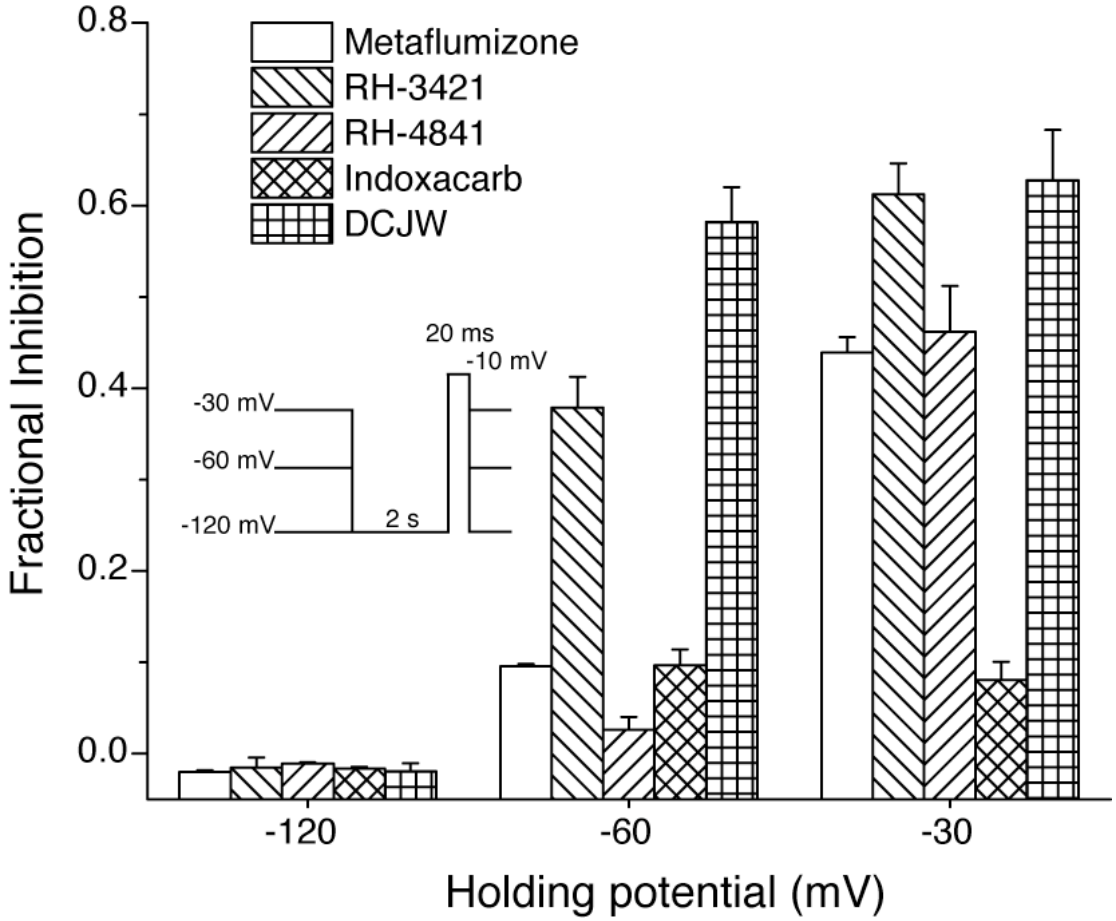
Metaflumizone
RH-3421
RH-4841
Indoxacarb
DCJW
20 ms
-10 mV
-30 mV
-60 mV
-120 mV
2 s
Fractional Inhibition
0.0
0.2
0.4
0.6
0.8
-120
-60
-30
Holding potential (mV)

Figure 3.5: Voltage dependence and development of steady-state slow inactivation for $Na_v1.4$, $Na_v1.4$/F1579A and $Na_v1.4$/Y1586A sodium channels expressed in *Xenopus* oocytes. (A) The voltage dependence of slow inactivation was examined using the standard protocol described in Fig. 3.2C and shown in the inset. Amplitudes of peak transient currents measured during a 20-ms depolarization to -10 mV ($Na_v1.4$ and $Na_v1.4$/F1579A) or 0 mV ($Na_v1.4$/Y1586A) following a 100-s conditioning prepulse from a holding potential (V_{hold}) of -120 mV to potentials ranging from -90 to 0 mV and a 50-ms hyperpolarization to -120 mV were normalized to the maximum current obtained during the inactivation protocol for that oocyte and plotted as a function of the conditioning potential. Values are means ± SE from 4-6 experiments in separate oocytes; curves are fitted to the Boltzmann equation. (B) The development of steady-state slow inactivation was assessed using a two-pulse protocol (see inset) in which oocytes were clamped at a V_{hold} of -30 mV ($Na_v1.4$), -35 mV ($Na_v1.4$/F1579A), or -50 mV ($Na_v1.4$/Y1586A) and stimulated every minute with a 20-ms test pulse to -10 mV ($Na_v1.4$ and $Na_v1.4$/F1579A) or 0 mV ($Na_v1.4$/Y1586A) that was preceded by a 2-s repolarization to -120 mV. Currents were normalized to peak test pulses elicited from a V_{hold} of -120 mV prior to depolarization; values are means ± SE from 9 experiments in separate oocytes. Curves were fitted with a single-exponential decay function.

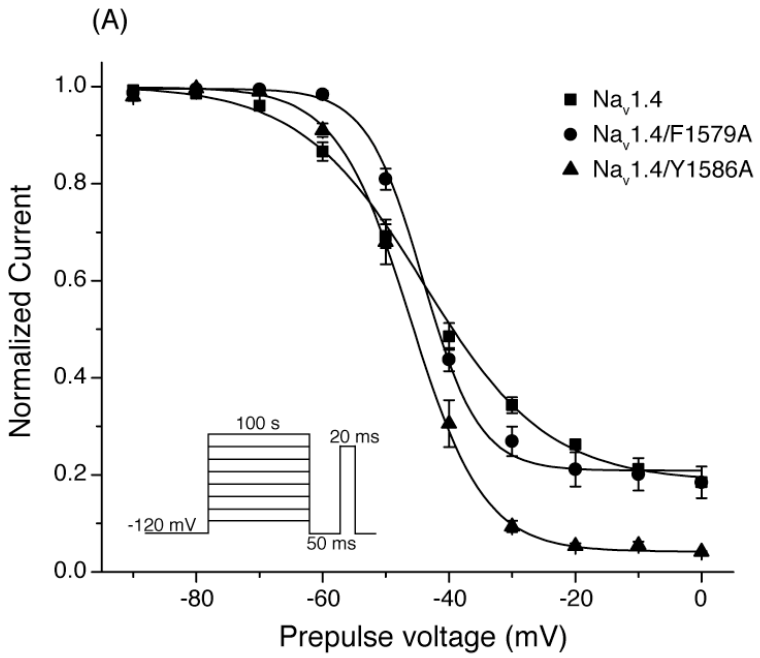
(A)
Normalized Current
Prepulse voltage (mV)
Na$_v$1.4
Na$_v$1.4/F1579A
Na$_v$1.4/Y1586A
100 s
20 ms
-120 mV
50 ms

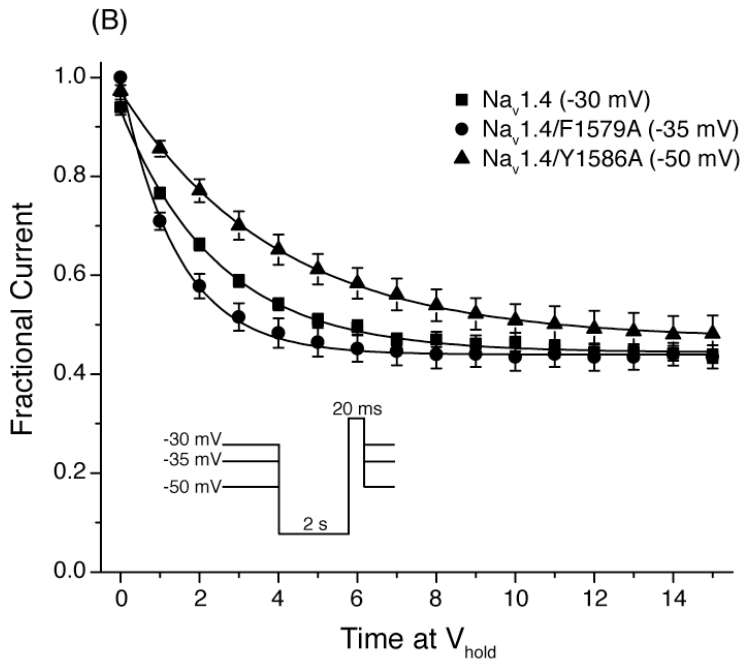
(B)
Fractional Current
Time at V$_{hold}$
Na$_v$1.4 (-30 mV)
Na$_v$1.4/F1579A (-35 mV)
Na$_v$1.4/Y1586A (-50 mV)
20 ms
-30 mV
-35 mV
-50 mV
2 s

to wildtype ($V_{1/2}$ = -44.9 ± 0.7 mV, k = 9.3 ± 0.6). A previous study (O'Reilly *et al.*, 2000) using transfected mammalian cells also reported that the $V_{1/2}$ of slow inactivation for $Na_v1.4$/Y1586A channels was not significantly altered, despite an increase in the extent of slow inactivation compared to wildtype channels. To avoid potential changes in insecticide potency arising indirectly from mutation-induced changes in the propensity of channels to occupy high affinity slow-inactivated states, oocytes were clamped at holding potentials of -35 mV ($Na_v1.4$/F1579A), or -50 mV ($Na_v1.4$/Y1586A). These holding potentials were empirically determined to produce fractional slow inactivation (~55%) equivalent to that in wildtype channels clamped at -30 mV (Fig. 3.5B).

I used the F1579A and Y1586A mutations to determine if metaflumizone shares common molecular determinants on mammalian sodium channels with other SCI insecticides. Fig. 3.6 shows the inhibition of sodium currents through $Na_v1.4$/F1579A channels by metaflumizone, RH-4841 and DCJW. Inhibition of $Na_v1.4$/F1579A channels by metaflumizone (Fig. 3.6A), RH-4841 (Fig. 3.6B), and DCJW (Fig. 3.6C) was significantly less compared to that of wildtype channels (Table 3.2). The time course of sodium current inhibition by SCI insecticides is illustrated in Fig. 3.6D. Paradoxically, the rate of inhibition of $Na_v1.4$/F1579A channels by metaflumizone and RH-4841 appeared to be much faster than for wildtype $Na_v1.4$ channels with steady-state inhibition being achieved after ~6 min of perfusion, whereas the rate of inhibition by DCJW did not appear to be affected by the F1579A mutation. Comparing first-order exponential decay fits of the time course of SCI insecticide inhibition demonstrated that the rate of inhibition by metaflumizone and RH-4841, but not DCJW was significantly greater compared to that of wildtype $Na_v1.4$ sodium channels (Table 3.3).

Fig. 3.7 illustrates the inhibition of $Na_v1.4$/Y1586A sodium channels by metaflumizone (Fig. 3.7A), RH-4841 (Fig. 3.7B), and DCJW (Fig. 3.7C). The time course of inhibition by SCI

Figure 3.6: Inhibition of $Na_v1.4$/F1579A sodium channels by SCI insecticides. (A-C) Representative traces of sodium currents through $Na_v1.4$/F1579A channels before and after 15 min of perfusion with 10 μM metaflumizone (A), RH-4841 (B), or DCJW (C). (D) Time course of sodium current inhibition caused by metaflumizone, RH-4841, and DCJW. Oocytes were held at a holding potential of -35 mV and stimulated once every minute with a test pulse (20 ms) to -10 mV that was preceded by a 2-s hyperpolarization to -120 mV. After 4 min of stable control recordings at -35 mV, insecticides were perfused into the bath for 15 min; peak sodium currents were normalized to the mean sodium current amplitude obtained during the 4 min of stable control recordings prior to insecticide perfusion. Data were fitted using a first-order exponential decay function that yielded a single time constant (τ_1); values are means ± SE of 4-5 individual experiments in separate oocytes.

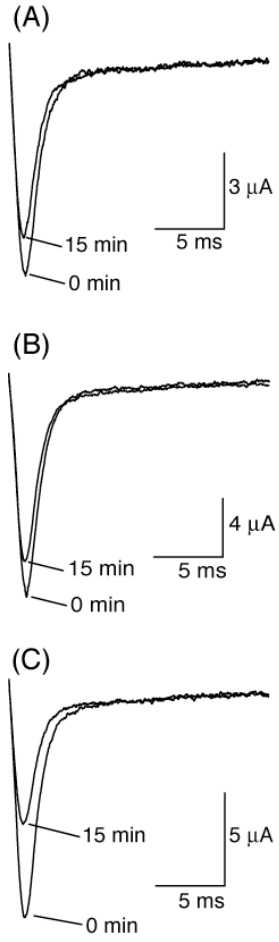
(A)
3 μA
15 min
5 ms
0 min
(B)
4 μA
15 min
5 ms
0 min
(C)
5 μA
15 min
5 ms
0 min

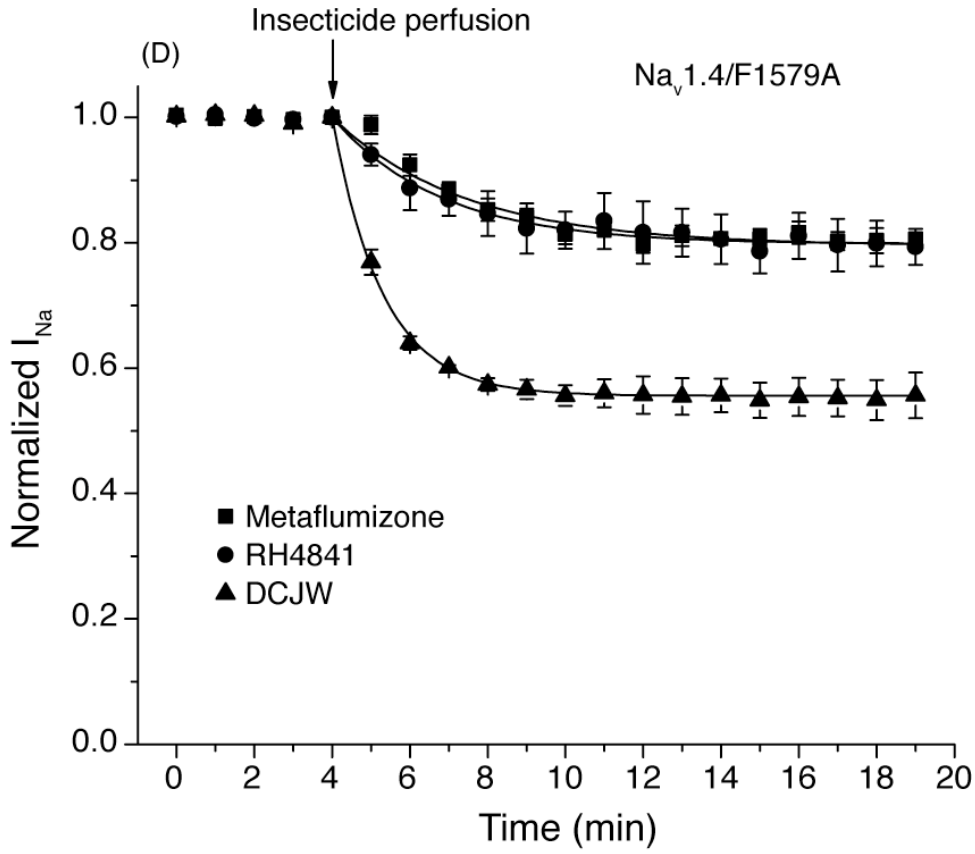
Insecticide perfusion
(D)
Na$_v$1.4/F1579A
Normalized I_{Na}
1.0
0.8
0.6
0.4
0.2
0.0
0
2
4
6
8
10
12
14
16
18
20
Time (min)
Metaflumizone
RH4841
DCJW

Figure 3.7: Inhibition of $Na_v1.4$/Y1586A sodium channels by SCI insecticides. (A-C) Representative traces of sodium currents through $Na_v1.4$/Y1586A channels before and after 15 min of perfusion with 10 μM metaflumizone (A), RH-4841 (B), or DCJW (C). (D) Time course of sodium current inhibition caused by metaflumizone, RH-4841, and DCJW. Oocytes were held at a holding potential of -50 mV and stimulated once every minute with a 20-ms test pulse to 0 mV that was preceded by a 2-s hyperpolarization to -120 mV. After 4 min of stable control recordings at -50 mV, insecticides were perfused into the bath for 15 min; peak sodium currents were normalized to the mean sodium current amplitude during the 4 min of stable control recordings prior to insecticide perfusion. Data were fitted using a first-order exponential decay function that yielded a single time constant (τ_1); values are means ± SE of 3 or more individual experiments in separate oocytes.

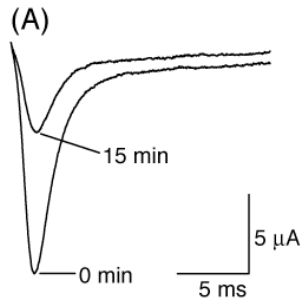
(A)
15 min
0 min
5 μA
5 ms

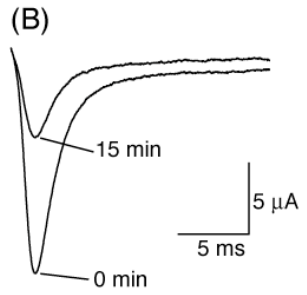
(B)
15 min
0 min
5 μA
5 ms

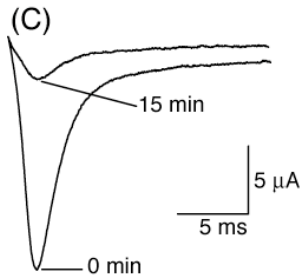
(C)
15 min
0 min
5 μA
5 ms

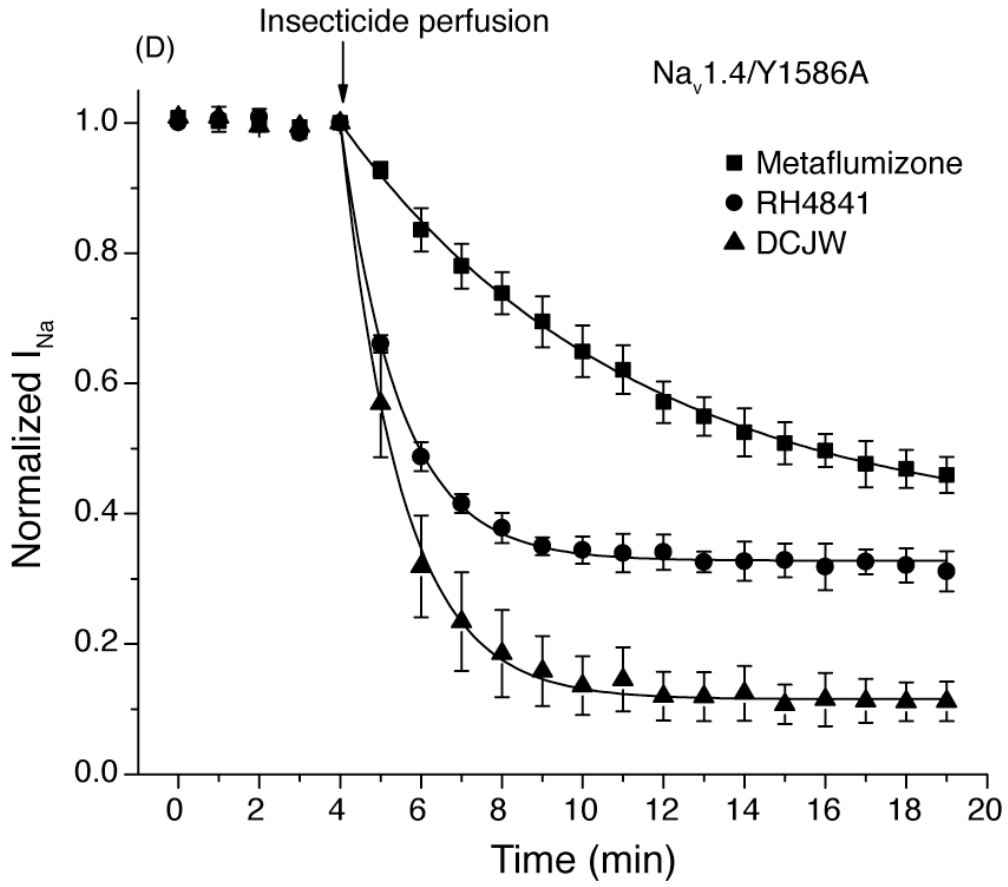
(D)
Insecticide perfusion
Na$_v$1.4/Y1586A
Metaflumizone
RH4841
DCJW
Normalized I_{Na}
1.0
0.8
0.6
0.4
0.2
0.0
0
2
4
6
8
10
12
14
16
18
20
Time (min)

insecticides are illustrated in Fig. 3.7D. The $Na_v1.4$/Y1586A sodium channels were significantly more sensitive to inhibition by all three SCI insecticides tested compared to wildtype $Na_v1.4$ and $Na_v1.4$/F1579A sodium channels (Table 3.2). Fitting the time course of SCI insecticide inhibition of $Na_v1.4$/Y1586A channels with a first-order decay indicated that the mutation had compound-specific effects on the rate of onset of inhibition. The rate of onset of inhibition by RH-4841, but not metaflumizone or DCJW, was significantly more rapid for $Na_v1.4$/Y1586A channels than for wildtype sodium channels (Table 3.3).

Fig. 3.8 illustrates the concentration-dependent inhibition of wildtype $Na_v1.4$ and $Na_v1.4$/Y1586A sodium channels by metaflumizone. The aqueous insolubility of metaflumizone at concentrations above 10 μM prevented me from achieving complete inhibition of sodium channels under the chosen experimental conditions. Although the relatively high insolubility of metaflumizone and low sensitivity of $Na_v1.4$ channels limited me from calculating an IC_{50} value for wildtype channels under these conditions, comparison of the partial curves shown in Fig. 3.8 suggests that the Y1586A mutation caused approximately a 10-fold increase in the sensitivity of $Na_v1.4$ sodium channels to metaflumizone.

Therapeutic SCI drugs have been shown previously to interfere with the ability of insecticidal SCIs to inhibit mammalian voltage-gated sodium channels under experimental conditions where no inhibition by the drugs is observed (Silver and Soderlund, 2005b). But, whether SCI insecticides are reciprocally capable of modulating the extent of inhibition by SCI drugs remains unclear. I assessed the effects of SCI insecticides on sodium channel inhibition by lidocaine to elucidate whether these insecticides bind to non-slow-inactivated channel states without inhibiting them. Fig. 3.9A shows the effects of high frequency (20 Hz) stimulation on the extent of sodium channel inhibition by 200 μM lidocaine alone and in the presence of 10 μM metaflumizone, RH-4841, or DCJW. The statistical analyses of steady-state use-dependent

Figure 3.8: Concentration dependence of metaflumizone inhibition of slow-inactivated wildtype (WT) and Y1586A mutant sodium channels. Oocytes were held at -30 mV (wildtype) or -50 mV (Y1586A) and sodium currents were recorded once every minute during a 20-ms test pulse to -10 mV that was preceded by a 2-s hyperpolarization to -120 mV. Each data point is the mean (± SE; n = 3-6) percent inhibition of sodium currents after 15 min of metaflumizone perfusion. Solid lines represent the best fit of the data points by the Hill equation.

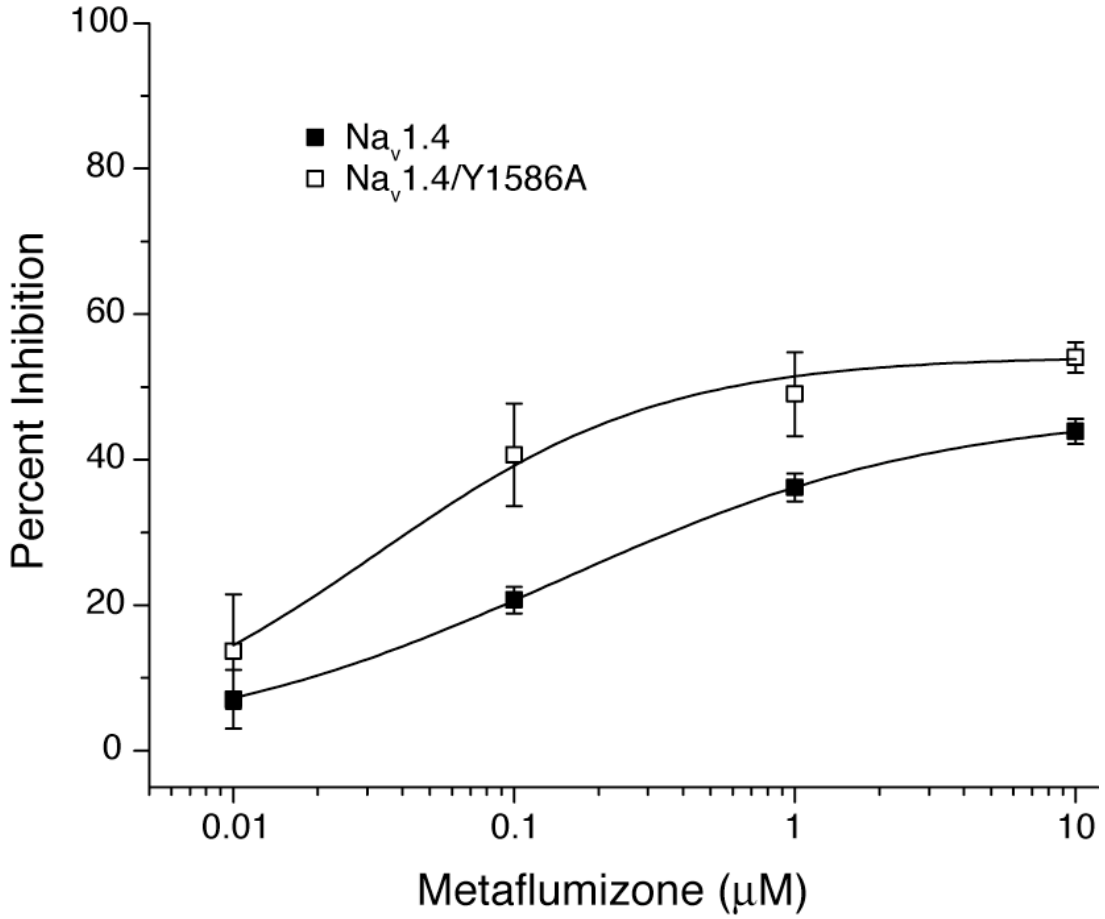
100
80
60
40
20
0
Percent Inhibition
Na$_v$1.4
Na$_v$1.4/Y1586A
0.01
0.1
1
10
Metaflumizone (μM)

Figure 3.9: Use-dependent lidocaine inhibition of sodium channels in the absence and presence of sodium channel inhibitor insecticides. (A) Effects of 10 μM metaflumizone, RH-4841 or DCJW on the extent of inhibition by lidocaine (200 μM) following 0-20 depolarizing prepulses (25 ms) from -120 mV to -50 mV at 20 Hz. Values were normalized to the mean peak sodium current amplitude measured from the same oocyte prior to the perfusion of lidocaine. Data points are means ± SE of 5 (lidocaine, metaflumizone+lidocaine, RH-4841+lidocaine) or 4 (DCJW+lidocaine) separate experiments with different oocytes; curves were fitted to mean data points using a single-exponential decay function. (B) Comparison of the extent of resting (after 0 prepulses) and fast-inactivated (after 10 prepulses) sodium channel inhibition by lidocaine in the absence or presence of metaflumizone, RH-4841, or DCJW. Values for use-dependent inhibition marked with an asterisk (*) are significantly ($p < 0.05$) different from use-dependent inhibition by lidocaine alone.

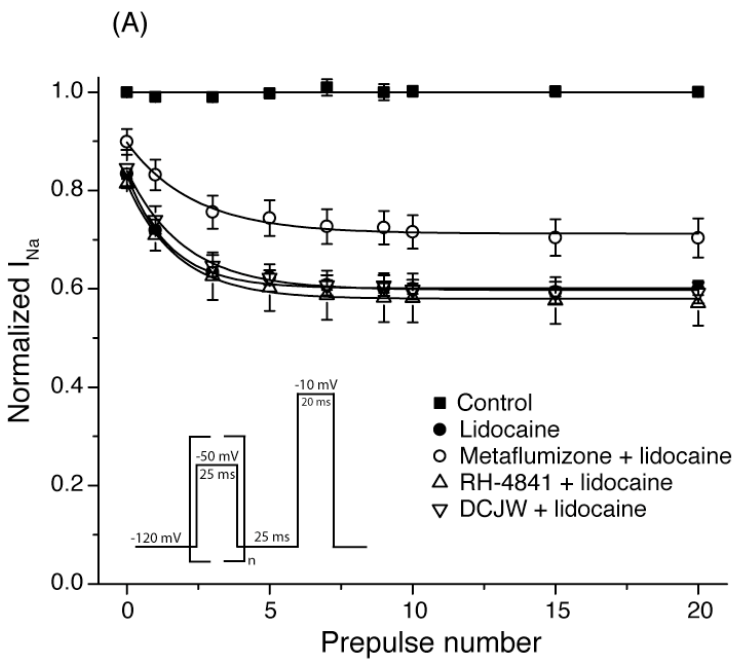
(A)
Normalized I_{Na}
Prepulse number
Control
Lidocaine
Metaflumizone + lidocaine
RH-4841 + lidocaine
DCJW + lidocaine
-120 mV
-50 mV
25 ms
25 ms
-10 mV
20 ms
n

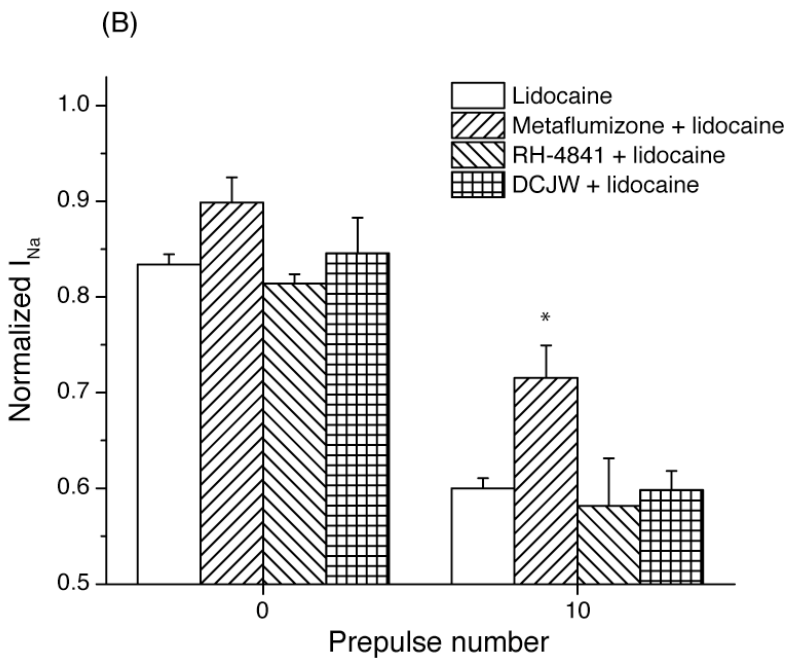
(B)
Normalized I_{Na}
Prepulse number
Lidocaine
Metaflumizone + lidocaine
RH-4841 + lidocaine
DCJW + lidocaine
*

inhibition are summarized in Fig. 3.9B. There was no effect of repeated depolarization on the stability of the peak transient sodium current in the absence of SCI drugs and insecticides. In the presence of lidocaine alone, peak currents were reduced by 16.6 ± 1.1% and 40.0 ± 1.0% after 0 and 10 depolarizing prepulses, respectively. Preliminary experiments verified that there was no significant increase in the extent of inhibition by lidocaine after 10 depolarizations (up to 100 depolarizations). None of the SCI insecticides exhibited any detectable use-dependent inhibition of sodium channels under these conditions (data not shown). However, in the presence of metaflumizone, the extent of lidocaine inhibition after 10 depolarizing prepulses was significantly reduced compared to inhibition by lidocaine alone. Metaflumizone also slightly reduced the extent of tonic sodium channel inhibition by lidocaine after 0 prepulses, but this effect was not statistically significant. Neither RH-4841 nor DCJW interfered with the tonic or use-dependent inhibition of sodium currents by lidocaine.

Discussion

This is the first report of the action of metaflumizone on mammalian voltage-gated sodium channels. I used the rat $Na_v1.4$ channel to enable me to place my findings in the context of previous studies (Silver and Soderlund, 2005b, 2006, 2007). I coexpressed the $Na_v1.4$ α subunit with the rat $\beta1$ subunit because these channels exhibit aberrant inactivation gating when expressed alone in *Xenopus* oocytes (Balser *et al.*, 1996, Kambouris *et al.*, 1998). The gating properties of $Na_v1.4+\beta1$ channel complexes that I describe here are in good agreement with the properties of these channels reported in previous studies. Slight quantitative differences between my data and previously published data can likely be explained by differences in experimental conditions, such as the choice of expression system or the details of the pulse protocols

employed.

Molecules that modify ion channel function often exhibit a preferential interaction with channels in one conformational state. At negative holding potentials, $Na_v1.4$ channels predominantly occupied the resting state and were insensitive to inhibition by the highest soluble concentration of metaflumizone or any other SCI insecticide tested. Holding the membrane potential at -60 mV caused partial inactivation of channels and facilitated inhibition by all insecticides tested. The extent of inhibition by metaflumizone, RH-4841, and RH-3421 was significantly greater at -30 mV, where inactivation was more complete, than at -60 mV. These findings are consistent with previous studies of other SCI insecticides (Silver and Soderlund, 2005b; Salgado and Hayashi, 2007) and have been interpreted as evidence that SCI insecticides preferentially interact with inactivated channels.

Fast inactivation in sodium channels terminates sodium conductance within milliseconds after depolarization and involves occlusion of the inner pore of the channel by the highly conserved inactivation gate in the intracellular linker between domains III and IV (Goldin, 2003). However, channel opening is not a prerequisite for fast inactivation because channels can enter the fast-inactivated state from the resting state following brief depolarization to potentials below the activation threshold (Ragsdale *et al.*, 1996; McDonough and Bean, 2006). Under my experimental conditions, metaflumizone had no effect on the voltage dependence of fast inactivation that was measured with standard 200-ms prepulses. This result is consistent with data from recent studies with metaflumizone on cloned cockroach sodium channels expressed in *Xenopus* oocytes (Silver *et al.*, 2009), and the current hypothesis that SCI insecticides inhibition occurs selectively only under experimental conditions that promote slow inactivation.

Slow inactivation in sodium channels is a voltage-dependent biophysical process that occurs following sustained depolarization or prolonged high-frequency stimulation and exhibits

development and recovery kinetics on the order of seconds to minutes (for reviews see Vilin and Ruben, 2001; Ulbricht, 2005). The molecular basis of slow inactivation is poorly understood, but it is different from fast inactivation because internal protease perfusion or amino acid substitutions that disable the fast-inactivation gate do not interfere with slow inactivation (Goldin, 2003). Slow inactivation of $Na_v1.4$ channels in my assays developed at potentials negative to channel opening but positive to fast inactivation, as previously reported (O'Reilly *et al.*, 2001; McNulty and Hanck, 2004). Metaflumizone enhanced the extent of slow inactivation and caused a modest hyperpolarizing shift in the voltage dependence of slow inactivation. These effects provide further evidence that SCI insecticides preferentially target and stabilize channels in a slow-inactivated state (Salgado, 1992). The very slow equilibration between metaflumizone and $Na_v1.4$ channels prevented a steady-state level of inhibition from being achieved during the 100-s conditioning pulses used to measure slow inactivation, so my data are likely to significantly underestimate the magnitude of the effects of metaflumizone on slow-inactivation gating parameters.

Substituting alanine at F1579 or Y1586 produced marked effects on metaflumizone and RH-4841 sensitivity that are consistent with previous studies describing the impact of these mutations on inhibition of $Na_v1.4$ channels by other SCI insecticides (Silver and Soderlund, 2007). The F1579A mutation reduced the sensitivity of channels to inhibition by metaflumizone, RH-4841, and DCJW. These results are consistent with the impact of the F1579A mutation on the action of SCI drugs at the LA receptor. The F1579 residue is undoubtedly the most significant determinant of the LA receptor to be identified. Amino acid substitution experiments indicate that resting-state affinity is dependent on the hydrophobicity of the residue at F1579, whereas high-affinity use-dependent inhibition is strongly determined by the aromaticity of the side chain at this position (Li *et al.*, 1999). These data have suggested that Phe-1579 stabilizes

drug binding to the open or inactivated states through either cation-π or aromatic-aromatic interactions between the aromatic amino acid side chain and the alkyl-substituted amino group of the drug molecule (Li *et al.*, 1999). Similarly, I hypothesize that the F1579A mutation may reduce SCI insecticide sensitivity through a disruption of important π-electron interactions between the aromatic side chain of F1579 and the *N*-phenyl moiety of SCI insecticides (see Fig. 3.1; Silver and Soderlund, 2007).

The Y1586A mutation increased SCI insecticide inhibition compared to wildtype. I estimate that that the Y1586A mutation enhanced the potency of metaflumizone by approximately 10-fold. However, the very slow kinetics of inhibition and limited aqueous solubility of metaflumizone prevented me from obtaining complete inhibition under my experimental conditions or calculating an IC_{50} value for inhibition of wildtype channels. Moreover, inhibition of $Na_v1.4$ or $Na_v1.4$/Y1586A channels by metaflumizone did not reach a steady-state level after 15 min, so my data are likely to slightly underestimate the potency of metaflumizone. The Y1586 residue appears to strongly influence the binding of LAs but not of other SCI drugs (for review see Mike and Lukacs, 2010). Moreover, studies of the impact of different amino acid substitutions at Y1717 in $rNa_v1.3$ channels (analogous to Y1586 in $rNa_v1.4$) expressed in *Xenopus* oocytes suggest that this residue does not directly contribute to the LA receptor (Li *et al.*, 1999). A molecular model of the LA receptor in $Na_v1.4$ channels indicates that the convergence of S6 segments constrains space in the inner pore, especially in the region of Y1586. The much smaller side chain of alanine at this position likely alleviates such space constraints (Lipkind and Fozzard, 2005). I hypothesize that the Y1586A mutation indirectly enhances SCI insecticide inhibition by reducing steric hindrance, thereby facilitating a more favorable interaction between the insecticide and other inner-pore residues that are directly involved in binding, as suggested previously (Silver and Soderlund, 2007). Further mutagenesis

experiments that alter the physiochemical properties at Y1586 are necessary to test this hypothesis.

The state-dependent inhibition of mammalian sodium channels by metaflumizone was similar to that of other SCI insecticides. However, perfusion of metaflumizone at a hyperpolarized holding potential reduced the voltage-dependent probability of sodium channel activation, as indicated by the depolarizing shift in the midpoint potential of the conductance-voltage (*G-V*) curve. Consequently, the amplitude of sodium currents measured during test pulses to sub-maximal activation potentials (*i.e.* -30 mV and -20 mV) were significantly reduced in the presence of metaflumizone compared to the control. These results imply that metaflumizone interacts with $Na_v1.4$ channels in the resting state. By contrast, other SCI insecticides do not affect the *G-V* relationship of rat $Na_v1.4$ channels expressed in oocytes (Silver and Soderlund, 2005b), TTX-S or TTX-R sodium channels in rat DRG neurons (Tsurubuchi *et al.*, 2001; Tsurubuchi and Kono, 2003; Zhao *et al.*, 2003), or sodium channels in cockroach DUM neurons (Lapied *et al.*, 2001). Nevertheless, other SCI insecticides may also interact with sodium channels in the resting state in a manner that does not produce block but modifies channel gating. Exposure of sodium channels in rat DRG neurons to indoxacarb or DCJW at a hyperpolarized membrane potential, at which no inhibition is observed, accelerates the development of slow inactivation following subsequent depolarization (Zhao *et al.*, 2003).

I examined the effect of metaflumizone and other SCI insecticides on use-dependent lidocaine inhibition to determine if SCI insecticides interact with non-slow-inactivated channels without blocking them. Although none of the insecticides alone exhibited any use dependence in response to high-frequency pulse trains that caused significant fast inactivation from the resting state, metaflumizone was unique in its ability to interfere with use-dependent inhibition by lidocaine. These results offer further evidence that binding of SCI insecticides to channels is not

always accompanied by channel inhibition (Silver and Soderlund, 2005b; Silver and Soderlund, 2007) and suggest further that the molecular determinants of action for metaflumizone are fundamentally different from other rigid, nearly planar SCI insecticides. Interestingly, metaflumizone did not significantly affect the level of resting inhibition by lidocaine that was evident upon depolarization following 0 prepulses. A recent study (Lenkey *et al.*, 2011) proposes that resting and inactivated sodium channels possess fundamentally distinct drug binding sites. The ability of metaflumizone to interfere with the binding of lidocaine to $Na_v1.4$ channels in the fast-inactivated state without significantly disrupting drug binding in resting channels offers further evidence that the drug binding sites on resting and inactivated sodium channels are fundamentally different.

Selective binding to sodium channels in slow-inactivated states may also produce therapeutically useful effects. The antihypertensive drug mibefradil (McNulty and Hanck, 2004), the anticonvulsant lacosamide (Errington *et al.*, 2008), and the investigational compound for neuropathic pain Z123212 (Hildebrand *et al.*, 2011) preferentially target sodium channels in one or more slow-inactivated state(s). However, the molecular basis by which slow-inactivation-specific SCIs produce neurotoxic or therapeutic effects is unknown. Therefore, SCI insecticides represent additional novel and unique chemical probes that may be useful for understanding the molecular details of ligand-receptor interactions that underlie toxic or therapeutic effects through slow inactivation and could thereby potentially facilitate the future design of safer and more effective insecticidal and therapeutic agents.

References

Bai C-X, Glaaser IW, Sawanobori T, Sunami A (2003) Involvement of local anesthetic binding sites on IVS6 of sodium channels in fast and slow inactivation. *Neurosci. Lett.* **337**:41-45.

Balser JR, Nuss HB, Orias DW, Johns DC, Marban E, and Tomaselli GF (1996) Local anesthetic as effectors of allosteric gating. *J. Clin. Invest.* **98**:2874-2886.

Bezanilla F and Armstrong CM (1977) Inactivation of the sodium channel. *J. Gen. Physiol.* **70**:549-566.

Bruhova I, Tikhonov DB, and Zhorov BS (2008) Access and binding of local anesthetics in the closed sodium channel. *Mol. Pharmacol.* **74**:1033-1045.

Errington AC, Stöhr T, Heers C, and Lees G (2008) The investigational anticonvulsant lacosamide selectively enhances slow inactivation of voltage-gated sodium channels. *Mol. Pharmacol.* **73**:157-169.

Goldin AL (1992) Maintenance of *Xenopus laevis* and oocyte injection. *Methods Enzymol.* **207**:266-297.

Goldin AL (2003) Mechanisms of sodium channel inactivation. *Curr. Opin. Neurobiol.* **13**:284-290.

Grosscurt AC, van Hes R, and Wellinga, K (1979) 1-Phenylcarbamoyl-2-pyrazolines, a new class of insecticides. 3. Synthesis and insecticidal properties of 3,4-diphenyl-1-phenylcarbamoyl-2-pyrazolines. *J. Agric. Food. Chem.* **27**:406-409.

Hasan R, Nishimura K, Okada M, Akamatsu M, Inoue M, and Ueno T (1996) Stereochemical basis for the insecticidal activity of carbamoylated and acylated pyrazoline. *Pestic. Sci.* **46**:105-112.

Hildebrand ME, Smith PL, Bladen C, Eduljee C, Xie JY, Chen L, Fee-Maki M, Doering CJ, Mezeyova J, Zhu Y, Belardetti F, Pajouhesh H, Parker D, Arneric SP, Parmar M, Porreca F, Tringham E, Zamponi GW, and Snutch TP (2011) A novel slow-inactivation-specific ion channel modulator attenuates neuropathic pain. *PAIN*® **152**:833-843.

Kallen RG, Sheng ZH, Yang J, Chen L, Rogart RB, and Barchi RL (1990) Structure and expression of a sodium channel characteristic of denervated skeletal muscle. *Neuron* **4**:233-242.

Kambouris NG, Hastings LA, Stepanovic S, Marban E, Tomaselli GF, and Balser JR. (1998) Mechanistic link between lidocaine block and inactivation probed by outer pore mutations in the rat μ1 skeletal muscle sodium channel. *J. Physiol.* **512**:693-705.

Lapied B, Grolleau F, and Sattelle DB (2001) Indoxacarb, an oxadiazine insecticide, block insect neuronal sodium channels. *Brit. J. Pharmacol.* **132**:587-595.

Lenkey N, Karoly R, Epresi N, Vizi ES, Mike A. (2011) Binding of sodium channel inhibitors to hyperpolarized and depolarized conformations of the channel. *Neuropharmacol.* **60**:191-200.

Li HL, Galue A, Meadows L, and Ragsdale DS (1999) A molecular basis for the different local anesthetic affinities of resting versus open and inactivated states of the sodium channel. *Mol. Pharmacol.* **55**:134-141.

Lipkind GM and Fozzard HA (2005) Molecular modeling of local anesthetic drug binding by voltage-gated sodium channels. *Mol. Pharmacol.* **68**:1611-1622.

McNulty MM and Hanck DA (2004) State-dependent mibefradil block of Na^+ channels. *Mol. Pharmacol.* **66**:1652-1661.

McDonough SI and Bean BP (2006) State-dependent drug interactions with ion channels, in *Voltage-Gated Ion Channels as Drug Targets* (Triggle DJ, Gopalakrishnan M, Rampe D, and Zheng W eds) pp 19-36, Wiley-VCH, Weinheim.

Mike A and Lukacs P (2010) The enigmatic drug binding site for sodium channel inhibitors. *Curr Mol. Pharmacol.* **3**:129-144.

O'Reilly JP, Wang S-Y, and Wang GK (2000) A point mutation in domain 4-segment 6 of the skeletal muscle sodium channel produces an atypical inactivation state. *Biophys.* **78**:773-784.

O'Reilly JP, Wang S-Y, and Wang GK (2001) Residue-specific effects on slow inactivation at V787 in D2-S6 of $Na_v1.4$ sodium channels. *Biophys. J* **81**:2100-2111.

Payne GT, Deecher DC, and Soderlund DM (1998) Structure-activity relationships for the action of dihydropyrazole insecticides on mouse brain sodium channels. *Pestic. Biochem. Physiol.* **60**:177-185.

Ragsdale DS, McPhee JC, Scheuer T, and Catterall, WA (1996) Common molecular determinants of local anesthetic, antiarrhythmic, and anticonvulsant block of voltage-gated Na^+ channels. *Proc. Natl. Acad. Sci. USA* **93**:9270-9275.

Salgado VL (1990) Mode of action of insecticidal dihydropyrazoles: selective block of impulse generation in sensory nerves. *Pestic. Sci.* **28**:389-411.

Salgado VL (1992) Slow voltage-dependent block of sodium channels in crayfish nerve by dihydropyrazole insecticides. *Mol. Pharmacol.* **41**:120-126.

Salgado VL and Hayashi JH (2007) Metaflumizone is a novel sodium channel blocker insecticide. *Vet. Parasitol.* **150**:182-189.

Silver KS and Soderlund DM (2005a) Action of pyrazoline-type insecticides at neuronal target sites. *Pestic. Biochem. Physiol.* **81**:136-143.

Silver KS and Soderlund DM (2005b) State-dependent block of rat $Na_v1.4$ sodium channels expressed in *Xenopus* oocytes by pyrazoline-type insecticides. *Neurotox.* **26**:397-406.

Silver KS and Soderlund DM (2006) Differential sensitvity of rat voltage-sensitive sodium channel isoforms to pyrazoline-type insecticides. *Toxicol Appl Pharmacol.* **214**:209-217.

Silver KS and Soderlund DM (2007) Point mutations at the local anesthetic receptor site modulate the state-dependent block of rat $Na_v1.4$ sodium channels by pyrazoline-type insecticides. *Neurotox.* **28**:655-663.

Silver KS, Nomura Y., Salgado VL, and Dong K (2009) Role of the sixth transmembrane segment of domain IV of the cockroach sodium channel in the action of sodium channel blocker insecticides. *Neurotox.* **30**:613-621.

Smith TJ and Soderlund DM (1998) Action of the pyrethroid insecticide cypermethrin on rat brain IIa sodium channels expressed in *Xenopus* oocytes. *Neurotox.* **19**:823-832.

Tatebayashi H and Narahashi T (1994) Differential mechanism of action of the pyrethroid tetramethrin on tetrodotoxin-sensitive and tetrodotoxin resistant sodium channels. *J. Pharmacol. Exp. Ther.* **270**:595-603.

Tsurubuchi Y, Zhao X, Nagata K, Kono Y, Nishimura K, Yeh JZ, and Narahashi T (2001) Modulation of tetrodotoxin-resistant sodium channels by dihydropyrazole insecticide RH-3421 in rat dorsal root ganglion neurons. *Neurotox.* **22**:743-753.

Tsurubuchi Y and Kono Y (2003) Modulation of sodium channels by the oxadiazine insecticide indoxacarb and its *N*-decarbomethoxylated metabolite in rat dorsal root ganglion neurons. *Pest. Manag. Sci.* **59**:999-1006.

Ulbricht W (2005) Sodium channel inactivation: molecular determinants and modulation. *Physiological Review* **85**:1271-1301.

Vilin YY and Ruben PC (2001) Slow inactivation in voltage-gated sodium channels, *Cell Biochem. Biophys.* **35**:171-190.

Wagner LE, Gingrich KJ, Kulli JC, and Yang J (2001) Ketamine blockade of voltage-gated sodium channels. *Anesthes.* **95**:1406-1413.

Wang GK, Quan C, and Wang S-Y (1998) A common local anesthetic receptor for benzocaine and etidocaine in voltage-gated μ1 Na^+ channels. *Pflugers Arch.* **435**:293-302.

Wellinga K, Grosscurt AC and van Hes R (1977) 1-Phenylcarbamoyl-2-pyrazoline: a new class of insecticides. 1. Synthesis and insecticidal properties of 3-phenyl-1-phenylcarbamoyl-2-pyrazoline. *J. Agric. Food Chem.* **25**: 987-992.

Wing KD, Andaloro JT, McCann SF, and Salgado VL (2005) Indoxacarb and the sodium channel blocker insecticides: chemistry, physiology, and biology in insects, in

Comprehensive Molecular Insect Science (Gilbert LI, Iatrou K, and Gill SS eds) pp 30–53, Elsevier, New York.

Zhao X, Ikeda T, Yeh JZ, and Narahashi T (2003) Voltage-dependent block of sodium channels in mammalian neurons by the oxadiazine insecticide indoxacarb and its metabolite DCJW. *Neurotox.* **24**:83-96.

CHAPTER FOUR

COMPOUND-SPECIFIC EFFECTS OF MUTATIONS AT V787 IN DII-S6 OF $NA_V1.4$ SODIUM CHANNELS ON SODIUM THE ACTION OF SODIUM CHANNEL INHIBITOR INSECTICIDES[1,2]

Introduction

Sodium channel inhibitor (SCI) insecticides are an emerging class of neurotoxic insect control agents that cause ataxia, convulsions, paralysis, and mortality in arthropods (Salgado, 1990). Although SCI insecticides were first discovered in the early 1970s, compounds with this novel mode of action have only become commercially available within the last decade. The oxadiazine indoxacarb (Fig. 4.1A), the first SCI insecticide to be commercially registered, is a proinsecticide that is efficiently converted in insects but not mammals to its more potent *N*-decarbomethoxylated metabolite, DCJW (Fig. 4.1A) (Wing *et al.*, 2005). The novel semicarbazone metaflumizone (Fig. 4.1B), the second SCI insecticide to be commercialized, is the first member of this insecticide class introduced for the animal health market because of its high efficacy for controlling fleas on domesticated pets (Salgado and Hayashi, 2007). Insecticidal dihydropyrazoles (*e.g*. RH-3421 and RH-4841; Fig 4.1C) are one of the prototypic

---

[1]Presented at the 26th Annual Meeting of Neurotoxicology, Portland, OR, June 6-10, 2010 and at the 40th Annual Meeting of the Society for Neuroscience, San Diego, CA, November 13-17, 2010.

[2]This chapter has been prepared for submission to *Neurotoxicology*

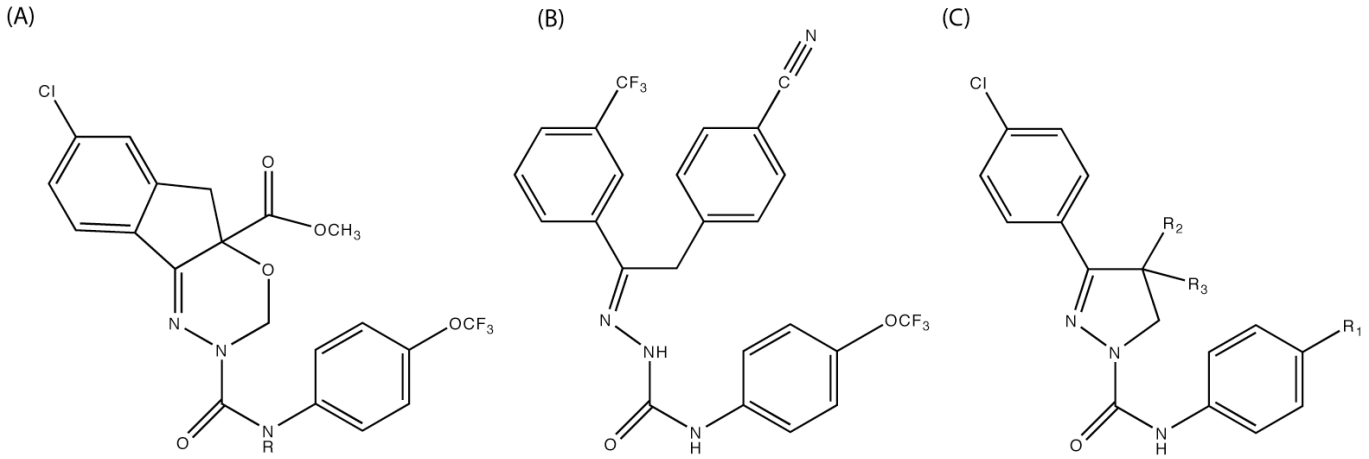

Indoxacarb

R = CO_2CH_3

DCJW

R = H

Metaflumizone

RH-3421

R_1 = CF_3
R_2 = CO_2CH_3
R_3 = CH_3

RH-4841

R_1 = Cl
R_2 = phenyl
R_3 = H

Figure 4.1: Structures of SCI insecticides. (A) Indoxacarb and DCJW. (B) Metaflumizone. (C) RH-3421 and RH-4841.

chemical subgroups of the SCI insecticide class that failed to be commercially registered because of the risks associated with their high subchronic toxicity to mammals (Payne *et al.*, 1998; Silver and Soderlund, 2005a). The continued efforts of the agrochemical industry to develop new, commercially viable SCI compounds reinforces both the value of this type of biological activity and the need to better understand the actions of these compounds that underlie their toxicological properties.

SCI insecticides block both insect and mammalian voltage-gated sodium channels through a preferential interaction with channels in the slow-inactivated state (Salgado, 1992; Lapied *et al.*, 2001; Zhou *et al.*, 2003; Silver and Soderlund, 2005b). However, the state-dependent details of insecticide-channel interactions are not completely understood. Experiments with crayfish axons showed that inhibition of sodium channels by a SCI insecticide (RH-1211) was not disrupted by progressive proteolytic removal of slow and fast inactivation by intracellular perfusion of trypsin and *N*-bromoacetamide, respectively (Salgado, 1992). Furthermore, metaflumizone differs from other SCI insecticides in its ability to interfere with use-dependent inhibition of fast-inactivated $Na_v1.4$ sodium channels by the local anesthetic lidocaine under experimental conditions that did not cause insecticide block (Chapter 3). These results not only imply a fundamental difference in the state-dependent action of metaflumizone compared to other SCI insecticides but also suggest that metaflumizone may bind to fast-inactivated channels without inhibiting them. The ability of other SCI insecticides to bind to sodium channels in the absence of block is also implied by the acceleration of the onset of slow sodium channel inactivation in rat DRG neurons following indoxacarb or DCJW perfusion at a hyperpolarized membrane potential, at which no inhibition is observed (Zhou *et al.*, 2003).

Therapeutic SCI drugs (local anesthetics, class I anticonvulsants and antiarrhythmics), which bind inside the inner pore at the "local anesthetic (LA) receptor," preferentially target

open or fast-inactivated channels (Ragsdale *et al.*, 1994; Ragsdale *et al.*, 1996). Studies employing site-directed mutagenesis have identified putative determinants of drug binding in the S6 transmembrane segments in all domains except domain II (Ragsdale *et al.*, 1994; Yarov-Yarovoy *et al.*, 2001; Yarov-Yarovoy *et al.*, 2002). Residues in domain IV-S6, particularly F1579 and Y1586 (rat $Na_v1.4$ numbering) appear to be essential for depolarization-dependent block by SCI drugs. Recent studies have shown that block of slow-inactivated channels by SCI insecticides is also modulated by mutations at F1579 and Y1586 (Silver and Soderlund, 2007; Chapter 3). Though, despite this apparent overlap of insecticide and drug binding sites, the larger size of insecticide molecules suggests that additional determinants of insecticide binding exist outside the LA receptor.

The present study was designed to elucidate the mechanism of state-dependent sodium channel block by SCI insecticides using specific mutations at V787 in $Na_v1.4$ sodium channels as a molecular modulator of slow inactivation. Mutations at the highly conserved V787 residue in sodium channel DII-S6 modulate slow inactivation in a residue-specific manner (O'Reilly *et al.*, 2001). Whereas the V787K mutation profoundly enhances slow inactivation, the V787A or V787C mutation variably inhibits slow inactivation compared to wildtype channels. I expressed wildtype $Na_v1.4$ channels and $Na_v1.4$ channels possessing the V787A, V787C, or V787K mutation in combination with the rat β1 subunit in *Xenopus* oocytes. Surprisingly, mutations at V787 modulated SCBI block in a residue- and compound-specific manner that was independent of mutation-induced changes in slow inactivation gating. These results suggest that the V787 residue in DII-S6 may be part of or in close proximity to the SCI insecticide binding site, which may differ precisely between members of this chemically diverse insecticide class.

Materials and Methods

The cDNA encoding the wildtype rat $Na_v1.4$ skeletal muscle α subunit (Kallen *et al.*, 1990) was obtained from R.G. Kallen (University of Pennsylvania, Philadelphia, PA) and the cloned rat brain β1 cDNA was obtained from W.A. Catterall (University of Washington, Seattle, WA). Sodium channel mutations were introduced by polymerase chain reaction using a commercial site-directed mutagenesis kit (QuikChange XL, Stratagene, La Jolla, CA) and oligonucleotide primers (Sigma Genosys, The Woodlands, TX) encoding for the mutation of interest at V787 in the rat $Na_v1.4$ cDNA. DNA sequencing of the region surrounding the mutation confirmed the structures of all mutated cDNAs. The cDNA plasmids were linearized with restriction enzymes to provide templates for *in vitro* cRNA synthesis using a commercial kit (mMessage mMachine, Ambion, Austin, TX). The integrity of all cRNAs was assessed by electrophoresis in 1% agarose-formaldehyde gels.

Ovaries from female *Xenopus laevis* toads (Nasco, Ft. Atkinson, WI) were washed with Ca^{2+}-free OR-2^{+} saline (containing in mM: 82.5 NaCl, 2 KCl, 1 $MgCl_2$, 5 HEPES, adjusted pH to 7.6 with NaOH) before being digested in 1 mg/mL collagenase (type 1A, Sigma-Aldrich, St. Louis, MO) for about 1 hr to degrade the ovarian tissue. This procedure was performed in accordance with National Institutes of Health guidelines and followed a protocol that was approved by the Cornell University Animal Care and Use Committee. Mature (stage V and VI) oocytes were selected and the outer follicle cells were manually removed with surgical forceps. Defolliculated oocytes were incubated overnight at 16° C in ND-96 (containing in mM: 96 NaCl, 2 KCl, 1.8 $CaCl_2$, 1 $MgCl_2$, and 5 HEPES, adjusted to pH 7.6 with NaOH) solution supplemented with 6% horse serum (Sigma-Aldrich), 0.5% penicillin/streptomycin and 2.5 mM sodium pyruvate (Goldin, 1992). Healthy oocytes were pressure-injected with a 1:2 (mass ratio)

mixture of wildtype or mutated rat $Na_v1.4$ channel α subunit and β1 cRNAs, respectively. The concentration of the β-subunit was between 0.5 and 12 ng/mL, which was sufficient to generate sodium currents with amplitudes between -10 and -30 μA. Oocytes were incubated at 16° C in supplemented ND-96 media for 2-5 days prior to use.

The two-microelectrode voltage-clamp technique was used to record macroscopic sodium currents from injected oocytes using a Geneclamp 500B amplifier (Axon Instruments, Foster City, CA) and pClamp 10.2 software (Axon Instruments, Burlingame, CA. All electrophysiological experiments were performed at room temperature (~23ºC) in disposable recording chambers manufactured from 0.25 in Plexiglass and a glass coverslip sealed together with ethyl cyanoacrylate as described elsewhere (Smith and Soderlund, 1998). Oocytes were continuously perfused with ND-96 saline at ~0.45 ml/min using a custom-designed passive capillary perfusion system similar to that described previously (Tatebayashi and Narahashi, 1994; Silver and Soderlund, 2005b) and the entire bath perfusate could be exchanged in ~1 min. Recording microelectrodes were pulled from borosilicate glass capillaries (World Precision Instruments, Inc.) and filled with a filtered 3 M KCl solution. Filled electrodes had 0.5- to 0.7 MΩ tip resistances when submerged in ND-96 saline. All perfusion capillaries, recording chambers, and recording electrodes were disposed of after single use, to prevent potential cross-contamination between experiments. Sodium currents were filtered at 5 kHz with a low-pass 4-pole Bessel filter and digitized at 50 kHz with a Digidata 1320A (Axon Instruments). Capacitive transient currents were subtracted using the P/N (N = 4) subtraction method (Bezanilla and Armstrong, 1977). Experiments with oocytes that expressed $Na_v1.4$, $Na_v1.4$/V787A, or $Na_v1.4$/V787C channels were performed >5 min after the membrane was clamped at a hyperpolarized potential of -120 mV to minimize increases in the sodium current amplitude arising from the recovery of slow inactivation following hyperpolarization from a typical resting

potential of about -55 mV (Catterall, 1976). The $Na_v1.4$/V787K channels typically required >10 min at a holding potential of -140 mV to stabilize the sodium current, reflecting the enhanced slow inactivation for this mutant.

Protocols used to characterize the voltage dependence of channel activation and inactivation were carried out at a holding potential (V_h) of -120 mV except for $Na_v1.4$/V787K, which were carried out at a V_h of -140 mV due to the altered voltage dependence of slow inactivation observed for this mutant channel. The voltage dependence of activation was determined by measuring sodium currents during a 20-ms depolarization to potentials ranging from -80 to 30 mV in 10-mV increments. To determine the voltage dependence of steady-state fast inactivation, sodium currents were measured during a 20-ms test pulse to -10 mV ($Na_v1.4$, $Na_v1.4$/V787C, and $Na_v1.4$/V787K) or 0 mV ($Na_v1.4$/V787A) after a 200-ms conditioning pulse to potentials ranging from -100 mV to 0 mV in 10-mV increments. To determine the voltage dependence of slow inactivation, a 100-s conditioning pulse to potentials ranging from V_h to 0 mV in 10-mV steps was followed by a 50-ms hyperpolarization to V_h (to fully recover fast-inactivated channels) and a 20-ms test pulse to -10 mV ($Na_v1.4$, $Na_v1.4$/V787C, and $Na_v1.4$/V787K) or 0 mV ($Na_v1.4$/V787A). For $Na_v1.4$/V787K, there was no difference in the extent of slow inactivation after a 10-s conditioning pulse compared to a 100-s conditioning pulse (data not shown) so I employed a 10-s conditioning pulse to characterize the voltage-dependence of slow inactivation in this mutant (O'Reilly *et al.*, 2001). Oocytes were held at V_h for >2 min between pulses in the slow inactivation protocol to allow recovery from slow inactivation caused by previous pulses. To assess the time course of inhibition by SCI insecticides, oocytes were held at a depolarized V_h of -30 mV and sodium currents were measured once every minute during a 20-ms test pulse preceded by a 2-s hyperpolarization to -120 mV to partially recover channels to the resting state except in V787K. In V787K, test pulses

were preceded by a 2-s step to -140 mV from either a V_h of -140 mV or -110 mV because of the enhanced slow inactivation caused by this mutation. Stable sodium currents were recorded for 15 min before insecticide perfusion and sodium currents were typically stable for >60 min in separate control experiments (data not shown). See figure legends for further details of voltage protocols.

Metaflumizone and indoxacarb were purchased from Sigma-Aldrich and ChemService (West Chester, PA), respectively. RH-3421 and RH-4841 were provided by G. Carlson (Rohm and Haas Company, Spring House, PA) and DCJW was a gift from K. Wing (DuPont Agricultural Product, Newark, DE). Stock solutions of insecticides (10 mM) were prepared in dimethyl sulfoxide (DMSO) and were diluted in ND-96 just prior to use to a final concentration of 10 μM, the highest soluble concentration obtainable. The DMSO concentration of the bath perfusate never exceeded 0.1% *v/v*, a concentration that had no effect on sodium currents.

Data was analyzed using Origin 8.1 (OriginLab Corp., Northampton, MA). The voltage dependence of sodium conductance and sodium channel inactivation plots were fitted using the Boltzmann equation [$y = (A_1\text{-}A_2)/\{1 + \exp[(V\text{-}V_{1/2})/k]\} + A_2$] where $V_{1/2}$ is the midpoint of the curve, k is the slope factor, and A_1 and A_2 are the maximum and minimum values in the fit, respectively. I calculated time constants for sodium current inhibition by fitting the time course of inhibition data with a single-exponential decay equation [$y = A_1 * \exp(-x/\tau_1) + y_0$], where x is time, τ_1 is the time constant, and y_0 is the non-inactivating component. All fitted data are given as the mean ± S.E. All statistical analyses were completed using Prism 5.0 (GraphPad Software, La Jolla, CA). The statistical significance of two or more mean values from a single control data set was determined by one-way analysis of variance (ANOVA) and Dunnett's *post-hoc* analysis. Differences were considered statistically significant when $p < 0.05$.

Results

I expressed the wildtype and mutated $Na_v1.4$ sodium channel α subunits in combination with the rat β1 subunit to produce channels that reflect the putative native heteromeric structure and exhibit more native-like gating properties in *Xenopus* oocytes (Isom, 2001). The activation (conductance-voltage) curve was significantly shifted in the direction of depolarization and less steep in $Na_v1.4$/V787A and $Na_v1.4$/V787C than in wildtype (Fig. 4.2A; Table 4.1). Although the V787K mutation did not significantly affect the midpoint potential ($V_{1/2}$) for activation, the slope of the voltage response was less steep compared to wildtype. The $V_{1/2}$ for steady-state fast inactivation was significantly more hyperpolarized in $Na_v1.4$/V787A and $Na_v1.4$/V787K, but not in $Na_v1.4$/V787C compared to wildtype (Fig. 4.2B; Table 4.1).

Amino acid substitutions at V787 strongly affected the propensity of sodium channels to occupy the slow-inactivated state in response to depolarization. In $Na_v1.4$/V787K, slow inactivation developed at more hyperpolarized potentials (~95% slow inactivation at -70 mV) than wildtype (~2% slow inactivation at -70 mV) and the $V_{1/2}$ of the steady-state slow inactivation curve was shifted ~50 mV in the direction of hyperpolarization compared to wildtype (Fig. 4.3; Table 4.1). In contrast, the steady-state probability of slow inactivation was significantly lower in $Na_v1.4$/V787A (~60% slow inactivation at 0 mV) and $Na_v1.4$/V787C (~34% slow inactivation at 0 mV) than in wildtype (~82% slow inactivation at 0 mV), though the midpoint potentials for steady-state slow inactivation in $Na_v1.4$/V787A (-39.8 ± 1.8 mV) and $Na_v1.4$/V787C (-41.4 ± 3.4 mV) did not differ significantly ($p > 0.05$) from that of wildtype (-45.8 ± 0.8 mV; Fig. 4.3; Table 4.1).

SCI insecticides had no effect on sodium currents through wildtype channels at a hyperpolarized holding potential (-120 mV) where channels predominantly occupied the resting

Figure 4.2: Voltage-dependent activation and steady-state fast inactivation of wildtype and mutated $Na_v1.4$ sodium channels. (A) Conductance-voltage plots for sodium channel activation; peak sodium currents measured on depolarization from -120 mV to test potentials ranging from -80 mV to 30 mV were transformed to conductances (G) using the equation $G = I/(V_t-V_{rev})$, where I is the peak current, V_t is the voltage of the test potential, and V_{rev} is the reversal potential; conductances were normalized to the maximal conductance (G_{max}) for that oocyte; values are means ± S.E. of 15 ($Na_v1.4$), 9 ($Na_v1.4$/V787A), 7 ($Na_v1.4$/V787C), or 11 ($Na_v1.4$/V787K) separate experiments with different oocytes. (B) Voltage dependence of steady-state fast inactivation; conditioning pulses (200 ms) from -120 mV to potentials ranging from -100 mV to 0 mV (V_p) were followed immediately by 20-ms test pulses to either -10 mV ($Na_v1.4$, $Na_v1.4$/V787C, $Na_v1.4$/V787K) or 0 mV ($Na_v1.4$/V787A); peak currents were normalized to the maximal current measured during the inactivation protocol for that oocyte; values are means ± S.E. of 11 ($Na_v1.4$), 9 ($Na_v1.4$/V787A), 5 ($Na_v1.4$/V787C), or 4 ($Na_v1.4$/V787K) separate experiments with different oocytes; curves were fitted to the mean values using the Boltzmann equation.

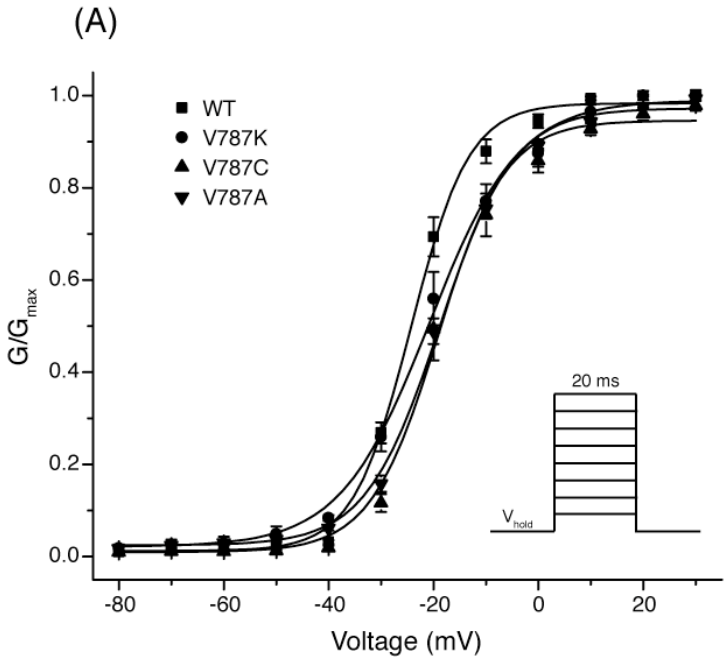
(A)
WT
V787K
V787C
V787A
G/G_max
1.0
0.8
0.6
0.4
0.2
0.0
-80
-60
-40
-20
0
20
Voltage (mV)
20 ms
V_hold

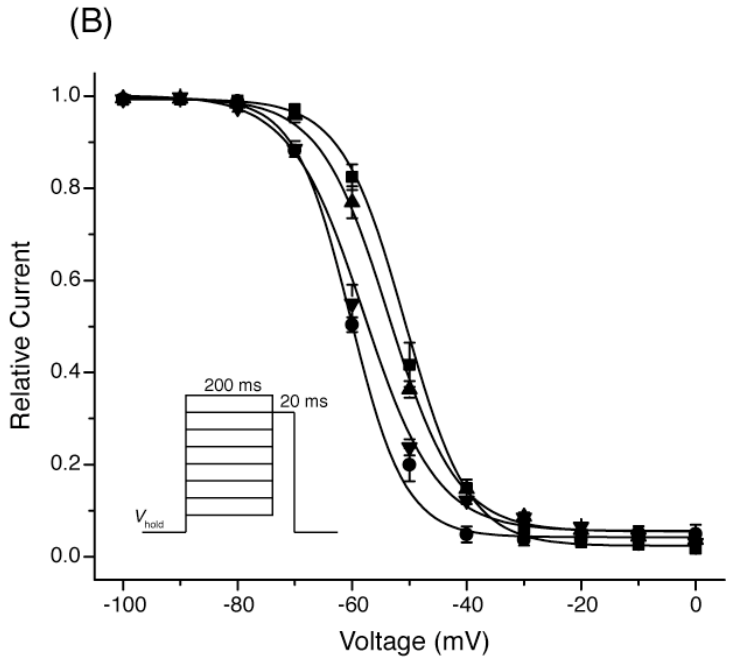
(B)
Relative Current
1.0
0.8
0.6
0.4
0.2
0.0
-100
-80
-60
-40
-20
0
Voltage (mV)
200 ms
20 ms
V_hold

Table 4.1:Voltage-dependent gating parameters for wildtype and V787 mutated $Na_v1.4$ sodium channels [a].

	Activation			Fast inactivation			Slow inactivation		
Channel	$V_{1/2}$ (mV)	k	[n]	$V_{1/2}$ (mV)	k	[n]	$V_{1/2}$ (mV)	k	[n]
$Na_v1.4$	-25.8 ± 0.4	5.0 ± 0.4	[15]	-52.2 ± 0.3	5.5 ± 0.2	[11]	-45.8 ± 0.8	9.4 ± 0.7	[7]
$Na_v1.4$/V787A	-18.8 ± 0.6*	7.0 ± 0.5*	[9]	-59.2 ± 0.6*	5.9 ± 0.5	[9]	-39.8 ± 1.8	10.8 ± 1.6	[4]
$Na_v1.4$/V787C	-18.3 ± 0.6*	6.6 ± 0.5†	[7]	-53.8 ± 0.4	5.6 ± 0.4	[5]	-41.4 ± 3.4	10.4 ± 2.9	[5]
$Na_v1.4$/V787K	-23.9 ± 0.7	6.6 ± 0.6§	[11]	-60.1 ± 0.5*	5.1 ± 0.5	[4]	-92.6 ± 1.2*	11.4 ± 1.0	[6]

[a] Values calculated from fits of mean data (Fig. 4.2 and Fig. 4.3) to the Boltzmann equation; $V_{1/2}$, midpoint potential (mV) for voltage-dependent activation or inactivation; k, slope factor.

Values are significantly different compared to wildtype ($^{*} = p < 0.001$, $^{\S} = p < 0.01$, $^{\dagger} = p < 0.05$; one-way ANOVA with Dunnett's *post-hoc* analysis).

Figure 4.3: Voltage dependence of slow inactivation of wildtype and mutated $Na_v1.4$ sodium channels. Oocytes were clamped at a holding potential (V_h) of either -120 mV ($Na_v1.4$, $Na_v1.4$/V787A, $Na_v1.4$/V787C channels) or -140 mV ($Na_v1.4$/V787K channels) and stimulated with either a 100-s ($Na_v1.4$, $Na_v1.4$/V787A, $Na_v1.4$/V787C) or 10-s ($Na_v1.4$/V787K) conditioning pulse to potentials ranging from V_h to 0 mV (V_p) followed by a 50-ms hyperpolarization to V_h and a test pulse to either -10 mV ($Na_v1.4$, $Na_v1.4$/V787C, $Na_v1.4$/V787K) or 0 mV ($Na_v1.4$/V787A); peak currents were normalized to the maximal current measured during the inactivation protocol for that oocyte; values are means ± S.E. of 7 ($Na_v1.4$, 4 ($Na_v1.4$/V787A), 5 ($Na_v1.4$/V787C), or 6 ($Na_v1.4$/V787K) separate experiments with different oocytes; curves were fitted to the mean values using the Boltzmann equation.

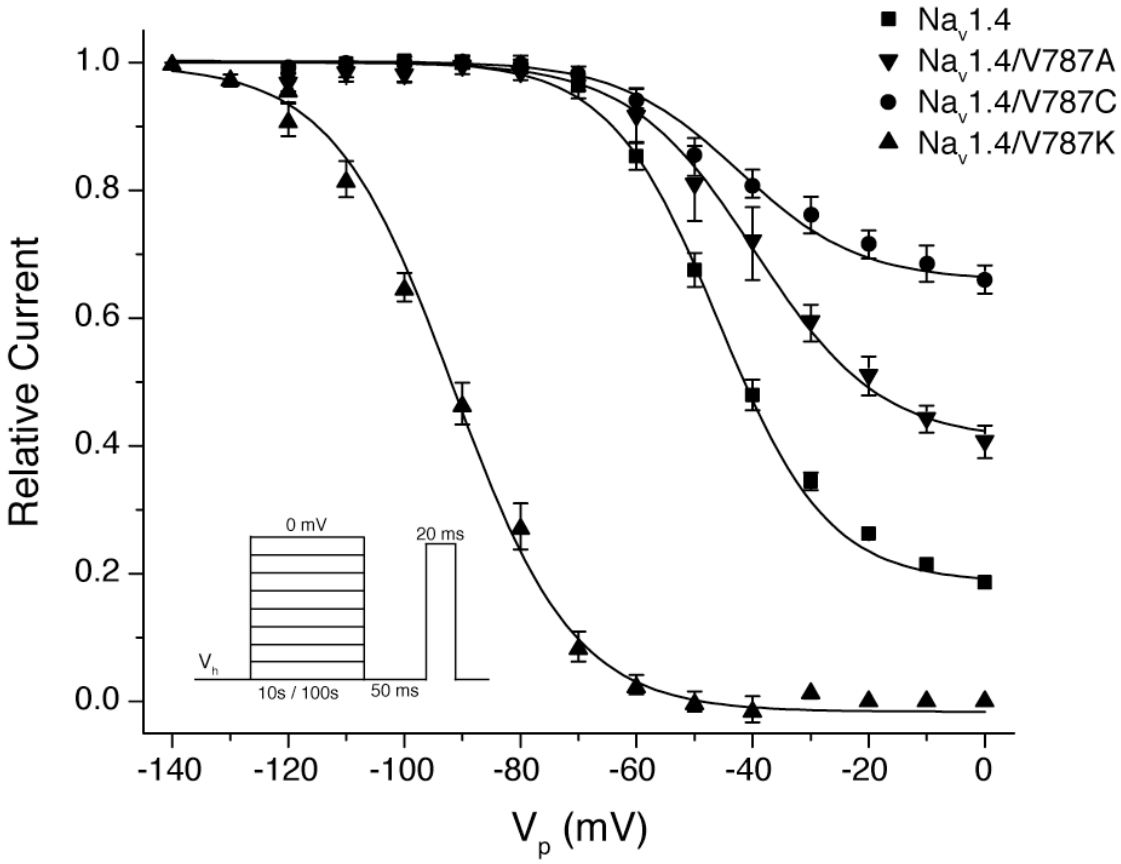
Na$_v$1.4
Na$_v$1.4/V787A
Na$_v$1.4/V787C
Na$_v$1.4/V787K
Relative Current
1.0
0.8
0.6
0.4
0.2
0.0
-140
-120
-100
-80
-60
-40
-20
0
V$_p$ (mV)
0 mV
20 ms
V$_h$
10s / 100s
50 ms

Figure 4.4: Time course of inhibition of (A) $Na_v1.4$, (B) $Na_v1.4$/V787A, (C) $Na_v1.4$/V787C, or (D) $Na_v1.4$/V787K sodium channels by SCI insecticides. Oocytes were clamped at a holding potential (V_h) of either -30 mV ($Na_v1.4$, $Na_v1.4$/V787A, $Na_v1.4$/V787C) or -140 mV ($Na_v1.4$/V787K); sodium currents were measured once every minute with a test pulse (20 ms) preceded by a hyperpolarization (2 s) to either -120 mV ($Na_v1.4$, $Na_v1.4$/V787A, $Na_v1.4$/V787C) or -140 mV ($Na_v1.4$/V787K); currents measured in the presence of an insecticide were normalized to the peak current recorded in that oocyte prior to insecticide perfusion; values are means ± S.E. of 3-5 experiments ($Na_v1.4$), 3-7 ($Na_v1.4$/V787A, $Na_v1.4$/V787C), or 4-5 ($Na_v1.4$/V787K) separate experiments with different oocytes; curves were fitted to the mean values using a single-exponential decay equation.

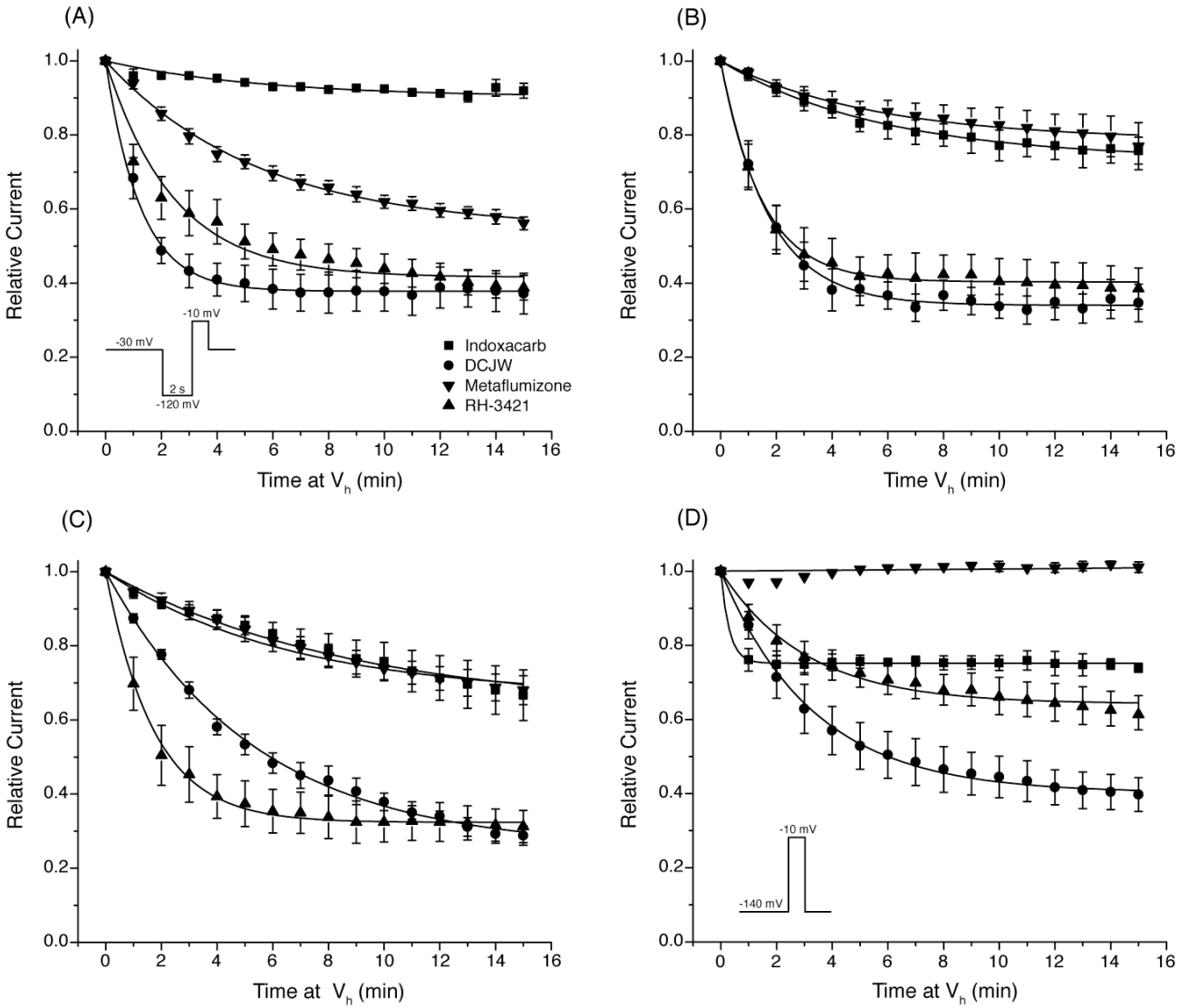
(A)
Relative Current
Time at V_h (min)
-30 mV
-10 mV
2 s
-120 mV
Indoxacarb
DCJW
Metaflumizone
RH-3421
(B)
Relative Current
Time V_h (min)
(C)
Relative Current
Time at V_h (min)
(D)
Relative Current
Time at V_h (min)
-10 mV
-140 mV

state (data not shown). Holding oocytes at a depolarized potential of -30 mV facilitated slow inactivation of wildtype channels and inhibition by SCI insecticides. Fig 4.4A shows the time course of inhibition of $Na_v1.4$ sodium channels by 10 μM indoxacarb, DCJW, metaflumizone, and RH-3421 at a holding potential of -30 mV. After 15 min of exposure, peak transient sodium currents were inhibited 8.3 ± 1.4% (n = 4), 62.8 ± 5.5% (n = 5), 43.9 ± 1.7% (n = 6), and 61.2 ± 3.3% (n = 3) by indoxacarb, DCJW, metaflumizone, and RH-3421, respectively. The time courses of inhibition were fitted best by a single-exponential decay equation that yielded first-order decay constants (τ) of 6.1 ± 1.1 min, 1.3 ± 0.1 min, 5.9 ± 0.6 min, and 1.4 ± 0.3 min for indoxacarb, DCJW, metaflumizone, and RH-3421, respectively.

Initial experiments verified that $Na_v1.4$ channels bearing either the V787A or V787C mutation were insensitive to inhibition by SCI insecticides at a holding potential of -120 mV (data not shown). The time course of inhibition of sodium currents through $Na_v1.4$/V787A (Fig 4.4B) and $Na_v1.4$/V787C (Fig. 4.4C) by SCI insecticides was assessed at a holding potential of -30 mV. At this potential, inhibition by indoxacarb after 15 min of perfusion was significantly greater in $Na_v1.4$/V787A (24.2 ± 3.6%; $p < 0.05$; n = 4) and $Na_v1.4$/V787C (33.3 ± 6.8%; $p < 0.01$; n = 7) than in wildtype. In contrast, the extent of inhibition by metaflumizone was significantly lower in $Na_v1.4$/V787A (20.4 ± 5.5% after 15 min; $p < 0.001$; n = 5), whereas inhibition by metaflumizone in $Na_v1.4$/V787C was not significantly ($p > 0.05$; n = 4) different from wildtype. Inhibition by DCJW or RH-3421 was not significantly ($p > 0.05$; $n \geq 3$) different in either $Na_v1.4$/V787A or $Na_v1.4$/V787C compared to wildtype. However, the V787C mutation significantly retarded the rate of onset of inhibition by indoxacarb (t = 11.9 ± 3.5 min; $p < 0.001$; n = 5) and DCJW (t = 4.5 ± 0.3 min; $p <$ 0.001; n = 4) compared to wildtype. Inhibition of $Na_v1.4$/V787C by indoxacarb and DCJW did not reach a steady-state plateau after 15 min of perfusion, so my results may underestimate the

extent to which this mutation enhanced inhibition by the oxadiazine insecticides.

I initially examined the time course of inhibition of $Na_v1.4$/V787K by SCI insecticides at a hyperpolarized holding potential of -140 mV (Fig. 4.4D) because of the propensity of this channel to enter slow inactivation at more hyperpolarized potentials (Fig 4.3). Limitations of the experimental system prohibited me from achieving a stable voltage-clamp of the membrane at potentials more hyperpolarized than -140 mV for the time (> 25 min) required to measure the slow inhibition of sodium channels by SCI insecticides. Sodium currents through $Na_v1.4$/V787K channels were significantly inhibited by 10 μM indoxacarb (26.3 ± 1.5%; *n* = 4), DCJW (60.3 ± 4.6%; *n* = 4), and RH-3421 (38.6 ± 5.1%; *n* = 4) after 15 min of perfusion, but were completely resistant to inhibition by 10 μM metaflumizone (*n* = 4). Inhibition by indoxacarb reached a steady-state level after about 1 min of perfusion, whereas DCJW and RH-3421 required ~15 min of perfusion to approach an apparent steady-state inhibition. First order fits of the time course of sodium current inhibition by DCJW and RH-3421 yielded time constants of 3.7 ± 0.2 min (*n* = 4) and 3.7 ± 0.4 min (*n* = 4), respectively. The rapid onset of inhibition by indoxacarb prevented an accurate first-order exponential decay fit of the time course of inhibition at a stimulation frequency of once per minute (0.0167 Hz).

To determine if insecticide block of $Na_v1.4$/V787K at -140 mV reflected insecticide binding to channels in the slow-inactivated state, I examined the effect that hyperpolarization to -150 mV had on the size of the peak sodium current in both the absence and presence of 10 μM indoxacarb (Fig. 4.5). Sodium current amplitudes increased in both the absence and presence of indoxacarb in response to hyperpolarization of the membrane to -150 mV. Oocytes were stimulated at a frequency of 0.05 Hz, which facilitated the onset of inhibition by indoxacarb to be fitted best by a first order decay function, which yielded a time constant of 0.7 ± 0.1 min (*n* = 7).

The extent of $Na_v1.4$ sodium channel inhibition by metaflumizone is strongly dependent

Figure 4.5: Effect of hyperpolarization on $Na_v1.4$/V787K currents and their inhibition by indoxacarb. Oocytes were clamped at a holding potential of (V_h) of -140 mV for 5 min followed by 5 min at a V_h of -150 mV while stimulated at a rate of 0.05 Hz with test pulse (20 ms) to -10 mV; sodium currents were normalized to the maximum current recorded in the same oocyte at -140 mV prior to indoxacarb perfusion; values are means ± S.E. of 7 separate experiments in different oocytes; curves were fitted to the mean values using a single-exponential decay equation.

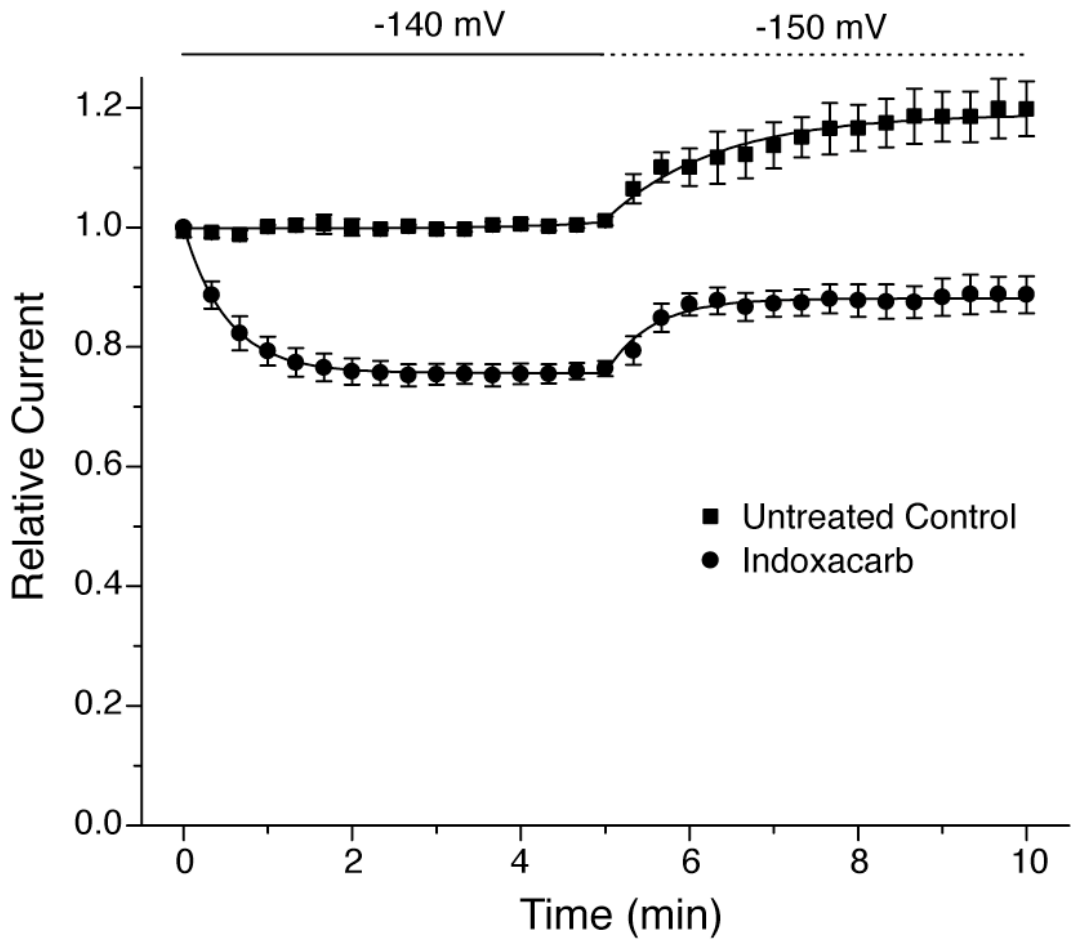
-140 mV
-150 mV
Relative Current
1.2
1.0
0.8
0.6
0.4
0.2
0.0
0
2
4
6
8
10
Time (min)
Untreated Control
Indoxacarb

on the relative fraction of channels in the slow-inactivated state (Chapter 3). Therefore, to determine if the resistance of $Na_v1.4$/V787K channels to inhibition by metaflumizone at -140 mV (Fig. 4.4D) reflected a relatively low steady-state probability of slow inactivation, I examined the time course of inhibition of currents through $Na_v1.4$/V787K channels at a more depolarized holding potential of -110 mV (Fig. 4.6). Holding oocytes at this potential in the absence of insecticides reduced the peak sodium current amplitude over several minutes to ~50% of the maximum current elicited from a holding potential of -140 mV (Fig. 4.6A), an extent of apparent slow inactivation that was comparable to the partial slow inactivation produced in wildtype channels at -30 mV (Fig. 4.6B). However, it is likely there was greater fractional slow inactivation in $Na_v1.4$/V787K at -110 mV compared to wildtype channels at -30 mV because some slow inactivation in $Na_v1.4$/V787K was evident at -140 mV (Fig. 4.5). The time course of the onset of $Na_v1.4$/V787K inhibition by SCI insecticides at -110 mV is illustrated in Fig. 4.6C and shows there was no difference in the extent of metaflumizone block compared to -140 mV (Fig. 4.4D). The statistical analyses of these data in comparison to inhibition of currents through wildtype channels after 15 min of perfusion at -30 mV are summarized in Fig. 4.6D. At a holding potential of -110 mV, the V787K mutation paradoxically increased sensitivity to 10 μM indoxacarb and conferred resistance to 10 μM metaflumizone, whereas the extent of inhibition by 10 μM DCJW and RH-3421 was not significantly different from wildtype. I also examined the impact of the V787K mutation on inhibition by RH-4841, a SCI insecticide that resembles a heterocylic ring-closed analog of metaflumizone. Sodium currents through $Na_v1.4$/V787K channels were significantly more sensitive to 10 μM RH-4841 than wildtype after 15 min of perfusion (Fig. 4.6D).

Figure 4.6: Comparative inhibition of $Na_v1.4$ and $Na_v1.4$/V787K sodium channels by SCI insecticides. (A) Representative sodium current traces from an oocyte expressing $Na_v1.4$/V787K at a holding potential of -140 mV and -110 mV in the absence of insecticides. (B) Representative sodium current traces from an oocyte expressing $Na_v1.4$ sodium channels at a holding potential (V_h) of -120 mV and -30 mV in the absence of SCI insecticides. (C) Time course of inhibition of $Na_v1.4$/V787K by SCI insecticides; oocytes were clamped at a V_h of -110 mV and stimulated once every minute with a test pulse (20 ms) to -10 mV preceded by a hyperpolarization (2 s) to -140 mV; currents measured in the presence of an insecticide were normalized to the peak sodium current recorded in that oocyte prior to insecticide perfusion; values are means ± S.E. of 5-7 separate experiments with different oocytes; curves were fitted to the mean values using a single-exponential decay equation. (D) Comparison of the fractional inhibition of $Na_v1.4$ (Fig. 4A) and $Na_v1.4$/V787K channels by SCI insecticides after 15 min of insecticide perfusion at a holding potential of either -30 ($Na_v1.4$) or -110 mV ($Na_v1.4$/V787K).

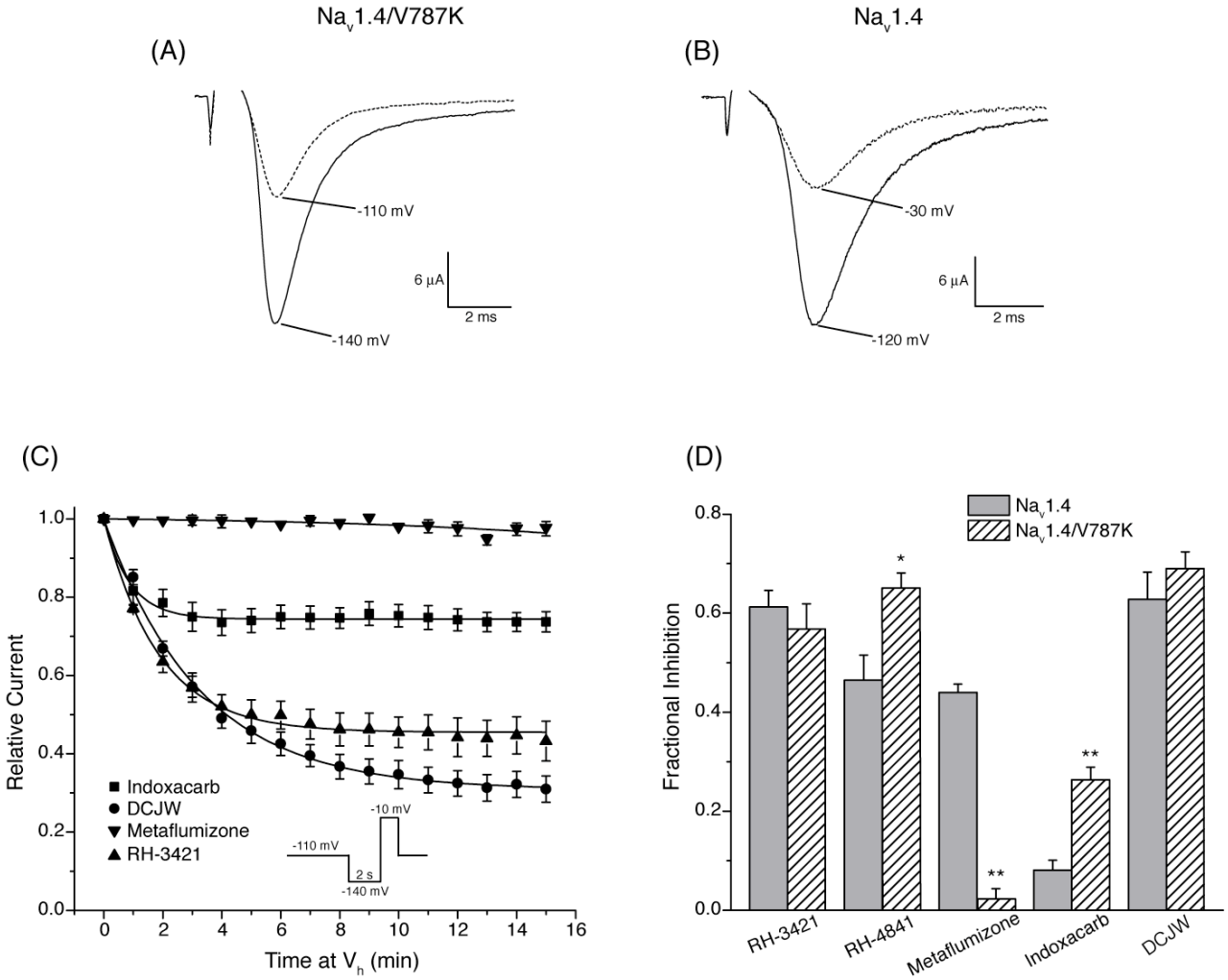
Na$_v$1.4/V787K
(A)
-110 mV
-140 mV
6 µA
2 ms
Na$_v$1.4
(B)
-30 mV
-120 mV
6 µA
2 ms
(C)
Relative Current
Time at V$_h$ (min)
Indoxacarb
DCJW
Metaflumizone
RH-3421
-10 mV
-110 mV
2 s
-140 mV
(D)
Na$_v$1.4
Na$_v$1.4/V787K
Fractional Inhibition
RH-3421
RH-4841
Metaflumizone
Indoxacarb
DCJW

Discussion

The current hypothesis for the state-dependent action of SCI insecticides on voltage-gated sodium channels proposes that inhibition involves a selective interaction with channels in the slow-inactivated state. The primary objective of this study was to determine if insecticide block of $Na_v1.4$ sodium channels was modulated by specific mutations at V787 in DII-S6 that exhibited altered slow inactivation. The rat skeletal muscle sodium channel ($Na_v1.4$) was chosen for the present study because it is a well-defined model system for studying the actions of SCI insecticides on cloned mammalian sodium channels (Silver and Soderlund, 2005b; Silver and Soderlund 2007). The use of $Na_v1.4$ also ensured that mutations at V787 yielded the expected residue-specific effects on slow inactivation that have been reported elsewhere (O'Reilly *et al.*, 2001). Furthermore, oocytes expressing $Na_v1.4$ channels consistently gave robust sodium currents that facilitated the reliable recording of currents under experimental conditions that promoted partial channel inactivation and insecticide block.

The effects of mutations at residue V787 on slow inactivation reported here are fully consistent with previous studies of these mutations in mammalian cells without the β1 subunit (O'Reilly *et al.*, 2001). Slow inactivation was severely inhibited in $Na_v1.4$/V787C and to a lesser extent in $Na_v1.4$/V787A, whereas slow inactivation in $Na_v1.4$/V787K was significantly enhanced compared to wildtype. The voltage dependence of slow inactivation in V787K was shifted ~50 mV in the direction of hyperpolarization compared to wildtype, which is quantitatively consistent with previous results (O'Reilly *et al.*, 2001). These studies also reported that the voltage dependence of steady-state slow inactivation in V787A and V787C was shifted ~24 mV in the direction of depolarization but I did not observe such dramatic shifts for these mutations compared to wildtype. These discrepancies may reflect differences in experimental conditions,

such as the choice of expression system, presence of the β1 subunit, or differences in the duration of conditioning prepulses used to assay slow inactivation (30 versus 100 s).

The interpretation of results from studies using site-directed mutagenesis to map binding determinants of state-dependent sodium channel inhibitors inside the inner pore are often confounded by the fact that mutations in this region of the channel can indirectly affect binding *via* modification of gating (Mike and Lukacs, 2010). However, my data for the effects of mutations at residue V787 on insecticide sensitivity cannot be fully explained by changes in slow inactivation gating. For example, the V787K mutation strongly enhanced slow inactivation relative to wildtype but completely abolished block by 10 μM metaflumizone. Furthermore, both V787A and V787C mutations destabilized slow inactivation but increased the sensitivity to block by indoxacarb compared to wildtype. These results indicate that the altered insecticide sensitivities caused by mutations at V787 do not correlate with the altered slow inactivation gating properties in mutated channels.

Although SCI insecticides are functionally unified by a common mechanism of action, this action is achieved by compounds with a variety of structures. The dihydropyrazoles (*e.g.* RH-3421 and RH-4841) contain a central pyrazoline ring, whereas indoxacarb contains a fused 3-ring system incorporating an oxadiazine ring and metaflumizone contains a linear semicarbazone motif in place of central heterocyclic elements. Although metaflumizone can be viewed as a ring-opened analog of RH-4841, the greater rotational flexibility conferred by the semicarbazone motif distinguishes it from other compounds in this insecticide class, which are very rigid, nearly planar molecules (Wellinga *et al.*, 1977; Grosscurt *et al.*, 1979; Hasan *et al.*, 1996).

The extent of use-dependent inhibition of fast-inactivated $Na_v1.4$ sodium channels by lidocaine was selectively attenuated by metaflumizone but not RH-4841 or DCJW (Chapter 3).

These data suggest that the state-dependent insecticide-channel interactions for metaflumizone may differ from other compounds in this insecticide class and may involve different binding determinants. Here, I have shown that mutations at residue V787 affect SCI insecticide sensitivity in a compound-specific manner. All mutations at V787 that I tested significantly increased the sensitivity to inhibition by indoxacarb, whereas metaflumizone sensitivity was significantly reduced in $Na_v1.4$/V787A and $Na_v1.4$/V787K compared to wildtype. Interestingly, the extent of inhibition by RH-4841 was significantly increased in $Na_v1.4$/V787K compared to wildtype. None of the mutations at residue V787 appeared to significantly affect the extent of inhibition by DCJW or RH-3421. These data indicate that the molecular determinants for the binding of SCI insecticides may not be identical for all members of this insecticide class. Consistent with this possibility, Silver and Soderlund (2005b) showed that co-application of indoxacarb was effective at reducing the sodium channel-blocking efficacy of DCJW but not RH-3421.

The orientation of the S6 helices of sodium channel domains I, II, and III in relation to the ion pore is uncertain (Mike and Lukacs, 2010). The orientation of DII-S6 is particularly ambiguous because no residues in this segment have been directly implicated in the binding of SCI drugs. Mike and Lukacs (2010) recently proposed a plausible orientation of the four S6 helices in the rat $Na_v1.2$ sodium channel. According to their model, residue V974 (analogous to V787 in $rNa_v1.4$) in DII-S6 is "buried" within the protein interface between domains II and III, at least in the open or fast-inactivated channel states that are the high-affinity conformations for the binding of numerous SCI drugs. Experiments using the substituted-cysteine accessibility method have demonstrated that the thiol group on V787C is only susceptible to covalent modification by the sulfhydryl-reactive agent methanethiosulfonate ethylammonium (MTSEA) under select experimental conditions that promote slow inactivation (O'Reilly *et al.*, 2001). These results

demonstrate that slow inactivation in sodium channels is associated with molecular rearrangement(s) at or near the V787 position. However, it is not clear whether MTSEA accesses the V787C residue via a hydrophilic (*i.e.* the pore) or a hydrophobic pathway (*i.e*. the membrane) since a significant fraction of MTSEA is un-protonated and neutral at physiological pH and can therefore reach the site through either pathway (O'Reilly *et al.*, 2001). Analogous experiments (O'Reilly and Shockett, 2006; Chancey *et al.*, 2007) were performed in the human $Na_v1.5$ sodium channel and have yielded similar results, suggesting that molecular rearrangement at or near V787 in DII-S6 plays an important role in conformational changes underlying slow inactivation.

At present, it cannot be clearly determined whether mutations at V787 affect individual SCI insecticide binding either directly or indirectly via allosteric changes. For indoxacarb, the increase in sensitivity caused by all three mutations at V787 was not well-correlated with the size or physiochemical properties of the substituted amino acid, which suggests that this residue does not likely contribute directly to the binding site for indoxacarb. I postulate that the increase in indoxacarb affinity caused by mutations at V787 may reflect an alleviation of steric hindrance that normally impedes the interaction between the insecticide and its receptor, as suggested for rat $Na_v1.4$ channels bearing the Y1586A mutation in DIV-S6 (Silver and Soderlund, 2007). In contrast, the effects of mutations at V787 on metaflumizone affinity were well-correlated with the hydrophobicity of the substituted amino acid. Replacing the native hydrophobic valine with a hydrophobic cysteine did not significantly affect metaflumizone affinity, whereas a less hydrophobic alanine substitution significantly lowered metaflumizone sensitivity and a hydrophilic lysine substitution rendered the channels completely insensitive to inhibition by 10 μM metaflumizone. These data suggest that V787 may participate directly with metaflumizone binding to slow-inactivated channels through hydrophobic interactions.

Further experiments involving replacement of Val787 amino acids with a broader range of physiochemical properties are needed to more definitively assess the involvement of V787 in metaflumizone binding. Nevertheless, my data provide provocative evidence that this residue directly interacts with metaflumizone. I conclude from these data that mutations at V787 modulate SCI insecticide sensitivity in a compound-specific manner that is independent of mutation-induced changes in slow inactivation gating. The data presented here provide new evidence for the involvement of residues outside the local anesthetic drug receptor in the binding and action of select SCI insecticides.

References

Bezanilla F and Armstrong CM (1977) Inactivation of the sodium channel. *J. Gen. Physiol.* **70**:549-566.

Catterall WA (1976) Membrane potential dependent binding of scorpion toxin to action potential Na^+ channel ionophore. *Proc. Natl. Acad. Sci. USA* **73**:2682-2686.

Chancey JH, Shockett PE and O'Reilly JP (2007) Relative resistance to slow inactivation of human cardiac Na^+ channel $hNa_v1.5$ is reversed by lysine or glutamine substitution at V930 in D2-S6. *Am. J. Physiol. Cell. Physiol.* **293**: C1895-C1905.

Goldin AL (1992) Maintenance of *Xenopus laevis* and oocyte injection. *Methods Enzymol.* **207**:266-297.

Grosscurt AC, van Hes R and Wellinga, K (1979) 1-Phenylcarbamoyl-2-pyrazolines, a new class of insecticides. 3. Synthesis and insecticidal properties of 3,4-diphenyl-1-phenylcarbamoyl-2-pyrazolines. *J. Agric. Food Chem.* **27**:406-409.

Hasan R, Nishimura K, Okada M, Akamatsu M, Inoue M and Ueno T (1996) Stereochemical basis for the insecticidal activity of carbamoylated and acylated pyrazoline. *Pestic. Sci.* **46**:105-112.

Isom I (2001) Sodium channel β subunits: anything but auxiliary. *Neuroscientist* **7**:42-54.

Kallen RG, Sheng ZH, Yang J, Chen L, Rogart RB and Barchi RL (1990) Structure and expression of a sodium channel characteristic of denervated skeletal muscle. *Neuron* **4**:233-242.

Lapied B, Grolleau F and Satelle DB (2001) Indoxacarb, an oxadiazine insecticide, blocks insect neuronal sodium channels. *Brit. J. Pharmacol.* **132**:587-595.

Mike A and Lukacs P (2010) The enigmatic drug binding site for sodium channel inhibitors. *Curr. Mol. Pharmacol.* **3**:129-144.

O'Reilly JP, Wang S-Y and Wang GK (2001) Residue-specific effects on slow inactivation at V787 in D2-S6 of $Na_v1.4$ sodium channels. *Biophys. J.* **81**:2100-2111.

O'Reilly JP and Shockett PE (2006) Slow-inactivation induced conformational change in domain 2-segment 6 of cardiac Na^+ channel. *Biochem. Biophys. Res. Commun.* **345**:59-66.

Payne GT, Deecher DC and Soderlund DM (1998) Structure-activity relationships for the action of dihydropyrazole insecticides on mouse brain sodium channels. *Pestic. Biochem. Physiol.* **60**:177-185.

Ragsdale DS, McPhee JC, Scheuer T and Catterall WA (1994) Molecular determinants of state-dependent block of Na^+ channels by local anesthetics. *Science* **265**:1724-1728.

Ragsdale DS, McPhee JC, Scheuer T and Catterall WA (1996) Common molecular determinants of local anesthetic, antiarrhythmic, and anticonvulsant block of voltage-gated Na^+ channels. *Proc. Natl. Acad. Sci. USA* **93**:9270-9275.

Salgado VL (1990) Mode of action of insecticidal dihydropyrazoles: selective block of impulse generation in sensory nerves. *Pestic. Sci.* **28**:389-411.

Salgado VL (1992) Slow voltage-dependent block of sodium channels in crayfish nerve by dihydropyrazole insecticides. *Mol. Pharmacol.* **41**:120-126.

Salgado VL and Hayashi JH (2007) Metaflumizone is a novel sodium channel blocker insecticide. *Vet. Parasitol.* **150**:182-189.

Silver KS and Soderlund DM (2005a) Action of pyrazoline-type insecticides at neuronal target sites. *Pestic. Biochem. Physiol.* **81**:136-143.

Silver KS and Soderlund DM (2005b) State-dependent block of rat $Na_v1.4$ sodium channels expressed in *Xenopus* oocytes by pyrazoline-type insecticides. *Neurotox.* **26**:397-406.

Silver KS and Soderlund DM (2006) Differential sensitvity of rat voltage-sensitive sodium channel isoforms to pyrazoline-type insecticides. *Toxicol. Appl. Pharmacol.* **214**:209-217.

Silver KS and Soderlund DM (2007) Point mutations at the local anesthetic receptor site modulate the state-dependent block of rat $Na_v1.4$ sodium channels by pyrazoline-type insecticides. *Neurotox.* **28**:655-663.

Smith TJ and Soderlund DM (1998) Action of the pyrethroid insecticide cypermethrin on rat brain IIa sodium channels expressed in *Xenopus* oocytes. *Neurotox.* **19**:823-832.

Tatebayashi H and Narahashi T (1994) Differential mechanism of action of the pyrethroid tetramethrin on tetrodotoxin-sensitive and tetrodotoxin resistant sodium channels. *J. Pharmacol. Exp. Ther.* **270**:595-603.

Wellinga K, Grosscurt AC and van Hes R (1977) 1-Phenylcarbamoyl-2-pyrazoline: a new class of insecticides. 1. Synthesis and insecticidal properties of 3-phenyl-1-phenylcarbamoyl-2-pyrazoline. *J. Agric. Food. Chem.* **25**:987-992.

Wing KD, Andaloro JT, McCann SF and Salgado VL (2005) Indoxacarb and the sodium channel blocker insecticides: chemistry, physiology, and biology in insects, in *Comprehensive Molecular Insect Science* (Gilbert LI, Iatrou K, and Gill SS eds) pp 30–53, Elsevier, New York.

Yarov-Yarovoy V, Brown J, Sharp EM, Clare JJ, Scheuer T and Catterall WA (2001) Molecular determinants of voltage-dependent gating and binding of pore-blocking drugs in transmembrane segment IIIS6 of the Na^+ channel α subunit. *J. Bio. Chem.* **276**:20-27.

Yarov-Yarovoy V, McPhee JC, Idsvoog D, Pate C, Scheuer T and Catterall WA (2002) Role of amino acid residues in transmembrane segments IS6 and IIS6 of the Na^+ channel α subunit in voltage-dependent gating and drug block. *J. Bio. Chem.* **277**:35393-35401.

Zhao X, Ikeda T, Yeh JZ and Narahashi T (2003) Voltage-dependent block of sodium channels in mammalian neurons by the oxadiazine insecticide indoxacarb and its metabolite DCJW. *Neurotox.* **24**:83-96.

CHAPTER FIVE

CONCLUSIONS AND FUTURE DIRECTIONS

Discrete Mechanisms of Slow Inactivation in Voltage-Gated Sodium Channels

Slow inactivation in voltage-gated sodium channels is a heterogeneous biophysical process that regulates sodium channel excitability over extended periods of time. In $Na_v1.4$ sodium channels expressed in *Xenopus laevis* oocytes, multiple kinetically distinct types of slow inactivation have been identified (intermediate, slow, ultra-slow inactivation) but the molecular distinction between these is unclear.

SCI insecticides have been reported to selectively inhibit $Na_v1.4$ sodium channels in the slow-inactivated state (Silver and Soderlund, 2005, 2007). However, the heterogeneity of slow inactivation in $Na_v1.4$ channels expressed in *Xenopus* oocytes in the absence of the β1 subunit confounds previous analyses of the state-dependent details of SCI insecticide action in this system. Therefore, it was first necessary for me to characterize slow inactivation in detail to determine the experimental conditions necessary to study the state-dependent action of SCI insecticides.

My results, presented in Chapter 2, showed that intermediate and slow inactivation in $Na_v1.4$ sodium channels expressed in *Xenopus* oocytes differed significantly in their voltage dependence, with intermediate inactivation occurring at more depolarized membrane potentials. Coexpression with the β1 subunit markedly inhibited intermediate inactivation, but only marginally impeded slow inactivation. Further, cysteine substitution at residue V787 in DII-S6 inhibited slow inactivation but did not disrupt intermediate inactivation. These data reveal that the intermediate- and slow-inactivated states are functionally distinct sodium channel

conformations that exhibit unique voltage dependence of gating. These data are consistent with previous studies demonstrating that the intermediate- and slow-inactivated states of $Na_v1.4$ channels are pharmacologically distinct with respect to their relative affinities for the local anesthetic lidocaine (Kambouris *et al.*, 1998).

Action of Metaflumizone on Mammalian Voltage-Gated Sodium Channels

The second experimental objective of this dissertation project was to investigate the state-dependent action of metaflumizone, a newly-commercialized insecticide in the animal health market, on mammalian voltage-gated sodium channels. Recent studies have demonstrated that metaflumizone is a potent state-dependent inhibitor of insect voltage-gated sodium channels (Salgado and Hayashi, 2007; Silver *et al.*, 2009).

My results, presented in Chapter 3, showed that rat $Na_v1.4$ sodium channels expressed in *Xenopus* oocytes were insensitive to metaflumizone application at hyperpolarized membrane potentials, where channels were predominantly in the resting state. However, metaflumizone caused significant reductions in the availability of sodium channels at depolarized membrane potentials that facilitated slow inactivation. Moreover, metaflumizone significantly shifted the voltage dependence of slow inactivation in the direction of hyperpolarization. Thus, the effects of metaflumizone on mammalian voltage-gated sodium channels are qualitatively consistent with other SCI insecticides, as well as previous studies with metaflumizone on insect sodium channels.

Data from this dissertation project also suggest that metaflumizone interacts with resting and fast-inactivated channels without blocking them in a manner that is distinct from other compounds in this insecticide class. Application of metaflumizone at a hyperpolarized membrane

potential caused a significant depolarizing shift in the voltage dependence of activation and reduced the amplitude of the sodium current measured at potentials of sub-maximal activation. Previous studies have indicated that other SCI insecticides (e.g. RH3421, indoxacarb, or DCJW) do not affect the voltage dependence of activation for rat $Na_v1.4$ channels expressed in *Xenopus* oocytes (Silver and Soderlund, 2005), TTX-S or TTX-R sodium channels in rat DRG neurons (Tsurubuchi *et al.*, 2001; Tsurubuchi and Kono, 2003; Zhao *et al.*, 2003), or sodium channels in cockroach DUM neurons (Lapied *et al.*, 2001). The observed shift in the voltage dependence of activation by metaflumizone implies an interaction of this compound with $Na_v1.4$ channels in the resting state that does not result in inhibition. Furthermore, in the absence of channel inhibition, metaflumizone selectively antagonized the use-dependent inhibition of fast-inactivated sodium channels by the local anesthetic lidocaine. These data imply that metaflumizone also interacts with $Na_v1.4$ sodium channels in the fast-inactivated state. There is only one other instance of SCI insecticides binding to, but not inhibiting sodium channels in a non-slow-inactivated conformation. Exposure of sodium channels in rat DRG neurons to indoxacarb or DCJW at a hyperpolarized membrane potential, at which no inhibition is observed, accelerates the subsequent entry of channels into the slow-inactivated state (Zhao *et al.*, 2003).

Site-directed mutagenesis experiments indicate that residues in DIV-S6, identified previously as molecular determinants of therapeutic drug binding (Ragsdale *et al.*, 1994; Ragsdale *et al.*, 1996; Li *et al.*, 1999), also are important determinants of SCI insecticide action (Silver and Soderlund, 2007). In particular, alanine substitution at residue F1579 significantly reduces the affinity of rat $Na_v1.4$ channels for SCI insecticides, whereas alanine substitution at residue Y1586 paradoxically increases the affinity for SCI insecticides. My results showed that alanine substitution at F1579 or Y1586 produced marked effects on the sensitivity of $Na_v1.4$ sodium channels to inhibition by metaflumizone. Whereas the F1579A mutation significantly

reduced the sensitivity of channels to inhibition by metaflumizone, the Y1586A mutation increased channel sensitivity compared to wildtype. These data indicate that metaflumizone shares common molecular determinants in DIV-S6 of $Na_v1.4$ sodium channels with other SCI insecticides and therapeutic drugs.

State-Dependent Mechanism of Sodium Channel Inhibition by SCI Insecticides

The current model for the inhibition of voltage-gated sodium channels by SCI insecticides is derived from the "modulated receptor hypothesis" (Hille, 1977), originally proposed to account for the voltage-dependent properties of sodium channel inhibition by local anesthetic drugs. The modulated receptor model predicts that changes in channel conformation that occur during channel gating alter the binding sites of drug molecules, thereby modulating the binding affinity of the receptor for therapeutic agents. Accordingly, the local anesthetic receptor, which binds therapeutic agents, has a higher binding affinity in the inactivated state than in the resting state. The binding of drug molecules in the inactivated state stabilizes this nonconducting channel conformation, thus reducing sodium channel availability and causing hyperpolarizing shifts in the voltage dependence of inactivation (McDonough and Bean, 2006).

SCI insecticides selectively inhibit mammalian voltage-gated sodium channels at depolarized membrane potentials that promote slow inactivation. Further, the insecticides cause hyperpolarizing shifts in the voltage dependence of slow inactivation for rat $Na_v1.4$ sodium channels (Chapter 3; Silver and Soderlund, 2005) and channels in rat DRG neurons (Zhao *et al.*, 2003). These data are consistent with a model proposed by Salgado (1992) in which SCI insecticides selectively inhibit voltage-gated sodium channels in the high-affinity slow-inactivated state. However, the apparent interactions between SCI insecticides and sodium

channels in the resting and fast-inactivated state (Chapter 3; Zhao *et al.*, 2003) in the absence of channel inhibition challenges the exclusive involvement of slow inactivation in the binding and action of these compounds.

The third objective of this dissertation project was to use site-directed mutagenesis to specifically alter slow inactivation in $Na_v1.4$ sodium channels and examine the effects on inhibition by SCI insecticides. Amino acid substitutions at residue V787 in DII-S6 modulate slow inactivation in rat $Na_v1.4$ sodium channels in a residue-specific manner (O'Reilly *et al.*, 2001). My results, presented in Chapter 4, showed that amino acid substitutions at V787 produced compound-specific effects on SCI insecticide potency that were independent of mutation-induced changes in slow inactivation. The V787K mutation, which enhanced slow inactivation, conferred resistance to metaflumizone, enhanced the sensitivity for indoxacarb and RH4841, and did not affect the sensitivity to DCJW or RH3421 compared to wildtype channels. The V787C mutation, which inhibited slow inactivation, enhanced the sensitivity for indoxacarb without significantly affecting that of metaflumizone, DCJW, or RH3421. Additionally, the V787A mutation, which also inhibited slow inactivation, enhanced the sensitivity for indoxacarb, reduced that of metaflumizone, and did not affect the sensitivity for DCJW or RH3421. The reduction in the extent of channel inhibition by metaflumizone caused by mutations at V787 appeared to correlate with the reduced hydrophobicity of the substituted side chain, whereas mutations at this position either enhanced or did not effect inhibition by other SCI insecticides tested. I conclude from these data that V787 may be a unique determinant of metaflumizone binding (Fig. 5.1). Previous studies with SCI insecticides on rat $Na_v1.4$ sodium channels expressed in *Xenopus* oocytes demonstrated that indoxacarb interferes with the inhibitory efficiency of DCJW but not RH3421, suggesting further that different chemical classes of SCI insecticides may bind to overlapping but non-identical sites (Silver and Soderlund, 2005).

Toxicological and Pharmacological Significance

Earlier compounds in the SCI insecticide class, from which indoxacarb and metaflumizone are chemically derived, were not developed into commercial insecticides due to their high sub-acute toxicity in mammals. Therefore, understanding the molecular mechanisms that may underlie the high sub-acute toxicity is vital from a human health perspective. Because metaflumizone is the first SCI insecticide in the animal health market, it is also the first compound in this insecticide class to which mammals are intentionally exposed.

Metaflumizone inhibited rat $Na_v1.4$ sodium channels in a slow-inactivated state-dependent manner (Chapter 3) that was consistent with its mode of action in insects (Salgado and Hayashi, 2007; Silver *et al.*, 2009). However, metaflumizone appears to interact with mammalian sodium channels in a manner that is distinct from other classes of SCI insecticides (Chapter 3). Further, the conformational flexibility of metaflumizone, and results from mutagenesis studies in support of this dissertation (Chapter 4), suggest that metaflumizone has binding determinants that are distinct from other SCIs insecticides. These differences may partially explain the reduced-risk toxicity of metaflumizone compared to most experimental compounds.

Although the majority of therapeutic SCI drugs preferentially target channels in the activated or fast-inactivated state, there are an increasing number of therapeutic agents that appear to selectively inhibit channels in the slow-inactivated state. The antihypertensive drug mibefradil (McNulty and Hanck, 2004), the anticonvulsant lacosamide (Errington *et al.*, 2008), and a new experimental drug for neuropathic pain Z123212 (Hildebrand *et al.*, 2011) all preferentially target sodium channels in the slow-inactivated state. However, unlike most SCI

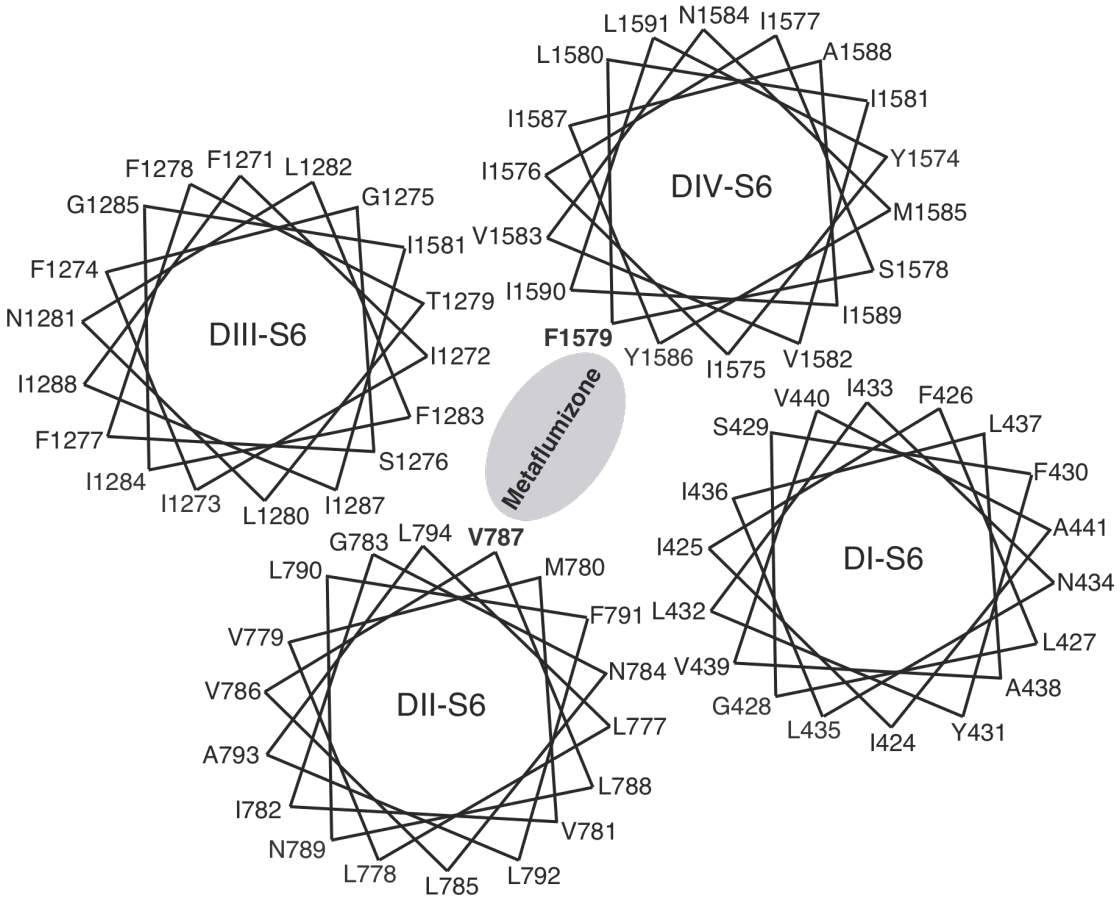

Figure 5.1: Proposed orientation of the four S6 helices of the rat $Na_v1.4$ sodium channel around the channel pore in the slow-inactivated conformation; residues implicated in metaflumizone binding are shown in **bold**.

drugs, the kinetics of sodium channel inhibition by insecticides is very slow, on the order of several minutes. The unique properties and structure-activity relationships of SCI insecticides makes them additional novel and unique chemical probes of the architecture of the inner pore in the slow-inactivated conformation.

The S6 transmembrane helices of each of the four sodium channel domains are thought to line the inner pore. The predicted orientation of the S6 segments in relation to the ion pore is based partially on homology models constructed from the crystal structures of distantly related voltage-gated potassium channels, as well as the positions of amino acid residues that are directly implicated in the binding of therapeutic drugs at the local anesthetic receptor.

Presently, the orientation of the S6 helices in domains I, II, and III is remains largely speculative (Mike and Lukacs, 2010). The orientation of DII-S6 is particularly uncertain since no residues in this domain are thought to participate in the formation of the local anesthetic drug receptor. The proposed involvement of V787 in DII-S6 in the binding of metaflumizone (Chapter 4) implies that this residue faces the ion pore in the slow-inactivated conformation. Fig. 5.1 is a helical wheel representation of the proposed orientation the four S6 helices in the slow-inactivated conformation. The orientation of DI-S6 and DIII-S6 is based on the recently proposed orientation of these segments in the high affinity states of therapeutic drug binding (Mike Lukacs, 2010). Experiments using the substituted-cysteine accessibility method demonstrated that the thiol group on V787C is only susceptible to covalent modification by methanethiosulfonate ethylammonium under conditions that promote slow inactivation (O'Reilly *et al.*, 2001). These data reveal that slow inactivation gating involves structural rearrangement(s) at or near residue V787, which may orient this residue towards the inner pore lumen.

Future Directions

Voltage-gated sodium channels in the slow-inactivated state are the molecular targets for both therapeutic and toxic agents. It is not possible to assess from the literature the basis for the distinction of therapeutically useful and toxic compounds with the same mode of action since previous studies with SCI drugs did not employ experimental methods that are directly comparable to those used in this dissertation project. Therefore, it would be useful to undertake a direct comparison of example compounds from the therapeutic and toxic classes to identify the attributes that determine a compound's therapeutic or toxic potential. Perhaps the very slow kinetics of inhibition by SCI insecticides is an important determinant of a compound's therapeutically useful or toxic effects.

SCI insecticides bind to a site on mammalian voltage-gated sodium channels that overlaps the local anesthetic receptor domain in DIV-S6 (Chapter 3; Silver and Soderlund, 2007). Data presented in this dissertation indicate that mutations at V787 in DII-S6, a domain not implicated in drug binding, causes effects on SCI insecticide sensitivity that appear to be related to side chain properties rather than indirect effects on slow inactivation. Further mutagenesis studies using a wider array of amino acid substitutions at V787 that exhibit a range of physical properties (*e.g*. size, hydrophobicity, aromaticity) are merited to clarify the role of this residue in SCI insecticide binding. Additionally, amino acid substitutions at residues adjacent to V787 are necessary to assess whether the observed effects on SCI insecticide sensitivity are region- or residue-specific. Previous studies demonstrated that a cysteine or lysine substitution at V787 does not disrupt inactivated sodium channel inhibition by local anesthetic drugs (Wang *et al.*, 2001; Kondratiev and Tomaselli, 2003). These data imply that V787 is not likely to be directly involved in drug binding, either because it not accessible in the high-affinity drug binding

conformations or because drug molecules are not able to span the asymmetrical inner pore to interact with residues in DII-S6. Because determinants of SCI insecticide binding exist in addition to those implicated in therapeutic drug binding (Fig. 5.1), the results of these studies would provide new insight into the molecular architecture of the inner pore of the channel in various conformational states.

Recent results from mutagenesis studies in DIV-S6 indicate that the SCI insecticide interactions identified with mammalian sodium channels (Chapter 3; Silver *et al.*, 2007) differ from those with insect channels (Silver *et al.*, 2009). In particular, the F1817A mutation in the German cockroach (*Blattella germanica*) sodium channel (corresponding to F1579A in $Na_v1.4$) increases the inhibitory efficiency of metaflumizone, but does not significantly affect that indoxacarb or DCJW. These data not only imply significantly different receptor sites for SCI insecticides on mammalian and insect sodium channels, but also imply a molecular distinction between metaflumizone and other SCI insecticides in terms of their interaction with the insect receptor. Further studies are required to define the role of the DII-S6 valine (V787 in $Na_v1.4$) in the binding of SCI insecticides, particularly metaflumizone, to insect sodium channels.

The structural and functional distinction between intermediate and slow inactivation in $Na_v1.4$ sodium channels identified in this dissertation project (Chapter 2) raises intriguing questions about the role of intermediate inactivation in channel inhibition by SCI insecticides. $Na_v1.4$ sodium channels in the intermediate-inactivated state have a seemingly higher affinity for lidocaine than channels in the slow-inactivated state (Kambouris *et al.*, 1998). Further studies are required to elucidate the inactivation state dependence of sodium channel inhibition by SCI insecticides. Mutations at W402 in the outer pore of $Na_v1.4$ channels have disparate effects on the intermediate and slow inactivation (Kambouris *et al.*, 1998). The W402S mutation significantly inhibits the intermediate component of inactivation and paradoxically enhances the

slow component of inactivation, whereas the W402A mutation inhibits both the intermediate and slow components of inactivation. Replacing the native tryptophan with another aromatic residue (phenylalanine; W402F) does not significantly alter either intermediate or slow inactivation.

If SCI insecticides selectively bind to slow-inactivated channels, one would predict that the W402S mutation would significantly increase insecticide inhibition, whereas the W402A mutation would decrease insecticide inhibition. If intermediate inactivation plays an important role in channel block by SCI insecticides, then both mutations would predictably decrease the inhibitory efficiency of these compounds, despite the disparate effects of the mutations on slow inactivation gating. If alterations in insecticide action were observed with sodium channels bearing the W402F mutation, it would imply that mutations at this position alter insecticide action independent of mutation-induced changes in intermediate or slow inactivation gating. The results from these studies would not only provide important insight into state-dependent mechanism of action of SCI insecticides, but also help delineate functional differences between insecticidal and therapeutic agents, as well as between nonconducting sodium channel conformations.

References

Errington AC, Stöhr T, Heers C, and Lees G (2008) The investigational anticonvulsant lacosamide selectively enhances slow inactivation of voltage-gated sodium channels. *Mol. Pharmacol.* **73**:157-169.

Hildebrand ME, Smith PL, Bladen C, Eduljee C, Xie JY, Chen L, Fee-Maki M, Doering CJ, Mezeyova J, Zhu Y, Belardetti F, Pajouhesh H, Parker D, Arneric SP, Parmar M, Porreca F, Tringham E, Zamponi GW, and Snutch TP (2011) A novel slow-inactivation-specific ion channel modulator attenuates neuropathic pain. *PAIN*® **152**:833-843.

Hille B (1977) Local anesthetics: hydrophilic and hydrophobic pathways for drug receptor reaction. *J. Gen. Physiol*. **69**:497-515.

Kambouris NG, Hastings LA, Stepanovic S, Marbán E, Tomaselli GF and Balser JR (1998) Mechanistic link between lidocaine block and inactivation probed by outer pore mutations in the rat μ1 skeletal muscle sodium channel. *J. Physiol*. **512**:693-705.

Kondratiev A and Tomaseli GF (200) Altered gating and local anesthetic block mediated by residues in the I-S6 and II-S6 transmembrane segments of voltage-dependent Na^+ channels. *Mol. Pharmacol.* **64**:741-752.

Lapied B, Grolleau F and Sattelle DB (2001) Indoxacarb, an oxadiazine insecticide, blocks insect neuronal sodium channels. *Brit. J. Pharmacol.* **132**:587-595.

Li HL, Galue A, Meadows L, and Ragsdale DS (1999) A molecular basis for the different local anesthetic affinities of resting versus open and inactivated states of the sodium channel. *Mol. Pharmacol.* **55**:134-141.

McDonough SI and Bean BP (2006) State-dependent drug interactions with ion channels, in *Voltage-Gated Ion Channels as Drug Targets* (Triggle DJ, Gopalakrishnan M, Rampe D, and Zheng W eds) pp 19-36, Wiley-VCH, Weinheim.

McNulty MM and Hanck DA (2004) State-dependent mibefradil block of Na^+ channels. *Mol. Pharmacol.* **66**:1652-1661.

Mike A and Lukacs P (2010) The enigmatic drug binding site for sodium channel inhibitors. *Curr. Mol. Pharmacol.* **3**:129-144.

O'Reilly JP, Wang S-Y and Wang GK (2001) Residue-specific effects on slow inactivation at V787 in D2-S6 of $Na_v1.4$ sodium channels. *Biophys. J.* **81**:2100-2111.

Ragsdale DS, McPhee JC, Scheuer T and Catterall WA (1994) Molecular determinants of state-dependent block of Na^+ channels by local anesthetics. *Science* **265**:1724-1728.

Ragsdale DS, McPhee JC, Scheuer T, and Catterall, WA (1996) Common molecular determinants of local anesthetic, antiarrhythmic, and anticonvulsant block of

Salgado VL (1992) Slow voltage-dependent block of sodium channels in crayfish nerve by dihydropyrazole insecticides. *Mol. Pharmacol.* **41**:120-126.

Salgado VL and Hayashi JH (2007) Metaflumizone is a novel sodium channel blocker insecticide. *Vet. Parasitol.* **150**:182-189.

Silver KS, Nomura Y, Salgado VL and Dong K (2009) Role of the sixth transmembrane segment of domain IV of the cockroach sodium channel in the action of sodium channel-blocker insecticides. *Neurotox.* **30**:613-621.

Silver KS and Soderlund DM (2005) State-dependent block of rat $Na_v1.4$ sodium channels expressed in *Xenopus* oocytes by pyrazoline-type insecticides. *Neurotox.* **26**:397-406.

Silver KS and Soderlund DM (2007) Point mutations at the local anesthetic receptor site modulate the state-dependent block of rat $Na_v1.4$ sodium channels by pyrazoline-type insecticides. *Neurotox.* **28**:655-663.

Tsurubuchi Y, Zhao X, Nagata K, Kono Y, Nishimuru K, Yeh JZ and Narahashi T (2001) Modulation of tetrodotoxin-resistant sodium channels by dihydropyrazole insecticide RH-3421 in rat dorsal root ganglion neurons. *Neurotox.* **22**:743-753.

Tsurubuchi Y and Kono Y (2003) Modulation of sodium channels by the oxadiazine insecticide indoxacarb and its *N*-decarbomethoxylated metabolite in rat dorsal root ganglion neurons. *Pest Manag. Sci.* **59**:999-1006.

Wang S-Y, Barile M and Wang GK (2001) Disparate role of Na^+ channel D2-S6 residues in batrachotoxin and local anesthetic action. *Mol. Pharmacol.* **59**:1100-1107.

Zhao X, Ikeda T, Yeh JZ and Narahashi T (2003) Voltage-dependent block of sodium channels in mammalian neurons by the oxadiazine insecticide indoxacarb and its metabolite DCJW. *Neurotox*. **24**:83-96.